TRANSFORMATION AND TRANSPORT OF DISSOLVED ORGANIC MATTER IN COASTAL SYSTEMS USING MOLECULAR AND OCEAN COLOR APPROACHES

by

RACHEL P. MARTINEAC

(Under the Direction of Patricia M. Medeiros)

ABSTRACT

Dissolved organic matter (DOM) is a critical component of the global carbon cycle; it has multiple sources including terrestrial runoff, riverine input, phytoplankton excretion, viral lysis, among others. These inputs have varying levels of contribution depending on temporal and spatial scales as well as environmental variables, making the characterization of the DOM increasingly complex. This dissertation used primarily molecular (ultrahigh resolution mass spectrometry - FT-ICR MS) and satellite-derived ocean-color techniques to investigate the transformation and transport of DOM in two important aquatic systems. In CHAPTER 2, FT-ICR MS in hand with metatranscriptomics were used to characterize the dominant patterns of variability modifying the DOM composition in a typical estuary off the Southeastern U.S. Results showed that after seasonal variations, long-term biodegradation was comparatively more important in the fall, while tidal variability was the second most important factor correlated to DOM compositional changes in the spring, when the freshwater content in the estuary was high. Microbial data revealed a similar pattern, with variability in gene expression occurring first at the seasonal scale, then by tidal influence. Over shorter time scales, however, the influence of

microbial processing on DOM compositional changes was small. In CHAPTER 3, two decades of ocean color observations from satellite were used to describe seasonal and interannual variability in terrigenous DOC (tDOC) content in the Amazon River plume. Seasonality accounted for 40% of the total variance in the plume core, and interannual variability in tDOC accounted for 15% of the total variance, likely associated with hydrological changes. Overall, we found MODIS-tDOC to be an effective tracer for the Amazon River plume, with great potential to be used for identifying events of increased off-shelf tDOC transport. Finally, in CHAPTER 4, MODIS-tDOC was used to estimate tDOC degradation over the shelf. A clear seasonal pattern was observed, with increased degradation occurring during the high discharge season. Also, a correlation was found between onshelf degradation and tDOC anomalies offshore with a lag-time of ~40 days. Overall, this dissertation uncovered the relative importance of various factors on DOM composition and degradation, especially in the context of combining various research techniques.

INDEX WORDS: Oceanography; Biogeochemistry; DOM Composition; DOM Processing; FT-ICR MS; Doboy Sound; Estuary; Georgia Coastal Ecosystem LTER; Amazon River Plume; Ocean Color; Remote Sensing; MODIS; SMOS

TRANSFORMATION AND TRANSPORT OF DISSOLVED ORGANIC MATTER IN COASTAL SYSTEMS USING MOLECULAR AND OCEAN COLOR APPROACHES

by

RACHEL P. MARTINEAC

BS, University of Connecticut, 2013
MS, University of Connecticut, 2015

A Dissertation Submitted to the Graduate Faculty of The University of Georgia

in Partial Fulfillment of the Requirements for the Degree

DOCTOR OF PHILOSOPHY

ATHENS, GEORGIA

2023

TRANSFORMATION AND TRANSPORT OF DISSOLVED ORGANIC MATTER IN COASTAL SYSTEMS USING MOLECULAR AND OCEAN COLOR APPROACHES

by

RACHEL P. MARTINEAC

Major Professor: Patricia M. Medeiros

Committee: Renato M. Castelao
Franklin E. Leach III
Mary Ann Moran
Amanda C. Spivak

Electronic Version Approved:

Ron Walcott
Vice Provost for Graduate Education and Dean of the Graduate School
The University of Georgia
May 2023

Dedicated to Kate and
her descendants.

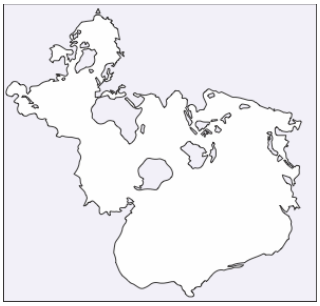

The Earth belongs to
future generations.

ACKNOWLEDGEMENTS

There are many who helped me along the way on this journey. First, I wish to thank my advisor, Patricia Medeiros. Her guidance and generosity are unmatched, and I am grateful she selected me as her student. I also thank my committee members, Renato Castelao, Franklin Leach, Mary Ann Moran, and Amanda Spivak. I am grateful to have an involved and supportive committee, and with their guidance was able to achieve a truly interdisciplinary dissertation. I would like to especially thank Patricia, Mary Ann, and Renato, with whom I am coauthors, for supporting me through the manuscript writing process.

Importantly, I would like to thank my funding sources for the financial support required to complete this degree – the National Science Foundation, the Georgia Coastal Ecosystem Long Term Ecological Research program, and the UGA Graduate School for funding this work. I would also like to thank the National High Magnetic Field Laboratory for providing me with training and support in the ultrahigh-resolution mass spectrometry analyses.

Next, I thank my lab-mates Maria Letourneau, Giovanna Utsumi, and Kellie White. I greatly look forward to having all of you as colleagues in the years ahead. Thanks for the proofreading, emotional support, and listening to me talk to myself.

Finally, I acknowledge my family. To my parents: thanks for listening to me on the phone nearly daily for five years. To my in-laws: thank you for the cat- and baby-sitting I needed to get my work done. To my husband, Luke, and my daughter, Kate: your support and understanding helped me through.

TABLE OF CONTENTS

LIST OF TABLES

Page

LIST OF FIGURES

Page

CHAPTER 1

INTRODUCTION AND LITERATURE REVIEW

The dissolved organic matter (DOM) pool in the ocean holds an amount of carbon comparable to the atmospheric carbon pool, making DOM an important component of the global carbon cycle (Hedges, 1992, Hansell, 2013). The marine DOM pool is estimated to be 662 Pg C (Hansell *et al.*, 2009), and comprises a major part of the carbon budget in marine ecosystems. Marine DOM composition is diverse, containing between tens to hundreds of thousands of distinct organic molecules (Kim *et al.*, 2003), and a wide range of lability depending on the variety of molecular compositions in different environments (e.g., Meyer *et al.*, 1987; Moran and Hodson, 1994; Amon and Benner, 1996). Additionally, DOM composition and quality are affected by the inputs of many different sources as well as the complex interactions of abiotic and biotic processes (Sholkovitz, 1978; Kieber *et al.*, 1990; Miller and Moran, 1997; Hernes and Benner, 2003).

Coastal ecosystems are important to our understanding of DOM composition due to a unique combination of carbon inputs from both marine and terrestrial sources (Hedges *et al.*, 1997). While studies have highlighted coastal regions as important links for carbon reservoirs in the open ocean (Walsh, 1991, Medeiros *et al.*, 2016), few efforts have been made to understand the fate and cycling of organic carbon in the coastal ocean, and eventual transport to the open ocean (e.g., Raymond and Bauer, 2001; Chen and Borges, 2009; Ward *et al.*, 2013; Medeiros *et*

al., 2016, 2017; Letourneau *et al.*, 2021). Exploring the differences between major DOM inputs to estuaries provides insight into how DOM from different sources may influence the patterns of transformation at the molecular level due to biodegradation (Medeiros *et al.*, 2017). For instance, seasonal changes in river discharge, as is typical in the Southeast U.S., have been shown to enhance the export of terrigenous DOM to estuaries (e.g., Medeiros *et al.*, 2017; Letourneau and Medeiros, 2019; Osburn *et al.*, 2019). Tides also have an impact on the DOM composition in estuaries as sources of DOM shift on short-time scales (Tzortziou *et al.*, 2008; Seidel *et al.*, 2014). Substantial transformations of DOM composition due to bacterial consumption have also been observed in Southeastern U.S. coastal waters (Moran and Hodson, 1989, 1994; Miller and Moran, 1997; Moran *et al.*, 1999; Medeiros *et al.*, 2015b, 2017; Vorobev *et al.*, 2018; Letourneau *et al.*, 2021). These environmental complexities make quantifying the influence of sources and biogeochemical processes affecting estuarine DOM composition in estuaries difficult.

Much remains to be learned about the fate of this terrigenous material in the ocean. Despite the large inputs, terrigenous DOC (tDOC) is thought to be altered over relatively short time scales (Benner and Opsahl, 2001; Hernes and Benner, 2003), with the coastal ocean serving as a major sink (Hedges *et al.*, 1997; Fichot and Benner, 2014). Main mechanisms responsible for removing tDOC in the coastal ocean include microbial degradation, photochemical processes, and flocculation (Sholkovitz, 1978; Hernes and Benner, 2003). One approach to uncovering changes in DOM between freshwater and marine waters values the observation of significant differences in DOM molecular composition (Sleighter & Hatcher, 2008; Medeiros *et al.*, 2015b), which is the major focus in CHAPTER 2. Relative to marine DOM, freshwater DOM is typically more enriched with compounds containing low H/C ratios consistent with more aromatic

structures, a characteristic of terrigenous material (Sleighter & Hatcher, 2008; Medeiros *et al.*, 2015a). Though terrigenous DOM is contributed in large volumes (0.25 Pg), it constitutes a small fraction of the open ocean DOM pool (Hedges, 1992; Opsahl & Benner, 1997) indicating this material may undergo rapid transformation in estuarine systems (Tzortziou *et al.*, 2008). Microorganisms are the most abundant marine organic matter producers and consumers, with the ocean microbiome containing estimated hundreds of thousands of distinctive bacterial, archaeal, and eukaryotic taxa (Pomeroy, 1974; Hertkorn *et al.*, 2006; Pomeroy *et al.*, 2007; Lechtenfeld *et al.*, 2015; Sunagawa *et al.*, 2015), and bacteria are the key drivers of the discrepancy between biological carbon fixation and remineralization (Lechtenfield *et al.*, 2015), as DOM is an important growth substrate for bacteria (Pomeroy, 1974). Though studies have investigated the microbial community composition to gain insight into their role modifying the molecular composition of the DOM pool (Moran *et al.*, 1994, 1999; Osterholz *et al.*, 2016, 2018; Vorobev *et al.*, 2018), the quality and quantity of DOM produced, consumed, and transformed by these organisms remains largely unknown (Borges *et al.*, 2005; Chen & Borges, 2009; Cai, 2011; Bauer *et al.*, 2013). In addition to the physical impacts on the DOM pool, CHAPTER 2 focuses on how biological changes are important to short-term shifts in molecular composition.

Many studies have indicated that ocean margins can act as major "filters" of tDOC between the land and ocean (Hedges *et al.*, 1997; Opsahl and Benner, 1997). This is especially of interest because riverine transport is the largest delivery of organic matter from land to ocean (Hedges *et al.*, 1997; Raymond and Spencer, 2015) supplying a quantity sufficient to support the turnover of dissolved organic carbon (DOC) throughout the ocean (Williams and Druffel, 1987). Estimates of global transport range from 0.17 Pg C yr^{-1} (Dai et al, 2012) to 0.36 Pg C yr^{-1} (Aitkenhead and McDowell, 2000), with many other estimates over the past five decades falling

in between (e.g., Meybeck, 1982; Smith and Hollibaugh, 1993; Ludwig *et al.*, 1996; Harrison *et al.*, 2005; Seitzinger *et al.*, 2005; Cai, 2011). Previous studies have found the driving control of DOM compositional change in many estuarine systems to be water mixing across a marine-freshwater gradient (Sleighter and Hatcher, 2008; Medeiros *et al.*, 2015b; Osterholz *et al.*, 2016), and recent studies have shown that over half of the tDOC from the Mississippi-Atchafalaya River system is mineralized along the northern Gulf of Mexico margin each year (Fichot and Benner, 2014). In fact, the metabolic state of ocean margins, including the role of CO_2 exchange with the atmosphere, is directly affected by the mineralization of tDOC (Smith and Hollibaugh, 1993; Hedges *et al.*, 1997; Opsahl and Benner, 1997; Bianchi, 2011; Cai, 2011; Letscher *et al.*, 2011; Fichot and Benner, 2014). Since it is likely that the terrigenous material will continue to be degraded as it is transported offshore, the fraction of terrigenous material exported from that continental margin is likely to be even smaller. Despite this intense mineralization, studies have demonstrated that some of the tDOC exported from rivers escapes the continental margin (Medeiros *et al.*, 2015a; Seidel *et al.*, 2015) and is transported to the open ocean (Medeiros *et al.*, 2017) and the deep ocean (Opsahl and Benner, 1997; Medeiros *et al.*, 2015c).

In CHAPTER 3 and CHAPTER 4, I shift my research area to the Amazon River to ocean continuum, where over 75% of the tDOC delivered to the ocean by the Amazon River can be exported from the continental margin, particularly during high discharge conditions (Medeiros *et al.*, 2015a). The Amazon River alone is responsible for discharging between 12-20% of the global riverine DOC flux to the ocean (Meybeck, 1982; Richey *et al.*, 1986; Moreira-Turcq *et al.*, 2003; Raymond and Spencer, 2015), and since the Amazon River discharge is predicted to increase in future climate scenarios (Manabe *et al.*, 2004; Nohara *et al.*, 2006) delivery of tDOC

to the ocean and the export from the coastal margin may increase even further (Medeiros *et al.*, 2015b).

Tracing the transport of tDOC in the ocean relying on *in situ* observations is challenging. Not only they are dependent on logistically difficult and expensive field campaigns that only provide snapshots in time, the transport often occurs in relatively narrow filaments that are easily missed by low-resolution *in situ* data. Long-term observations of that transport over large areas in the ocean can only be achieved via the use of well-calibrated satellite algorithms. Algorithms based on remote sensing reflectance (Rrs) data from the Moderate Resolution Imaging Spectroradiometer (MODIS) have been developed to estimate the spectral slope coefficient of CDOM absorbance from satellite ocean color data (Fichot *et al.*, 2013; 2014). Recent studies have shown that the spectral slope coefficient of chromophoric dissolved organic matter (CDOM) between 275 and 295 nm ($S_{275\text{-}295}$) can be used as a tracer of the percent tDOC in river-influenced ocean margins (Fichot and Benner, 2012; Fichot *et al.*, 2014; Medeiros *et al.*, 2017a). Fichot *et al.* (2014) showed that $S_{275\text{-}295}$ from satellites agree with *in situ* $S_{275\text{-}295}$ measurements with an average uncertainty of 10%. By using a nonlinear regression to model the relationship between *in situ* $S_{275\text{-}295}$ and tDOC concentration, estimates of tDOC content from ocean color can be obtained (Fichot *et al.*, 2014). Thus, CHAPTER 3 focuses on quantifying the cross-shelf transport of tDOC using satellite observations.

Although much has been learned about the distribution of Amazon River plume waters (e.g., Salisbury *et al.*, 2011; Fournier *et al.*, 2015) and the mechanisms driving offshore advection of freshwater into the tropical Atlantic Ocean (e.g., Fournier *et al.*, 2017) using satellite observations, many of these previous studies relied on relatively short time series lasting only a few years. This precluded the characterization of plume variability at seasonal and/or

lower frequencies. With almost 20 years of satellite observations of ocean color now available, we adapted and refined the algorithm developed by Fichot *et al.* (2013, 2014) to provide a detailed characterization of seasonal and interannual variability in the distribution of terrigenous DOC from the Amazon River in the Atlantic Ocean. Identifying areas of enhanced offshore transport of tDOC as well as the mechanisms controlling the offshore transport are the focuses of CHAPTER 4.

References

Aitkenhead, J. A. and W. H. McDowell (2000). Soil C:N ratio as a predictor of annual riverine DOC flux at local and global scales. Global Biogeochem. Cycles, 14(1), 127-138. doi: 10.1029/1999GB900083

Amon, R. M. W. and R. Benner (1996). Bacterial utilization of different size classes of dissolved organic matter. Limnol. Oceanogr., 41(1), 41-51. doi: 10.4319/lo.1996.41.1.0041

Bauer J., Cai, W.J., Raymond, P., Bianchi, T.S., Hopkinson, C.S., and Regnier, P.A.G. (2013). The changing carbon cycle of the coastal ocean. Nature. 504, 61-70. doi: 10.1038/nature12857

Benner, R., and Opsahl, S. (2001). Molecular indicators of the sources and transformations of dissolved organic matter in the Mississippi River plume. Org. Geochem., 32, 4, 597–611. doi: 10.1016/s0146-6380(00)00197-2

Bianchi, T. S. (2011). The role of terrestrially derived organic carbon in the coastal ocean: A changing paradigm and the priming effect. Proc. Natl. Acad. Sci. U.S.A., 108(49), 19473-19481. doi:10.1073/pnas.1017982108

Borges, A. V., Delille, B., and Frankignoulle, M. (2005). Budgeting sinks and sources of CO2 in the coastal ocean: Diversity of ecosystems counts, Geophys. Res. Lett., 32(14).

Cai, W. (2011). Estuarine and Coastal Ocean Carbon Paradox: CO2 Sinks or Sites of Terrestrial Carbon Incineration?. Annu. Rev. Mar. Sci., 3(1), 123-145. doi: 10.1146/annurev-marine-120709-142723

Chen, C. A. and Borges, A. V. (2009). Reconciling opposing views on carbon cycling in the coastal ocean: Continental shelves as sinks and near-shore ecosystems as sources of atmospheric CO2, Deep Sea Res. Part II Top. Stud. Oceanogr., 56(8-10), 578-590.

Fichot, C. G., Kaiser, K., Hooker, S., Amon, R., Babin, M., Belanger, S., Walker, S., and Benner, R. (2013). Pan-Arctic distributions of continental runoff in the Arctic Ocean, Sci. Rep., 3, 1053. doi:10.1038/srep01053

Fichot, C. G. and Benner, R. (2014). The fate of terrigenous dissolved organic carbon in a river-influenced ocean margin. Global Biogeochem. Cycles, 28(3), 300-318. doi: 10.1002/2013GB004670

Fournier, S., Chapron, B., Salisbury, J., Vandemark, D. and Reul, N. (2015). Comparison of spaceborne measurements of sea surface salinity and colored detrital matter in the Amazon plume. J. Geophys. Res. Oceans, 120(5), 3177-3192. doi: 10.1002/2014JC010109

Fournier, S., Vandemark, D., Gaultier, L., Lee, T., Jonsson, B. and Gierach, M. M. (2017). Interannual Variation in Offshore Advection of Amazon-Orinoco Plume Waters: Observations, Forcing Mechanisms, and Impacts. J. Geophys. Res. Oceans, 122(11), 8966-

8982. doi: 10.1002/2017JC013103

Hansell, D.A., Carlson, C.A., Repeta, D.J., and Schlitzer, R. (2009). Dissolved organic matter in the ocean: A controversy stimulates new insights. Oceanography. 22, 202-211. doi: 10.5670/oceanog.2009.109

Hansell, D. A. (2013). Recalcitrant Dissolved Organic Carbon Fractions, Annu. Rev. Mar. Sci., 5(1), 421-445. doi: 10.1146/annurev-marine-120710-100757

Harrison, J. A., Caraco, N. and Seitzinger, S. P. (2005). Global patterns and sources of dissolved organic matter export to the coastal zone: Results from a spatially explicit, global model. Global Biogeochem. Cycles, 19(4). doi: 10.1029/2005GB002480

Hedges, J. I. (1992). Global biogeochemical cycles: progress and problems. Mar. Chem., 39(1), 67-93. doi: 10.1016/0304-4203(92)90096-S

Hedges, J. I., Keil, R. G. and Benner, R. (1997). What happens to terrestrial organic matter in the ocean?. Org. Geochem., 27(5), 195-212. doi: 10.1016/S0146-6380(97)00066-1

Hernes, P. J. and R. Benner (2003). Photochemical and microbial degradation of dissolved lignin phenols: Implications for the fate of terrigenous dissolved organic matter in marine environments, J. Geophys. Res., 108. doi: 10.1029/2002JC001421

Hertkorn, N., Benner, R., Frommberger, M., Schmitt-Kopplin, P., Witt, M., Kaiser, K., Kettrup, A., and Hedges, J. I. (2006). Characterization of a major refractory component of marine dissolved organic matter, Geochim. Cosmochim. Acta, 70(12), 2990-3010.

Hopkinson Jr, C. S. (1985). Shallow-water benthic and pelagic metabolism: evidence of heterotrophy in the nearshore Georgia Bight, Mar. Biol., 87(1), 19-32.

Kieber, R. J., Zhou, X., and Mopper, K. (1990). Formation of carbonyl compounds from UV-induced photodegradation of humic substances in natural waters: Fate of riverine carbon in the sea, Limnol. Oceanogr., 35(7), 1503-1515.

Kim, S., Kramer, R. W., and Hatcher, P. G. (2003). Graphical Method for Analysis of Ultrahigh-Resolution Broadband Mass Spectra of Natural Organic Matter, the Van Krevelen Diagram, Anal. Chem., 75(20), 5336-5344. doi: 10.1021/ac034415p

Lechtenfeld, O. J., Hertkorn, N., Shen, Y., Witt, M., and Benner, R. (2015). Marine sequestration of carbon in bacterial metabolites, Nat. Commun., 6(1), 6711.

Letourneau, M. L. and Medeiros, P. M. (2019). Dissolved Organic Matter Composition in a Marsh-Dominated Estuary: Response to Seasonal Forcing and to the Passage of a Hurricane, J. Geophys. Res. Biogeosci., 124(6), 1545-1559. doi: 10.1029/2018JG004982

Letourneau, M. L., Schaefer, S. C., Chen, H., McKenna, A. M., Alber, M., and Medeiros, P. M. (2021). Spatio-temporal changes in dissolved organic matter composition along the salinity gradient of a marsh-influenced estuarine complex, Limnol. Oceanogr., 66(8), 3040-3054.

doi: 10.1002/lno.11857

Letscher, R., D. A. Hansell, and D. Kadko. (2011). Rapid removal of terrigenous dissolved organic carbon over the Eurasian shelves of the Arctic Ocean. Mar. Chem., 123:78–87. doi: 10.1016/j.marchem.2010.10.002

Ludwig, W., Probst, J. and Kempe, S. (1996). Predicting the oceanic input of organic carbon by continental erosion. Global Biogeochem. Cycles, 10(1), 23-41. doi: 10.1029/95GB02925

Manabe, S., Wetherald, R. T., Milly, P., Delworth, T. L., and Stouffer, R. J. (2004). Century-scale change in water availability: CO 2-quadrupling experiment, Clim. Change, 64, 59-76.

Medeiros, P.M., Seidel, M., Dittmar, T., Whitman, W.B., and Moran, M.A. (2015a). Drought-induced variability in dissolved organic matter composition in a marsh-dominated estuary. Geophys. Res. Lett. 42, 6446-6453. doi:10.1002/ 2015GL064653

Medeiros, P. M., Seidel, M., Ward, N. D., Carpenter, E. J., Gomes, H. R., Niggemann, J., Krusche, A. V., Richey, J. E., Yager, P. L. and Dittmar, T. (2015b). Fate of the Amazon River dissolved organic matter in the tropical Atlantic Ocean. Global Biogeochem. Cycles, 29(5), 677-690. doi: 10.1002/2015GB005115

Medeiros, P. M., Seidel, M., Powers, L. C., Dittmar, T., Hansell, D. A., and Miller, W. L. (2015c). Dissolved organic matter composition and photochemical transformations in the northern North Pacific Ocean, Geophys. Res. Lett., 42(3), 863-870.

Medeiros, P.M., Babcock-Adams, L., Seidel, M., Castelao, R.M., Di Iorio, D., Hollibaugh, J. T., *et al.* (2017a). Export of terrigenous dissolved organic matter in a broad continental shelf. Limnol. Oceanogr. 62, 1718-1731. doi: 10.1002/lno.10528

Meybeck, M. (1982). Carbon, nitrogen, and phosphorus transport by world rivers, Am. J. Sci., 282(4), 401. doi: 10.2475/ajs.282.4.401

Meyer, J. L., Edwards, R. T., and Risley, R. (1987). Bacterial growth on dissolved organic carbon from a blackwater river, Microb. Ecol., 13(1), 13-29. doi: 10.1007/BF02014960

Miller, W.L., and Moran, M.A. (1997). Interaction of photochemical and microbial processes in the degradation of refractory dissolved organic matter from a coastal marine environment. Limnol. Oceanogr. 42, 1317-1324. doi: 10.4319/lo.1997.42.6.1317

Moran, M. A. and Hodson, R. E. (1989). Formation and bacterial utilization of dissolved organic carbon derived from detrital lignocellulose, Limnol. Oceanogr., 34(6), 1034-1047.

Moran, M. A. and Hodson, R. E. (1994). Dissolved humic substances of vascular plant origin in a coastal marine environment, Limnol. Oceanogr., 39(4), 762-771.

Moran, M. A., Sheldon, W. M., and Sheldon, J. E. (1999). Biodegradation of riverine dissolved organic carbon in five estuaries of the southeastern United States, Estuaries, 22, 55-64.

Nohara, D., Kitoh, A., Hosaka, M., and Oki, T. (2006). Impact of climate change on river discharge projected by multimodel ensemble, J. Hydrometeorol., 7(5), 1076-1089.

Opsahl, S. and Benner, R. (1997). Distribution and cycling of terrigenous dissolved organic matter in the ocean, Nature, 386(6624), 480-482. doi: 10.1038/386480a0

Osburn, C.L., Atar, J.N., Boyd, T.J., and Montgomery, M.T. (2019). Antecedent precipitation influences the bacterial processing of terrestrial dissolved organic matter in a North Carolina estuary. Estuar. Coast. Shelf Sci. 221, 119-131. doi: 10.1016/j.ecss.2019.03.016

Osterholz, H., Kirchman, D. L., Niggemann, J., and Dittmar, T. (2016b). Environmental drivers of dissolved organic matter molecular composition in the Delaware Estuary, Front. Earth Sci., 4, 95.

Osterholz, H., Kirchman, D. L., Niggemann, J., and Dittmar, T. (2018). Diversity of bacterial communities and dissolved organic matter in a temperate estuary. FEMS Microbiol. Ecol. 94:8. doi: 10.1093/femsec/fiy119

Pomeroy, L. R. (1974). The ocean's food web, a changing paradigm. Bioscience, 24(9), 499-504.

Pomeroy, L. R, Williams, P. J. leB., Azam, F., and Hobbie, J. E. (2007). The microbial loop, Oceanography, 20(2), 28-33.

Raymond, P. A., and J. E. Bauer (2001). Riverine export of aged terrestrial organic matter to the North Atlantic Ocean. Nature, 409, 497–500.

Raymond, P. A. and R. G. M. Spencer (2015). “Chapter 11 - Riverine DOM”, in Biogeochemistry of Marine Dissolved Organic Matter (Second Edition), ed Hansell, D.A. and Carlson, C.A. (Boston MA: Academic Press) pp. 509-533.

Salisbury, J., Vandemark, D., Campbell, J., Hunt, C., Wisser, D., Reul, N., and Chapron, B. (2011). Spatial and temporal coherence between Amazon River discharge, salinity, and light absorption by colored organic carbon in western tropical Atlantic surface waters. J. Geophys. Res., 116, C7. doi: 10.1029/2011jc006989

Seidel, M., Beck, M., Riedel, T., Waska, H., Suryaputra, I. G. N. A., Schnetger, B., *et al.* (2014). Biogeochemistry of dissolved organic matter in an anoxic intertidal creek bank. Geochim. Cosmochim. Acta. 140, 418-434. doi: 10.1016/j.gca.2014.05.038

Seidel, M., Yager, P. L., Ward, N. D., Carpenter, E. J., Gomes, H. R., Krusche, A. V., Richey, J. E., Dittmar, T., and Medeiros, P. M. (2015). Molecular-level changes of dissolved organic matter along the Amazon River-to-ocean continuum. Mar. Chem., 177, 218–231. doi: 10.1016/j.marchem.2015.06.019

Seitzinger, S. P., Harrison, J. A., Dumont, E., Beusen, A. H. W., and Bouwman, A. F. (2005). Sources and delivery of carbon, nitrogen, and phosphorus to the coastal zone: An overview of Global Nutrient Export from Watersheds (NEWS) models and their application, Global Biogeochem. Cycles, 19(4). doi: 10.1029/2005GB002606

Sholkovitz, E.R. (1976). Flocculation of dissolved organic and inorganic matter during the mixing of river water and seawater. Geochim. Cosmochim. Acta. 4, 831-845.

Sleighter, R.L., and Hatcher, P.G. (2008). Molecular characterization of dissolved organic matter (DOM) along a river to ocean transect of the lower Chesapeake Bay by ultrahigh resolution electrospray ionization Fourier transform ion cyclotron resonance mass spectrometry. Mar. Chem. 110, 140-152. doi: 10.1016/j.marchem.2008.04.008

Smith, S. V. and J. T. Hollibaugh (1993). Coastal metabolism and the oceanic organic carbon balance. Rev. Geophys., 31(1), 75-89. doi: 10.1029/92RG02584

Sunagawa, S., Coelho, L. P., Chaffron, S., Kultima, J. R., Labadie, K., Salazar, G., Djahanschiri, B, Zeller, G., Mende, D. R., and Alberti, A. (2015). Structure and function of the global ocean microbiome, Science, 348(6237), 1261359.

Tzortziou, M., Neale, P.J., Osburn, C.L., Megonigal, J. P., Maie, N., and Jaffe, R. (2008). Tidal marshes as a source of optically and chemically distinctive colored dissolved organic matter in the Chesapeake Bay. Limnol. Oceanogr. 53, 148-159.

Tzortziou, M., P. J. Neale, J. P. Megonigal, C. L. Pow, and M. Butterworth (2011). Spatial gradients in dissolved carbon due to tidal marsh outwelling into a Chesapeake Bay estuary, Mar. Ecol. Prog. Ser., 426, 41-56.

Vorobev, A., S. Sharma, M. Yu, J. Lee, B. J. Washington, W. B. Whitman, F. Ballantyne IV, P. M. Medeiros, and M. A. Moran (2018). Identifying labile DOM components in a coastal ocean through depleted bacterial transcripts and chemical signals, Environ. Microbiol., 20(8), 3012-3030.

Walsh, J. J. (1991). Importance of continental margins in the marine biogeochemical cycling of carbon and nitrogen, Nature, 350(6313), 53-55.

Ward, N. D., R. G. Keil, P. M. Medeiros, D. C. Brito, A. C. Cunha, T. Dittmar, P. L. Yager, A. V. Krusche, and J. E. Richey (2013). Degradation of terrestrially derived macromolecules in the Amazon River, Nat. Geosci., 6, 530–533.

Williams, P. M. and E. R. M. Druffel (1987). Radiocarbon in dissolved organic matter in the central North Pacific Ocean, Nature, 330(6145), 246-248. doi: 10.1038/330246a0

CHAPTER 2

ASSESSING THE CONTRIBUTION OF SEASONALITY, TIDES, AND MICROBIAL PROCESSING TO DISSOLVED ORGANIC MATTER COMPOSITION VARIABILITY IN A SOUTHEASTERN U.S. ESTUARY[1]

[1]Martineac, R.P., Vorobev, A.V., Moran, M.A., and Medeiros, P.M., 2021. *Frontiers in Marine Science,* 8:781580. Reprinted here with permission of the publisher.

Abstract

Uncovering which biogeochemical processes have a critical role controlling dissolved organic matter (DOM) compositional changes in complex estuarine environments remains a challenge. In this context, the aim of this study is to characterize the dominant patterns of variability modifying the DOM composition in an estuary off the Southeastern U.S. We collected water samples during three seasons (July and October 2014 and April 2015) at both high and low tides and conducted short- (1 day) and long-term (60 days) dark incubations. Samples were analyzed for bulk DOC concentration, and optical (CDOM) and molecular (FT-ICR MS) compositions and bacterial cells were collected for metatranscriptomics. Results show that the dominant pattern of variability in DOM composition occurs at seasonal scales, likely associated with the seasonality of river discharge. After seasonal variations, long-term biodegradation was found to be comparatively more important in the fall, while tidal variability was the second most important factor correlated to DOM composition in spring, when the freshwater content in the estuary was high. Over shorter time scales, however, the influence of microbial processing was small. Microbial data revealed a similar pattern, with variability in gene expression occurring primarily at the seasonal scale and tidal influence being of secondary importance. Our analyses suggest that future changes in the seasonal delivery of freshwater to this system have the potential to significantly impact DOM composition. Changes in residence time may also be important, helping control the relative contribution of tides and long-term biodegradation to DOM compositional changes in the estuary.

Keywords: Dissolved organic matter; DOM composition; Microbial degradation; FT-ICR MS; marsh-dominated estuary; GCE-LTER; Southeastern U.S.

1. Introduction

The world ocean is one of the largest reservoirs of organic matter on Earth, containing approximately the same amount of carbon as atmospheric carbon dioxide (Hedges, 1992; Walther, 2013). The marine dissolved organic matter (DOM) pool is estimated to be 662 Pg C (Hansell *et al.*, 2009), and comprises a major part of the carbon budget in marine ecosystems. Marine DOM composition is diverse, containing between tens to hundreds of thousands of distinct organic molecules (Kim *et al.*, 2003), and a wide range of lability depending on the variety of molecular compositions in different environments (e.g., Meyer *et al.*, 1987; Moran and Hodson, 1994; Amon and Benner, 1996). Additionally, DOM composition and quality are affected by the inputs of many different sources as well as the complex interactions of abiotic and biotic processes (Sholkovitz, 1976; Kieber *et al.*, 1990; Miller and Moran, 1997; Hernes and Benner, 2003).

Coastal ecosystems are specifically important to our understanding of DOM composition and transformation due to the combination of carbon inputs from both marine and terrestrial sources (Hedges *et al.*, 1997). Researching DOM composition in estuaries can elucidate processes involved in organic carbon production (Bianchi, 2006) and sequestration (Watanabe and Kuwae, 2015) in these areas. By uncovering how estuaries process DOM, we gain insight into fluxes of dissolved organic carbon (DOC) to the ocean and fluxes of CO_2 to the atmosphere, especially because these regions can be both carbon sources and sinks (Bauer *et al.*, 2013; Noriega and Araujo, 2014; Canuel and Hardison, 2015). Therefore, determining the biogeochemical processes that affect DOM composition is important to our understanding of carbon cycling in estuaries.

Exploring the differences between major DOM inputs to estuaries provides insight into which biogeochemical factors are most important in considering transformations in a given region. For instance, seasonal changes in river discharge, as is typical in the Southeast U.S., have been shown to enhance the export of terrigenous DOM to estuaries (e.g., Medeiros *et al.*, 2017b; Letourneau and Medeiros, 2019; Osburn *et al.*, 2019). Tides also have an impact on the DOM composition in estuaries as sources of DOM shift on short-time scales (Tzortziou *et al.*, 2008; Seidel *et al.*, 2014). Substantial transformations of DOM composition due to bacterial consumption have also been observed in Southeastern U.S. coastal waters (Moran and Hodson, 1989, 1994; Miller and Moran, 1997; Moran *et al.*, 1999; Medeiros *et al.*, 2015a, 2017b; Vorobev *et al.*, 2018; Letourneau *et al.*, 2021). These environmental complexities make quantifying the influence of sources and biogeochemical processes affecting estuarine DOM composition in estuaries difficult. Previous studies have found the driving control of DOM compositional change in many estuarine systems to be water mixing across a marine-freshwater gradient (Sleighter and Hatcher, 2008; Medeiros *et al.*, 2015a; Osterholz *et al.*, 2016a). Medeiros *et al.* (2017b) described how DOM from different sources may influence the patterns of transformation at the molecular level due to biodegradation. Additionally, studies have investigated the microbial community composition to gain insight into their role modifying the molecular composition of the DOM pool (Osterholz *et al.*, 2016a, 2018; Vorobev *et al.*, 2018).

This study aims to build upon prior research by characterizing the most important patterns of variability modifying the DOM composition in a typical estuary of the Southeastern U.S. over three seasons. In this context, we used dark incubations on short (1 day) and long (60 days) timescales to compare biodegradation of DOM to seasonal and tidally-driven changes in

DOM composition using bulk, optical and molecular chemical techniques coupled with metatranscriptomic data to assess composition variability at the molecular level.

2. Methods

2.1 Sample Collection and Incubation

Surface water samples were collected in three seasons (July and October 2014, and April 2015) at Marsh Landing in Doboy Sound, Georgia, U.S. (**Figure 2.1**). Temperatures at the time of collection were ~30°C, 26°C and 21.5°C for July, October and April, respectively. Doboy Sound is characterized by marine influence augmented with terrestrial inputs from the Altamaha River (Medeiros *et al.*, 2015a), the dominant source of freshwater to the area (Schaefer and Alber, 2007). This study location was selected due to extensive prior research on the gene expression from ambient microbial communities (e.g., Poretsky *et al.*, 2005, 2010; Gifford *et al.*, 2011; Hollibaugh *et al.*, 2011, 2013) coupled with characterization of the DOM pool (Medeiros *et al.*, 2015a, 2017b; Letourneau *et al.*, 2021). Samples from July and October 2014 analyzed here have been previously described in Vorobev *et al.* (2018).

In the three seasons, water samples were collected at high and low tide into triplicate 20 L acid-washed carboys for initial (T_0), and short-term (1 day; T_1) dark incubations. Long-term (60 days; T_{60}) dark incubations were also pursued for high tide samples in October 2014 and April 2015. Triplicate T0 samples were processed immediately, while triplicate T1 water containers were wrapped in black plastic and immediately returned to Doboy Sound for a 1-day (24 hours) incubation before processing. Samples were processed by filtering 3 L through 3 μm pore-size filters (Capsule Pleated Versapor Membrane filters; Pall Life Sciences) to remove eukaryotic cells, then through 0.2 μm pore-size filters (Supor polyethersulfone filter; Pall Life

Sciences) to collect bacterial cells. The 0.2 μm filters were placed in Whirl-Pak plastic bags and flash-frozen in liquid nitrogen for metatranscriptomic analysis, which was conducted on July and October samples (Vorobev *et al.*, 2018). Sample filtrates were collected for bulk DOC concentration, and optical (CDOM) and molecular (FT-ICR MS) composition analyses. Aliquots for DOC and CDOM analyses were collected and stored frozen (-20ºC) and refrigerated (4ºC), respectively. The remaining filtrates (2 L) were acidified to pH 2 (using HCl), and DOM was extracted with solid phase extraction (SPE) using styrene divinyl benzene polymer (Agilent Bond Elut PPL) as described in Letourneau and Medeiros (2019).

For the long-term incubations, 4 L water samples were immediately transported to the laboratory, where inorganic nutrients (20 μM Na_2PO_4 and 50 μM NH_4Cl) were added to the raw seawater to alleviate inorganic nutrient limitation on bacterial carbon processing. Samples were then filtered through pre-combusted (5 h at 450ºC) 2.7 μm pore size filters (GF/D; Whatman) before dark-incubating in triplicate for 60 days at 24ºC. After incubations were complete, samples were filtered through Pall Supor membrane filters (0.2 μm) and filtrates were collected for DOC, CDOM and FT-ICR MS analyses as described above.

2.2 Bulk DOC and Chromophoric DOM

Dissolved organic carbon concentrations from T_0, T_1, and T_{60} water samples and SPE-DOC extracts (dried and resuspended in ultrapure water) were measured using a Shimadzu TOC-L_{CPH} analyzer with potassium hydrogen phthalate as a standard. Milli-Q water blanks were tested before sample analysis and throughout instrument use. Accuracy and precision were tested against deep-sea reference material (Hansell, 2005) and were better than 5%. SPE extraction

efficiency across all samples (the SPE extract versus DOC concentration in the original sample) was 71% ± 4% of the DOC. Biodegradation of DOC (%) was determined as

$$\frac{DOC_{T_0} - DOC_{T_{end}}}{DOC_{T_0}} \times 100 \quad (1)$$

where DOC_{T0} is the concentration of DOC in the samples before incubations, and DOC_{Tend} is the concentration of DOC in samples after either 1-day or 60-day incubations.

Absorbance measurements of water samples for CDOM were taken at room temperature using an Agilent 8453 UV-visible spectrophotometer with a 1 cm quartz cuvette. Blank calibrations using Milli-Q water were performed prior to sample measurement to achieve a baseline background level. Absorbance was measured from wavelengths 190 to 1,100 nm and was converted to absorption coefficients as in D'Sa *et al.* (1999). The ratio of absorption coefficients at λ = 250 nm to λ = 365 nm ($a_g(250):a_g(365)$) was calculated for each sample. The CDOM absorption ratio is inversely correlated to DOM aromaticity and molecular weight (Peuravuori and Pihlaja, 1997). The spectral slope ($S_{275\text{-}295}$) was calculated between 275 nm and 295 nm as in Helms *et al.* (2008) and has been shown to be correlated negatively with terrigenous DOM (Fichot and Benner, 2012).

2.3 Molecular Analysis using FT-ICR MS

The molecular composition of DOM extracts (200 mg C L^{-1} in methanol) was analyzed using a 9.4 T Fourier transform ion cyclotron resonance mass spectrometer (FT-ICR MS) at the National High Magnetic Field Laboratory (NHMFL, Florida State University, Tallahassee, FL, USA) with electrospray ionization (ESI; negative mode). Samples were processed as described in Vorobev *et al.* (2018). Briefly, each *m/z* spectrum was internally calibrated with respect to an abundant homologous alkylation series whose members differ in mass by integer multiples of

14.01565 Da (mass of a CH_2 unit) confirmed by isotopic fine structure (Savory *et al.*, 2011), achieving a mass error of <0.5 ppm. Molecular formulae were assigned for masses in the range of 150 and 750 Da by applying the following restrictions: $^{12}C_{1\text{-}100}$ $^{1}H_{1\text{-}200}$ $O_{1\text{-}25}$ $^{14}N_{0\text{-}4}$ $S_{0\text{-}2}$, where the subscripts indicate the range in the number of atoms considered when assigning formulae. Molecular formulae assignment was performed by Kendrick mass defect analysis (Wu *et al.*, 2004) using PetroOrg software (Corilo, 2014) as in Letourneau and Medeiros (2019). Compounds with a signal-to-noise ratio smaller than 6 were discarded from the analysis to eliminate inter-sample variability based on peaks that were close to the detection limit. The peak intensity of each molecular formula was normalized by the sum peak intensities of the total identified peaks in each sample.

2.4 Microbial Analysis

Bioinformatic processing via differential gene expression (DGE) was performed using the DESeq2 package in R (Love *et al.*, 2014). Genes were mapped on marine microbial genomic databases (SILVA database, www.arb-silva.de) to identify taxa associated with gene expression. Separately, principal component (PC) analysis was performed using the normalized gene expression data from DEseq2 to capture patterns of variability in the microbial samples. A detailed description of the microbial data processing is presented in Vorobev *et al.* (2018).

2.5 Ancillary data

River discharge at the Altamaha River is routinely measured by the U.S. Geological Survey (USGS) at Doctortown, GA (available at http://waterdata.usgs.gov). Temperature and salinity time series at multiple locations in the estuary are available as part of the Georgia

Coastal Ecosystem Long Term Ecological Research (GCE-LTER) program (https://gce-lter.marsci.uga.edu). Long-term monitoring site GCE6 is located about 3 km from our sampling site **(Figure 2.1**).

3. Results

The estuary around Sapelo Island is characterized by strong seasonal variability. Peak Altamaha River discharge generally occurs in March and April, and discharge is reduced during summer and fall (Di Iorio and Castelao, 2013). From mid-2014 to early 2015, the Altamaha River discharge was close to the long-term average (**Figure 2.2**), with low discharge during the July and October 2014 sampling periods, and high discharge in April 2015. Consistent with that, the lowest salinity at the sampling site was observed in April 2015 (Table 1). Salinity in July 2014 was the highest, with October 2014 being characterized by intermediate values. For each season, salinity at low tide was 1-3 psu lower than during high tide (**Table 2.1**).

3.1 Patterns of DOC and CDOM Variability

Concentrations of DOC for T0 samples were variable between different seasons and tidal conditions. During the sampling period, DOC ranged from 194 to 337 μM, with larger values for each season observed at low tide, which is consistent with observations from other systems (e.g., Tzortziou *et al.*, 2008; Osterholz *et al.*, 2018). During July and October, mean high tide DOC concentrations were not significantly different from one another (t-test, p=0.18). In April, when river discharge was high, mean DOC concentration was significantly different (1.5 times higher) from both previous seasons (for both, t-test, p<0.01). During low tide, each season's DOC concentration was significantly different from one another (ANOVA, F=174.6, df=2,8, p<0.01),

with July having the lowest DOC concentration, followed by October and then April (**Table 2.1**). Seasonal differences in DOC have been observed in previous studies of the region, where DOC concentrations tend to peak in spring as compared to summer and fall (e.g., Medeiros *et al.*, 2017a; Letourneau and Medeiros, 2019).

Differences in DOM composition between seasons were quantified by analyzing optical properties (**Table 2.1**). At both high and low tides, the observed absorption ratio at λ = 250 nm to λ = 365 nm was smaller in April than July or October, though all months were significantly different from one another (ANOVA, high tide: F=14.5, df=2,5, p=0.02; low tide: F=504, df=2,8, p<0.05). Decreased values for absorption ratios indicate a shift toward more aromatic structures (Peuravuori and Pihlaja, 1997), which is a typical characteristic of terrigenous DOM (Sleighter and Hatcher, 2008; Medeiros *et al.*, 2015b). Spectral slope coefficients in April were also reduced compared to July and October, which is consistent with increased terrigenous content during spring. No differences in the mean absorption ratio were observed between samples collected at high or low tides for July and October (t-test, p>0.05), while for April the difference in the ratio for high and low tide was marginally significant (t-test, p=0.047). $S_{275\text{-}295}$ were not significantly different for samples collected at high and low tide in all seasons (t-test, p>0.05).

Biodegradation over a short time scale (1-day long incubation) resulted in only small and non-significant changes in DOC concentrations. Long-term dark incubations (60 days; T60) performed on high tide samples revealed larger changes, however. The percent of DOC biodegraded was slightly higher in October (11.7%) than in April (9.0%). The absorption ratio ($a_g(250):a_g(365)$) decreased in most incubations (**Table 2.1**), indicating a shift toward more aromatic structures in the remaining DOM pools.

3.2 Drivers of DOM Composition Variability

DOM composition was investigated at the molecular level using FT-ICR MS analysis. Over 5,000 molecular formulae were assigned for triplicate samples over three seasons. The vast majority of the molecular formulae identified were observed in all seasons. Considering all replicates, there were only 36, 10 and 8 formulae that were observed exclusively in July, October and April, respectively. There were 157 formulae that were observed in October and April but not in July, however. These formulae were characterized by small H/C and especially O/C ratios (H/C = 1.02 ± 0.31, O/C = 0.29 ± 0.17), suggesting that some of the most aromatic compounds may have been missing from samples collected during summer.

To decipher environmental drivers of DOM variability using FT-ICR MS, DOM composition for pre- and post-incubation (1 day) samples collected in different seasons and tidal conditions were decomposed into principal components (Bro and Smilde, 2014). Analyses were run in Matlab using all replicates simultaneously after normalization by the standard deviation between samples and mean centering (**Figure 2.3**). Only modes that were statistically significant (95% confidence level) are shown (Overland and Preisendorfer, 1982). Plots of PC scores are related to van Krevelen diagrams of the loadings; for a given sample, where the score of a PC is positive, DOM is relatively enriched with compounds associated with molecular formulae whose loadings for that PC are positive and relatively depleted with those whose loadings are negative.

The dominant PC (PC 1) accounted for 28% of the total variance in DOM composition in Doboy Sound during the sampling period and separated samples according to sample month. The analysis showed samples from months with lower salinities (**Table 2.1**) tending toward higher PC 1 scores (**Figure 2.3A**). Analysis of a van Krevelen diagram of the loading of PC 1 showed a tendency for high positive loadings to cluster at low H/C ratios, and low negative loadings to

cluster at high H/C ratios (**Figure 2.3B**). This is similar to the pattern observed in river-to-ocean transects (Medeiros *et al.*, 2015b), as the terrigenous vs. marine gradient of DOM sources in the system has previously been defined (Medeiros *et al.*, 2015a), and terrigenous DOM is known to be enriched with molecular formulae with low H/C ratios (Sleighter and Hatcher, 2008). Thus, DOM samples were enriched with compounds with more terrigenous characteristics in April and shifted toward having a more marine character during July. This corroborates previous studies in this region that found that DOM has a more terrigenous character during spring than summer and fall (e.g., Letourneau and Medeiros, 2019), and suggests that the most important pattern of DOM variability in the estuary occurs at seasonal scales, likely associated with variations in river discharge (**Figure 2.2**).

Within the same analysis, high and low tide samples from each season were separated along PC 2 (**Figure 2.3A**), which represented 10% of the total variance in DOM composition for the samples. This suggests the secondary mode of variance in DOM composition is influenced by tidal variability. High tide samples were relatively enriched with compounds found near the center of the van Krevelen diagram (shown in blue in **Figure 2.3C**), while low tide samples for all seasons were comparatively enriched with compounds near the periphery of the diagram (shown in red in **Figure 2.3C**). A separate plot (not shown), which contours the molecular mass of each formula as a function of its O/C and H/C ratios in van Krevelen space, indicates that compounds near the center of the diagram are generally characterized by higher molecular mass. Indeed, comparing the loading of PC 2 with the molecular mass of the respective compounds indicates that molecular formulae relatively enriched during low tide (~8% of all formulae) were characterized by low molecular mass (< ~300 Da), while formulae relatively enriched during high tide (~12% of all formulae) were characterized by high molecular mass (> ~400 Da)

(**Figure 2.4**). Although low tide samples were enriched with formulae found at the lower sector of the diagram (low H/C ratios; 3.9% of all formulae), which are characterized by high aromaticity (Koch and Dittmar, 2006; 2016), they were also enriched with formulae with high H/C ratios (4.1% of all formulae), which are less aromatic (**Figure 2.3C**). This suggests that the overall aromaticity of the DOM may not have been strongly affected by tides. This could help explain the results described earlier based on the optical data, which showed that low and high tide samples were not significantly different with respect to the absorption ratio at $\lambda = 250$ nm to $\lambda = 365$ nm and to $S_{275\text{-}295}$ (**Table 2.1**), which are related to DOM aromaticity (Peuravuori and Pihlaja, 1997) and to the terrigenous content of the DOM (Fichot and Benner, 2012), respectively.

In all cases including different seasons and tidal conditions, the impact of short-time scale biodegradation on DOM composition was comparatively small. No significant differences were observed between the PC scores for samples within a given month and tidal phase before and after the 1-day incubations (**Figure 2.3A**). Collectively, the analyses revealed that the dominant factor controlling DOM composition during the study period varied at seasonal scale. That was followed by tidal variability, with microbial degradation over short time scales having a smaller effect.

3.3 Drivers of change in gene expression

Changes in DOM chemical composition are difficult to measure on short time scales because the highly labile compounds make up a small proportion of total DOM at any one time (Hansell, 2013; Moran *et al.*, 2016). Further, methods for concentrating DOM are not efficient at capturing low molecular weight (LMW) and polar compounds, typically important components

of the most labile DOM (Kujawinski, 2011). Instead, we used differences in gene expression by microbial taxa as a proxy for chemical differences in DOM composition over the 1-day incubations (Vorobev *et al.*, 2018). Homology searches of metatranscriptomic reads against marine microbial genomic data allowed expression of individual genes to be associated with their taxonomic origin.

Vorobev *et al.* (2018) used metatranscriptome and FT-ICR MS analyses together to characterize components of labile DOM in these samples. Here, given that gene expression data are only available for July and October 2014, we repeated the analysis of DOM composition using only samples collected in those months (**Figure 2.5A**), which yielded results consistent with those described before. Despite the fact that the chemical (FT-ICR MS) and microbiological (functional assignments of transcripts) assessments largely tracked different components of the DOM pool, we noted that the important scales over which changes occurred coincided. The largest differences in both cases were observed between seasons and then for different tidal phases, with short-term incubations having a comparatively smaller effect (**Figure 2.5A,B**). Yet, analysis of specific gene functions differentiated shifts in microbial uptake and metabolism after the 1-day incubation (Vorobev *et al.*, 2018). Within the 50 highest transcript-recruiting reference genomes, July had statistically elevated transcript abundance of Actinobacteria (p=0.01), Nitrosomondales (p=0.04), Rhodospiralles (p<0.05), SAR 11 (p=0.02), and SAR 86 (p=0.03) as compared to October, while in October the Archaea taxon Euryarchaeota (p<0.05) was the greatest contributor to metatranscriptomes (**Figure 2.6**). Following the pattern of DOM driver importance, tides secondarily impacted taxon-based gene expression patterns. Specifically, we observed small variations in the taxa contributing most to gene expression for different tidal stages within a season. While no differences in transcript production by taxon was observed

between tides during October, in July the Verrucomicrobia population for T0 samples increased during low tides (p<0.05) (**Figure 2.6**). Kara and Shade (2009) reported that over a time scale of a few days (74 h), the microbial community composition near Doboy Sound was most impacted by tides, which is consistent with our observations that once seasonality is removed, the influence of tides becomes more evident.

3.4 *DOM Compositional Variability on Long Timescales*

In the absence of highly labile compounds, microbial transformation is constrained to the components of DOM that are more recalcitrant and less energetically favorable to metabolize. Over time, these slower microbial transformations of DOM accumulate and can typically be observed after several weeks (e.g., Medeiros *et al.*, 2017b; Logozzo *et al.*, 2021). To observe effects of long-term biodegradation on DOM and quantify the relative importance in comparison to other processes, analyses were repeated including the samples collected at the end of the 60-day long incubations (T60). Given the constraints imposed by the PC analyses, however, it is difficult to interpret transformations associated with tidal variability and long-term biodegradation considering all samples together, since additional modes of variability must be orthogonal to the dominant mode associated with seasonal variability. This often results in variability associated with processes of secondary importance being split into more than one mode (Medeiros *et al.*, 2017b). Thus, we chose to remove the influence of seasonal variability by repeating the analysis separately for each season. This allowed us to assess the relative contributions of tidal variability versus long-term biodegradation to changes in DOM composition in each season.

During October 2014, the dominant PC separated the high tide T60 samples from both T0 and T1 collected during high or low tide, indicating that the change in DOM composition due to the long-term degradation was larger than the differences in DOM composition observed between different tidal phases (**Figure 2.7A**). Conversely, during April 2015 the high tide T0-T60 samples represented a smaller difference in DOM composition compared to the difference found between high tide and low tide T0 samples (**Figure 2.7B**). Thus, the change in DOM composition due to long-term incubations was larger than due to tidal variability in October, but the opposite was true in April. We note that the salinity difference between high and low tide conditions at an oceanographic mooring located ~3 km from our sampling location was significantly higher in April 2015 than in October 2014, and the average salinity was lower in spring (**Figure 2.8**). This is consistent with river discharge data and indicates that more freshwater was present in the system in April (**Table 2.1**).

4. Discussion

Dissolved organic matter composition and transformation play an important role in a variety of processes in estuaries, including nutrient availability, bacterial production, and carbon export to the coastal ocean (Hedges *et al.*, 1997; Aitkenhead-Peterson *et al.*, 2003; Crump *et al.*, 2009; Moran *et al.*, 2016; Medeiros *et al.*, 2017a). Several processes are known to influence DOM composition in estuarine settings at various spatial and temporal scales. Here, we assess the relative importance of seasonality, tides and microbial processing on variations in DOM composition in the estuary around Sapelo Island, off the Southeastern U.S. Our analyses revealed that the primary mode of variability in DOM composition in Doboy Sound occurs at the seasonal scale and is associated with the terrigenous content of the DOM. This is consistent with previous

studies that have shown that the seasonal delivery of freshwater to the system plays an important role controlling DOM composition in the estuary (Medeiros *et al.*, 2015a). Given that our samples were collected during 3 instances in the year, we cannot compute correlations between DOM composition and environmental drivers such as river discharge. However, Letourneau and Medeiros (2019) analyzed monthly time series of DOM composition at the mouth of the Altamaha River to show that the terrigenous signature of the DOM delivered to the estuary is highly correlated with river discharge when river flow is higher than 150 $m^3 s^{-1}$, while for low discharge conditions the signature of marsh-derived inputs can be observed. Letourneau and Medeiros (2019) samples were all collected in high tide conditions, however, so they were not able to assess the relative importance of seasonal variability associated with riverine inputs and variability at semi-diurnal scales associated with tides, which has been shown to be of critical importance in other estuaries (e.g., Tzortziou *et al.*, 2008; Cao and Tzortziou, 2021). By analyzing samples from different seasons collected twice on each tidal cycle, we were able to expand on Letourneau and Medeiros (2019) analyses by directly comparing the relative importance of riverine inputs and tidal stage.

Although seasonal variability likely due to riverine inputs is dominant, the analyses also revealed significant increases in DOC during low tide conditions, which is consistent with results of Tzortziou *et al.* (2008) for Chesapeake Bay. Optical analyses (absorption ratio at λ = 250 nm to λ = 365 nm; spectral slope: $S_{275\text{-}295}$) revealed no significant differences in DOM composition between high and low tide conditions, however. This is surprising, considering that Tzortziou *et al.* (2008) reported strong tidal modulation in optical properties in Chesapeake Bay, with a clear signature of marsh-exported CDOM during low tide. Given that our samples were collected in a relatively wide (~220 m) channel close to the main channel of Doboy Sound (which is itself 1.6

km wide and 10 m deep), relatively far from narrow and shallow tidal creeks (see **Figure 2.1** for sampling location), it is possible that the influence of marsh-derived DOM introduced at low tide was diluted at our study site, resulting in a smaller difference in DOM composition between high and low tide conditions. The chemical analyses at the molecular level revealed that DOM at high and low tide conditions have distinct compositions, though. During low tide, DOM in all seasons was relatively enriched with highly aromatic compounds (Koch and Dittmar, 2006; 2016), which is consistent with the observations from Chesapeake Bay (Tzortziou *et al.*, 2008). However, DOM during low tide was also relatively enriched with aliphatic compounds characterized by high H/C ratios (Seidel *et al.*, 2014). Thus, the overall aromaticity of the added DOM may not be much different than the original signature, which could contribute to the optical signatures reflecting the average aromaticity of the DOM (Peuravuori and Pihlaja, 1997) not being significantly different between low and high tide. We were not able to quantify the specific contribution of the input of the aromatic or aliphatic compounds to the optical signature of each sample since that would depend on the change in concentration and in the extinction coefficient of each compound, none of which are known.

We were also able to identify the relative contribution of microbial degradation to DOM compositional changes, which showed that on short time scales transformations due to microbial activity were small when compared to variations associated with seasonal or tidal variability. This is likely affected by the low inventory of biologically labile compounds maintained in seawater combined with the poor capture efficiency of LMW molecules by solid-phase extraction methods (Kujawinski, 2011; Moran *et al.*, 2016). Short-term incubations were done with whole seawater to mimic *in situ* conditions as close as possible, and thus included a full range of trophic levels including bacterial grazers. The bacterial cell number decreased by ~20%

during the incubation; however, numbers were between 1.3 and 2.4 million cells per milliliter, and therefore were sufficient in number to assimilate available DOM.

Collectively, this analysis provided an assessment of the relative importance of these three processes in modifying DOM composition during the study period. The metatranscriptomics data largely mirrored these results, with tidal scale being of secondary importance relative to seasonal scale. As was the case for DOM composition, short-term incubations were found to have a smaller effect on variability in the microbial data. It is likely that both DOM chemical composition and the microbial response to DOM composition primarily followed terrestrial versus marine water mass budgets in the estuary (e.g., higher influence of freshwater in April during peak river discharge; high influence of oceanic water during high tide for each season) as has been observed in the Delaware Estuary (Osterholz *et al.*, 2018).

Although short-term biodegradation was found to have a comparatively small effect on DOM composition, our analyses indicate that over longer time scales microbial activity significantly altered the DOM chemistry. Indeed, while DOM composition changes in the 1-day incubations reported here have been previously shown to be consistent with microbial cleavage of functional groups from semi-polar compounds (Vorobev *et al.*, 2018), changes over longer time scales are consistent with progressive transformation of functional groups of intermediates in degradation pathways, resulting in larger net changes in DOM composition (Medeiros *et al.*, 2017b). Our analyses indicate that over these longer scales, microbial biodegradation can produce DOM composition differences comparable to that observed in response to tides, previously recognized to be important (e.g., Tzortziou *et al.*, 2008; Cao *et al.*, 2018; Cao and Tzortziou, 2021). Thus, if estuarine residence time is large in comparison to the time scale of biodegradation, microbial activity can exert a first-order effect on DOM composition. Here,

estuarine water was incubated for 60 days, which is longer than the residence time in the system (Wang *et al.*, 2017). However, Medeiros *et al.* (2017b) pursued dark incubations of Doboy Sound water for different durations and identified molecular formulae whose relative abundances were enriched or depleted during the incubations. They showed that the difference in the average mass of these formulae was similar for incubations lasting 35 and 70 days. This suggests that significant changes in DOM composition occur on times scales of 1 month. Logozzo *et al.* (2021) used dark incubations of Chesapeake Bay water to show that significant changes in DOC concentration and DOM composition due to microbial activity can occur on time scales of 2 weeks. Microbial activity can therefore play an important role controlling DOM dynamics in at least some areas of the estuary. Residence time at the Altamaha River averages only a few days (Sheldon and Alber, 2002) but can reach several weeks in many parts of the estuary (Wang *et al.*, 2017). For example, DOM composition was significantly enriched in terrigenous molecules 30 days after the passage of Hurricane Irma in 2017, indicating a residence time of at least 1 month for organic material introduced during the passage of the storm (Letourneau *et al.*, 2021) and sufficient time for microbial transformation before export to the coastal ocean.

The relative importance of tidal variability versus long-term incubation differed between October 2014 and April 2015. While tidal variability drove larger DOM changes than did long-term biodegradation in spring, the opposite was true in the fall. This may be related to seasonal differences in DOM lability, which has often been linked to DOM source (Obernosterer and Benner, 2004), including for this system (e.g., Medeiros *et al.*, 2017b). More labile components of the DOM may have been available to microbes in October 2014 than in April 2015, resulting in larger DOM transformation. Indeed, we observed slightly more DOC long-term degradation in October (11.7%) than in April (9.0%) (**Table 2.1**). Alternatively, the high and low tide difference

in DOM composition in April 2015 could be related to a greater freshwater content in the estuary during that time. Time series data of salinity at the main channel of Doboy Sound (see **Figure 2.1** for location), ~3 km from our sampling site, indicated that the salinity difference between high and low tide conditions in October 2014 was about 2 psu, but in April 2015 that difference was about 6 psu (**Figure 2.8**). Thus, it is possible that the comparatively larger importance of tidal variability in April 2015 was simply because a stronger gradient in freshwater content (and presumably in DOM composition) was advected back and forth by tidal currents across our sampling location. This also highlights an important aspect of the influence of tides on DOM composition in estuaries. Although in some cases variability may be associated with an input of organic matter, such as from salt marshes (Tzortziou *et al.*, 2008), representing an actual alteration of DOM composition, other tidally-linked changes in DOM composition at a given site may be due to a gradient of dissolved organic matter advected back and forth across the site.

We note that our analyses cannot fully resolve seasonal variability, given that samples were collected in three different months in a single 12-month period. As such, variability at different scales (e.g., interannual) may have been aliased into the seasonal component of variability extracted by our analyses. Our results for different months are consistent with those reported by Letourneau and Medeiros (2019), however, suggesting that a similar pattern of variability is observed in different years. Similarly, because of sampling constraints, only 2 samples (with triplicates) were collected to represent tidal differences in each season, one at high and another at low tide. Although this does not allow for tidal variability to be fully resolved or for correlations with sea level height to be computed, the fact that results were quantitatively similar for all seasons (i.e., shift in second principal component for low tide samples was similar for all months; **Figure 2.3**) suggests that the change in composition reported here is robust and

repeatable for different tidal cycles. Our analyses indicate that short-term transformations due to biodegradation are small compared to other drivers for the fraction of the DOM captured by our analysis, which excludes LMW compounds known to be highly labile (Kujawinski, 2011) as well as classes of compounds often targeted by microorganisms (e.g., polysaccharides, Rich *et al.*, 1996). Thus, the true importance of biodegradation changing DOM composition in estuaries over short-time scales may be underestimated by our analyses. Lastly, we focused on only a few factors that could be affecting DOM composition in estuaries, representing a first step toward assessing their relative importance. Future studies attempting to isolate and quantify the relative importance of other drivers, such as photochemistry, flocculation, and inputs associated with phytoplankton and zooplankton activity (Hedges, 1992), will advance our understanding of DOM dynamics in complex coastal environments.

Assessing the contribution of different drivers to DOM composition in estuaries is critically important to understand future changes in these systems. The atmospheric supply of water vapor to the Southeastern U.S. is predicted to be modestly reduced in the future (Seager *et al.*, 2009), and the frequency of low Altamaha River discharge conditions has shown signs of increasing in recent decades (e.g., Medeiros *et al.*, 2015a). Given that change in DOM composition at seasonal scales, likely associated with river discharge, is the most important mode of variability in the system, predicted changes in the hydroclimate can be accompanied by changes in DOM composition. Future changes in river discharge (and other factors driving local circulation, such as wind forcing) will likely also affect estuarine residence time (Sheldon and Alber, 2002; Wang *et al.*, 2017) and therefore the time available for microbial activity to modify the DOM before export to the coastal ocean. Lastly, understanding the relative contributions of the various processes investigated here is important to highlight the likely factors explaining

spatial and/or temporal differences in DOM composition in estuarine regions, and to set the context for observed differences in DOM composition between different systems.

References

Aitkenhead-Peterson, J.A., McDowell, W.H., and Neff, J.C. (2003). "Sources, Production, and Regulation of Allochthonous Dissolved Organic Matter Inputs to Surface Waters." In Aquatic Ecosystems (Cambridge, MA: Elsevier), p. 25-70.

Amon, R. M. W. and R. Benner (1996). Bacterial utilization of different size classes of dissolved organic matter. Limnol. Oceanogr., 41(1), 41-51. doi: 10.4319/lo.1996.41.1.0041

Bauer J., Cai, W.J., Raymond, P., Bianchi, T.S., Hopkinson, C.S., and Regnier, P.A.G. (2013). The changing carbon cycle of the coastal ocean. Nature. 504, 61-70. doi: 10.1038/nature12857

Bianchi, T.S. (2006). "Organic Matter Cycling," in Biogeochemistry of Estuaries. (New York, NY: Oxford University Press), p. 177-221.

Bro, R., and Smilde, A. (2014). Principal component analysis. Anal. Methods. 6, 2812-2831.

Canuel, E.A., and Hardison, A.K. (2016). Sources, ages, and alteration of organic matter in estuaries. Ann. Rev. Mar. Sci. 8, 409-434. doi:10.1146/annurev-marine-122414-034058

Cao, F., Tzortziou, M., Hu, C., Mannino, A., Fichot, C.G., Del Vecchio, R., Najjar, R.G., and Novak, M. (2018). Remote sensing retrievals of colored dissolved organic matter and dissolved organic carbon dynamics in North American estuaries and their margins. Remote Sens. Environ. 205, 151-165. doi: 10.1016/j.rse.2017.11.014

Cao, F., and Tzortziou, M. (2021). Capturing dissolved organic carbon dynamics with Landsat-8 and Sentinel-2 in tidally influenced wetland–estuarine systems. Sci. Total Environ. 777, 145910. doi: 10.1016/j.scitotenv.2021.145910

Corilo, Y.E. (2014). PetroOrg software. Florida State University. All rights reserved. (https://nationalmaglab.org/user-facilities/icr/icr-software).

Crump, B.C., Peterson, B.J., Raymond, P.A., Amon, R.M.W., Rinehart, A., McClelland, J.W., and Holmes, R.M. (2009). Circumpolar synchrony in big river bacterioplankton. Proc. Natl. Acad. Sci. U.S.A. 106, 21208-21212. doi: 10.1073/pnas.0906149106

Di Iorio, D., and Castelao, R.M. (2013). The dynamical response of salinity to freshwater discharge and wind forcing in adjacent estuaries on the Georgia coast. Oceanography. 26, 44-51. doi: 10.5670/oceanog.2013.44

D'Sa, E.J., Steward, R.G., Vodacek, A., Blough, N. V., and Phinney, D. (1999). Determining optical absorption of colored dissolved organic matter in seawater with a liquid capillary waveguide. Limnol. Oceanogr. 44, 1142-1148. doi: 10.4319/ lo.1999.44.4.1142

Fichot, C. G. and Benner, R. (2012). The spectral slope coefficient of chromophoric dissolved organic matter (S275–295) as a tracer of terrigenous dissolved organic carbon in river-influenced ocean margins. Limnol. Oceanogr., 57(5), 1453-1466. doi:

10.4319/lo.2012.57.5.1453

Gifford, S.M., Sharma, S., Rinta-Kanto, J.M., and Moran, M.A. (2011). Quantitative analysis of a deeply sequenced marine microbial metatranscriptome. ISME J. 5, 461-472.

Gifford, S.M., Sharma, S., Booth, M., and Moran, M.A. (2013). Expression patterns reveal niche diversification in a marine microbial assemblage. ISME J. 7, 281-298.

Hansell, D.A. (2005). Dissolved organic carbon reference material program. Eos. 86:35, 318-318. doi: 10.1029/2005EO350003

Hansell, D.A., Carlson, C.A., Repeta, D.J., and Schlitzer, R. (2009). Dissolved organic matter in the ocean: A controversy stimulates new insights. Oceanography. 22, 202-211. doi: 10.5670/oceanog.2009.109

Hansell, D. A. (2013). Recalcitrant Dissolved Organic Carbon Fractions, Annu. Rev. Mar. Sci., 5(1), 421-445. doi: 10.1146/annurev-marine-120710-100757

Hedges, J. I. (1992). Global biogeochemical cycles: progress and problems. Mar. Chem., 39(1), 67-93. doi: 10.1016/0304-4203(92)90096-S

Hedges, J. I., Keil, R. G. and Benner, R. (1997). What happens to terrestrial organic matter in the ocean?. Org. Geochem., 27(5), 195-212. doi: 10.1016/S0146-6380(97)00066-1

Helms, J.R., Stubbins, A., Ritchie, J.D., Minor, E.C., Kieber, D.J., and Mopper, K. (2008). Absorption spectral slopes and slope ratios as indicators of molecular weight, source, and photobleaching of chromophoric dissolved organic matter. Limnol. Oceanogr. 53, 955-969.

Hernes, P. J. and R. Benner (2003). Photochemical and microbial degradation of dissolved lignin phenols: Implications for the fate of terrigenous dissolved organic matter in marine environments, J. Geophys. Res., 108. doi: 10.1029/2002JC001421

Hollibaugh, J., Gifford, S., Sharma, S., Bano, N. and Moran, M.A. (2011). Metatranscriptomic analysis of ammonia-oxidizing organisms in an estuarine bacterioplankton assemblage. ISME J. 5, 866-878. doi: 10.1038/ismej.2010.172

Hollibaugh, J., Gifford, S., Moran, M.A., Ross, M.J., Sharma, S., and Tolar, B.B. (2013). Seasonal variation in the metratranscriptomes of a Thaumarchaeota population from SE USA coastal waters. ISME J. 8, 685-698. doi: 10.1038/ismej.2013.171

Kara, E., and Shade, A. (2009). Temporal dynamics of south end tidal creek (Sapelo Island, Georgia) bacterial communities. Appl. Environ. Microbiol. 75, 1058-1064.

Kieber, R. J., Zhou, X., and Mopper, K. (1990). Formation of carbonyl compounds from UV-induced photodegradation of humic substances in natural waters: Fate of riverine carbon in the sea, Limnol. Oceanogr., 35(7), 1503-1515.

Kim, S., Kramer, R. W., and Hatcher, P. G. (2003). Graphical Method for Analysis of Ultrahigh-

Resolution Broadband Mass Spectra of Natural Organic Matter, the Van Krevelen Diagram, Anal. Chem., 75(20), 5336-5344. doi: 10.1021/ac034415p

Koch, B.P., and Dittmar, T. (2006). From mass to structure: an aromaticity index for high-resolution mass data of natural organic matter. Rapid Commun. Mass Spectrom., 20, 926-932. doi: 10.1002/rcm.2386

Koch, B.P., and Dittmar, T. (2016). From mass to structure: an aromaticity index for high-resolution mass data of natural organic matter. Rapid Commun. Mass Spectrom., 30, 250. doi: 10.1002/rcm.7433.

Kujawinski, E.B. (2011). The impact of microbial metabolism on marine dissolved organic matter. Ann. Rev. Mar. Sci. 3, 567-599. doi: 10.1146/annurev-marine-120308-081003

Letourneau, M. L. and Medeiros, P. M. (2019). Dissolved Organic Matter Composition in a Marsh-Dominated Estuary: Response to Seasonal Forcing and to the Passage of a Hurricane, J. Geophys. Res. Biogeosci., 124(6), 1545-1559. doi: 10.1029/2018JG004982

Letourneau, M. L., Schaefer, S. C., Chen, H., McKenna, A. M., Alber, M., and Medeiros, P. M. (2021). Spatio-temporal changes in dissolved organic matter composition along the salinity gradient of a marsh-influenced estuarine complex, Limnol. Oceanogr., 66(8), 3040-3054. doi: 10.1002/lno.11857

Logozzo, L., Tzortziou, M., Neale, P., and Clark, J.B. (2021). Photochemical and microbial degradation of chromophoric dissolved organic matter exported from tidal marshes, J. Geophys. Res.-Biogeosci., 126. doi:10.1029/2020JG005744

Love, M.I., Huber, W. and Anders, S. (2014). Moderated estimation of fold change and dispersion for RNA-seq data with DESeq2. Genome Biol. 15, 550. doi: 10.1186/s13059-014-0550-8

Medeiros, P.M., Seidel, M., Dittmar, T., Whitman, W.B., and Moran, M.A. (2015a). Drought-induced variability in dissolved organic matter composition in a marsh-dominated estuary. Geophys. Res. Lett. 42, 6446-6453. doi:10.1002/ 2015GL064653

Medeiros, P. M., Seidel, M., Ward, N. D., Carpenter, E. J., Gomes, H. R., Niggemann, J., Krusche, A. V., Richey, J. E., Yager, P. L. and Dittmar, T. (2015b). Fate of the Amazon River dissolved organic matter in the tropical Atlantic Ocean. Global Biogeochem. Cycles, 29(5), 677-690. doi: 10.1002/2015GB005115

Medeiros, P.M., Babcock-Adams, L., Seidel, M., Castelao, R.M., Di Iorio, D., Hollibaugh, J. T., *et al.* (2017a). Export of terrigenous dissolved organic matter in a broad continental shelf. Limnol. Oceanogr. 62, 1718-1731. doi: 10.1002/lno.10528

Medeiros, P.M., Seidel, M., Gifford, S.M., Ballantyne, F., Dittmar, T., Whitman, W. B., *et al.* (2017b). Microbially-mediated transformations of estuarine dissolved organic matter. Front. Mar. Sci. 4. doi:10.3389/fmars.2017.00069

Meyer, J. L., Edwards, R. T., and Risley, R. (1987). Bacterial growth on dissolved organic carbon from a blackwater river, Microb. Ecol., 13(1), 13-29. doi: 10.1007/BF02014960

Miller, W.L., and Moran, M.A. (1997). Interaction of photochemical and microbial processes in the degradation of refractory dissolved organic matter from a coastal marine environment. Limnol. Oceanogr. 42, 1317-1324. doi: 10.4319/lo.1997.42.6.1317

Moran, M. A. and Hodson, R. E. (1989). Formation and bacterial utilization of dissolved organic carbon derived from detrital lignocellulose, Limnol. Oceanogr., 34(6), 1034-1047.

Moran, M. A. and Hodson, R. E. (1994). Dissolved humic substances of vascular plant origin in a coastal marine environment, Limnol. Oceanogr., 39(4), 762-771.

Moran, M. A., Sheldon, W. M., and Sheldon, J. E. (1999). Biodegradation of riverine dissolved organic carbon in five estuaries of the southeastern United States, Estuaries, 22, 55-64.

Moran M.A, Kujawinski E.B., Stubbins A., Fatland R., Aluwihare L.I., Buchan A., *et al.* (2016). Deciphering ocean carbon in a changing world. Proc. Natl. Acad. Sci. U.S.A. 113, 3143-3151. doi: 10.1073/pnas.1514645113

Noriega, C., and Araujo, M. (2014). Carbon dioxide emissions from estuaries of northern and northeastern Brazil. Sci. Rep. 4, 6164. doi: 10.1038/srep06164

Obernosterer, I., and Benner, R. (2004). Competition between biological and photochemical processes in the mineralization of dissolved organic carbon. Limnol. Oceanogr. 49, 117-124.

Osburn, C.L., Atar, J.N., Boyd, T.J., and Montgomery, M.T. (2019). Antecedent precipitation influences the bacterial processing of terrestrial dissolved organic matter in a North Carolina estuary. Estuar. Coast. Shelf Sci. 221, 119-131. doi: 10.1016/j.ecss.2019.03.016

Osterholz, H., Singer, G., Wemheuer, B., Daniel, R., Simon, M., Niggemann, J., *et al.* (2016a). Deciphering associations between dissolved organic molecules and bacterial communities in a pelagic marine system. ISME J. 10, 1717-1730. doi: 10.1038/ismej.2015.231

Osterholz, H., Kirchman, D. L., Niggemann, J., and Dittmar, T. (2018). Diversity of bacterial communities and dissolved organic matter in a temperate estuary. FEMS Microbiol. Ecol. 94:8. doi: 10.1093/femsec/fiy119

Overland, J. E. and Preisendorfer, R. W. (1982). A Significance Test for Principal Components Applied to a Cyclone Climatology. Mon. Weather Rev., 110(1), 1-4. doi: 10.1175/1520-0493(1982)110

Peuravuori, J., and Pihlaja, K. (1997). Molecular size distribution and spectroscopic properties of aquatic humic substances. Anal. Chim. Acta. 337, 133-149. doi: 10.1016/s0003-2670(96)00412-6

Poretsky, R.S., Bano, N., Buchan, A., LeCleir, G. Kleikemper, J., Pickering, M., *et al.* (2005).

Analysis of microbial gene transcripts in environmental samples. Appl. Environ. Microbiol. 71, 7. doi: 10.1128/AEM.71.7.4121-4126.2005

Poretsky, R.S., Sun, S., Mou, X., and Moran, M.A. (2010). Transporter genes expressed by coastal bacterioplankton in response to dissolved organic carbon. Environ. Microbiol. 12, 616-627. doi: 10.1111/j.1462-2920.2009.02102.x

Rich, J., Ducklow, H., and Kirchman, D.L. (1996). Concentrations and uptake of neutral monosaccharides along 14°W in the equatorial Pacific: Contribution of glucose to heterotrophic bacterial activity and the DOM flux. Limnol. Oceanogr. 41, 595-604.

Savory, J.J., Kaiser, N.K., McKenna, A.M., Xian, F., Blakney, G.T., Rodgers, R.P., Hendrickson, C.L., and Marshall, A.G. (2011). Parts-per-billion Fourier transform ion cyclotron resonance mass measurement accuracy with a "walking" calibration equation. Anal. Chem. 83, 1732-1736, doi: 10.1021/ac102943z

Schaefer, S.C., and Alber, M. (2007). Temperature controls a latitudinal gradient in the proportion of watershed nitrogen exported to coastal ecosystems. Biogeochemistry. 85, 333-346.

Seager, R., Tzanova, A., and Nakamura, J. (2009). Drought in the southeastern United States: causes, variability over the last millennium, and the potential for future hydroclimate change. J. Clim. 22, 5021-5045. doi: 10.1175/2009jcli2683.1

Seidel, M., Beck, M., Riedel, T., Waska, H., Suryaputra, I. G. N. A., Schnetger, B., *et al.* (2014). Biogeochemistry of dissolved organic matter in an anoxic intertidal creek bank. Geochim. Cosmochim. Acta. 140, 418-434. doi: 10.1016/j.gca.2014.05.038

Sheldon, J.E., and Alber, M. (2002). A comparison of residence time calculations using simple compartment models of the Altamaha River estuary, Georgia. Estuar. Coast. 25, 1304-1317. doi: 10.1007 /bf02692226

Sholkovitz, E.R. (1976). Flocculation of dissolved organic and inorganic matter during the mixing of river water and seawater. Geochim. Cosmochim. Acta. 4, 831-845.

Sleighter, R.L., and Hatcher, P.G. (2008). Molecular characterization of dissolved organic matter (DOM) along a river to ocean transect of the lower Chesapeake Bay by ultrahigh resolution electrospray ionization Fourier transform ion cyclotron resonance mass spectrometry. Mar. Chem. 110, 140-152. doi: 10.1016/j.marchem.2008.04.008

Tzortziou, M., Neale, P.J., Osburn, C.L., Megonigal, J. P., Maie, N., and Jaffe, R. (2008). Tidal marshes as a source of optically and chemically distinctive colored dissolved organic matter in the Chesapeake Bay. Limnol. Oceanogr. 53, 148-159.

Vorobev, A., S. Sharma, M. Yu, J. Lee, B. J. Washington, W. B. Whitman, F. Ballantyne IV, P. M. Medeiros, and M. A. Moran (2018). Identifying labile DOM components in a coastal ocean through depleted bacterial transcripts and chemical signals, Environ. Microbiol., 20(8), 3012-3030.

Walther, J.V. (2013). “Understanding the Earth's natural resources: An introduction,” in Earth's Natural Resources, (Burlington, MA: Jones and Bartlett Learning), p 1-26.

Wang, Y., Castelao, R.M., and Di Iorio, D. (2017). Salinity variability and water exchange in interconnected estuaries. Estuar. Coast. 40, 917-929. doi: 10.1007/s12237-016-0195-9

Watanabe, K., and Kuwae, T. (2015). How organic carbon derived from multiple sources contributes to carbon sequestration processes in a shallow coastal system? Glob. Change Biol. 21, 2612-2623. doi: 10.1111/gcb.12924

Wu, Z., Rodgers, R.P., and Marshall, A.G. (2004). Two- and three-dimensional van Krevelen diagrams: A graphical analysis complementary to the Kendrick mass plot for sorting elemental compositions of complex organic mixtures based on ultrahigh-resolution broadband Fourier transform ion cyclotron resonance mass measurements. Anal. Chem. 76, 2511-2516. doi: 10.1021/ ac0355449

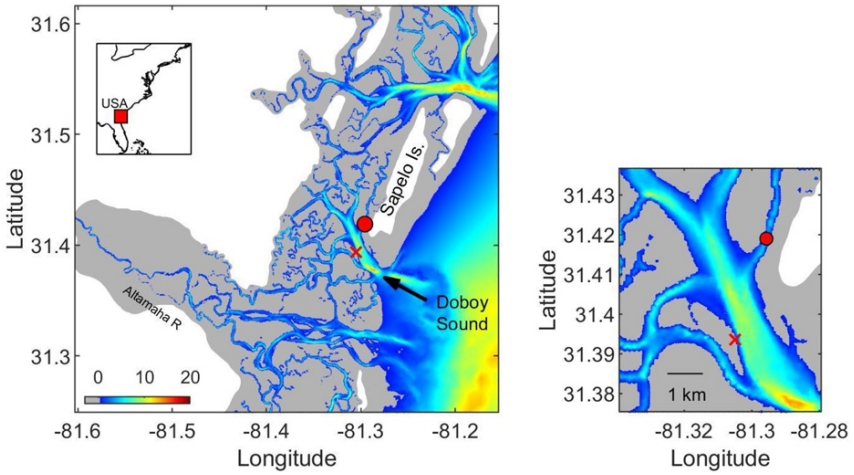

Figure 2.1: (**left**) Sampling location in Doboy Sound, GA (red circle). Salt marshes and uplands are shown in gray and white, respectively. Colors indicate bottom topography in meters. Location of oceanographic mooring GCE6, where salinity time series was obtained (see Figure 2.8), is shown by red cross. (**right**) Region around sampling site is shown in detail.

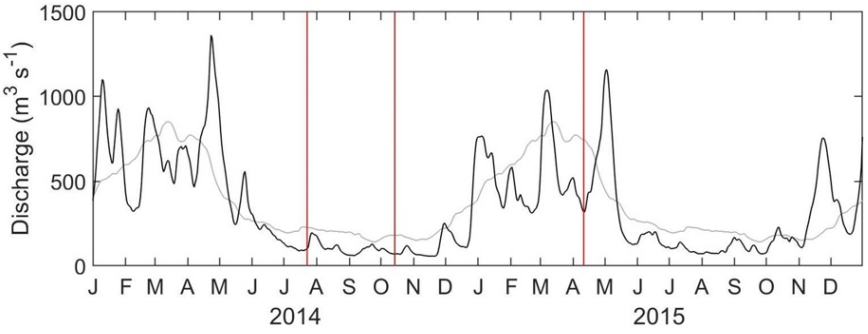

Figure 2.2: Time series of Altamaha River discharge at Doctortown, Georgia (black). Long-term average is shown in gray. Red vertical lines indicate sampling periods.

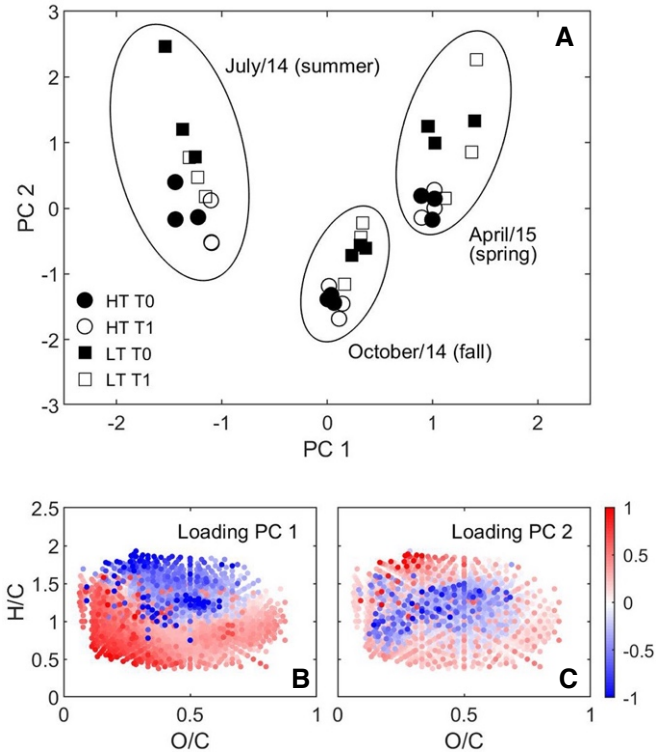

Figure 2.3: Principal component analysis of DOM composition. (**A**) Scores of the principal components from the same month are circled and labelled. Solid and open symbols represent T0 and T1, respectively. Circle and square symbols represent high tide and low tide, respectively. Van Krevelen diagrams color coded with loadings of (**B**) PC 1 and (**C**) PC 2 are also shown. The first and second principal components explained 28% and 10% of the variance.

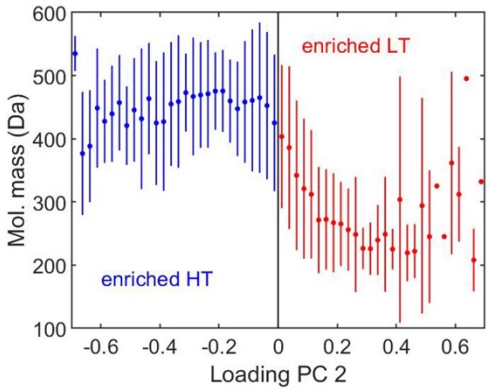

Figure 2.4: Average ± 1 standard deviation of molecular mass as a function of the loading of PC 2 shown in Figure 2.3C. Positive loadings (shown in red) represent molecular formulae enriched in samples collected at low tide (LT), while negative loadings (shown in blue) represent formulae enriched in samples collected at high tide (HT).

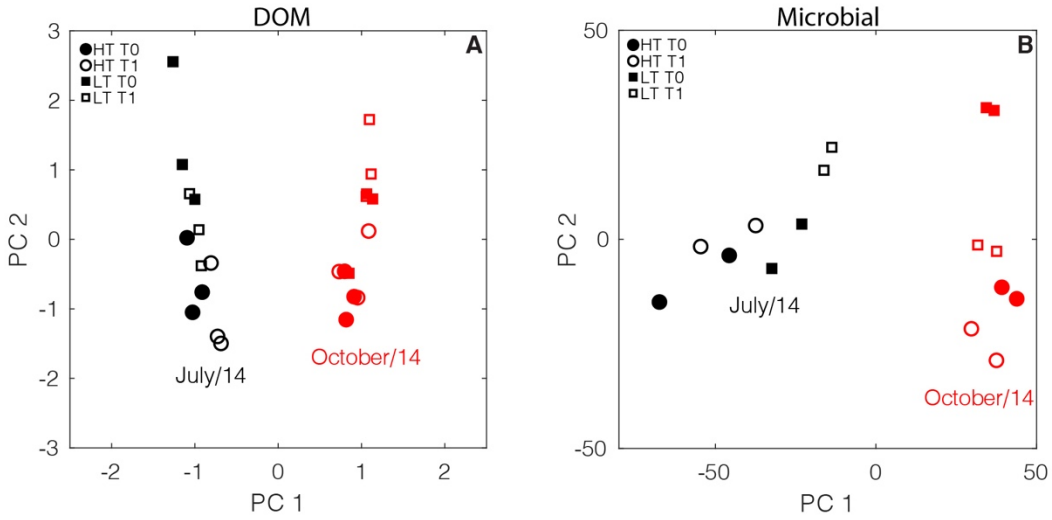

Figure 2.5: Comparison of patterns of variability between chemical and microbial data. Black and red symbols represent July and October, respectively. Solid and open symbols represent T0 and T1, respectively. Circle and square symbols represent high tide and low tide, respectively. (**A**) PCA scores of DOM composition. The first and second principal components explained 32% and 9% of the variance. (**B**) Corresponding PCA scores for gene expression data. The first and second principal components explained 66% and 13% of the variance.

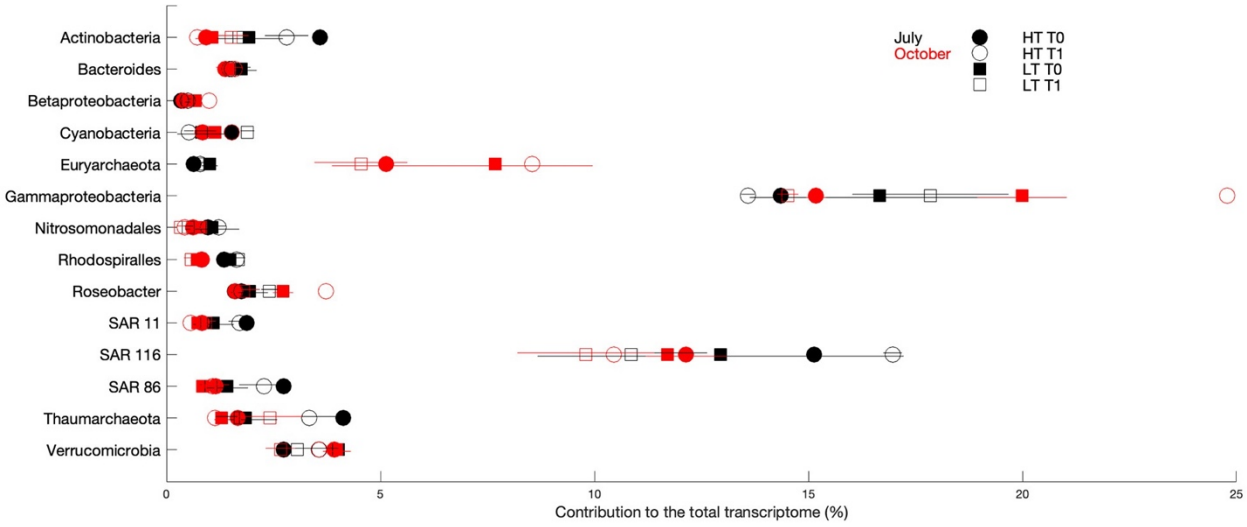

Figure 2.6: Percent contribution to the total transcriptome for the 50 highest transcript-recruiting reference genomes categorized by taxonomic group. Black and red symbols represent July and October, respectively. Solid and open symbols represent T0 and T1, respectively. Circle and square symbols represent high tide and low tide, respectively. In some cases, error bars are smaller than symbols.

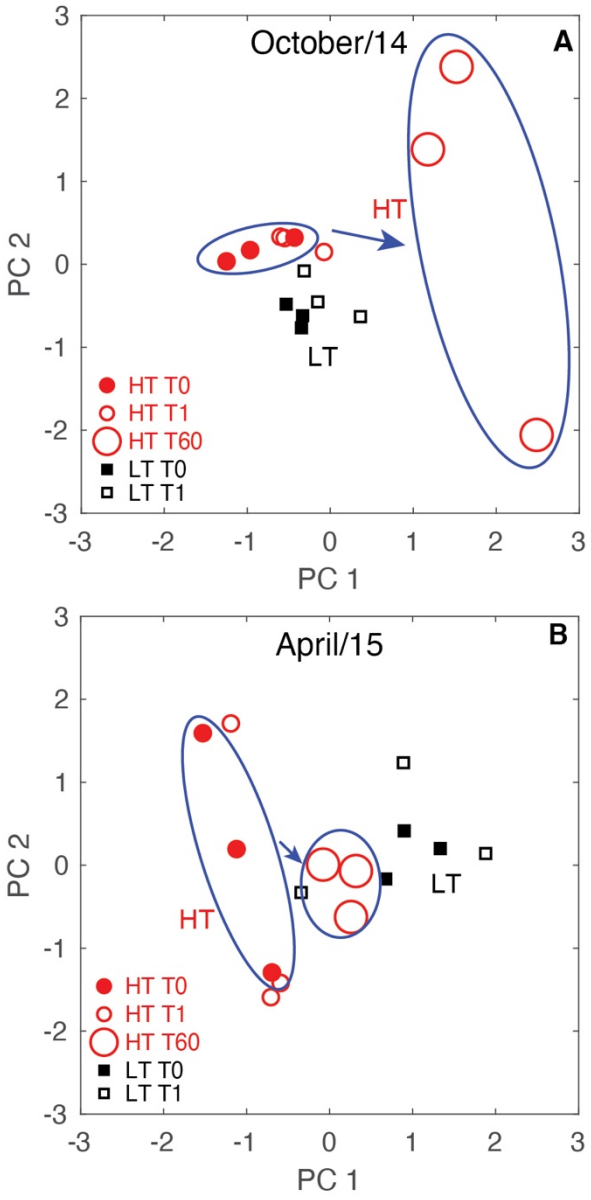

Figure 2.7: Principal component analyses of DOM composition including long-term incubations for (**A**) October 2014 and (**B**) April 2015. T0 and T60 samples are grouped with ellipses for emphasis, while arrows emphasize the extent of DOM transformation over the incubation period based on the first two principal components. The first and second principal components explained 26% and 21% of the variance in (**A**) and 24% and 13% in (**B**).

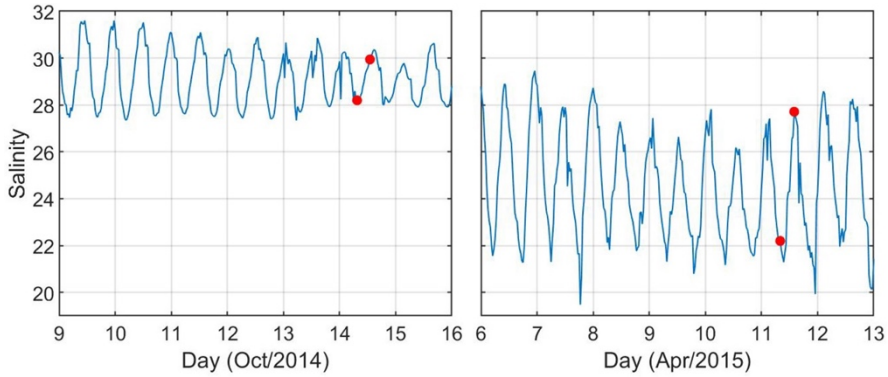

Figure 2.8: Time series of salinity at oceanographic mooring GCE6 at the main channel of Doboy Sound (see Figure 2.1 for location) during October 2014 and April 2015 collections. Red circles indicate timing of sample collection.

Table 2.1: Environmental, bulk and optical measurements for seasonal DOM samples collected at Doboy Sound (GA) at high and low tides.

	July 2014		**October 2014**		**April 2015**	
	High tide	**Low tide**	**High tide**	**Low tide**	**High tide**	**Low tide**
			Salinity			
	33	30	28	27	25	23
			DOC *(μM)*			
T0	194.0 ± 6.7	249.3 ± 7.8	198.2 ± 5.8	324.9 ± 4.2	291.1 ± 6.3	337.1 ± 6.2
T1	190.1 ± 7.1	250.9 ± 8.7	193.0 ± 3.4	309.4 ± 9.4	288.6 ± 6.3	331.6 ± 4.2
T60	-	-	175.1 ± 3.3	-	264.8 ± 5.7	-
			$a_g(250):a_g(365)$			
T0	6.04 ± 0.22	5.97 ± 0.10	6.33 ± 0.12	6.39 ± 0.21	5.59 ± 0.04	5.68 ± 0.03
T1	6.08 ± 0.05	5.86 ± 0.30	6.19 ± 0.06	6.20 ± 0.20	5.55 ± 0.01	5.66 ± 0.01
T60	-	-	6.09 ± 0.14	-	5.51 ± 0.02	-
			$S_{275-295}$ ($\times 10^3$ nm^{-1})			
T0	17.27 ± 0.25	16.80 ± 0.14	17.11 ± 0.11	17.38 ± 0.19	15.67 ± 0.06	15.66 ± 0.05
T1	17.30 ± 0.10	16.57 ± 0.40	17.15 ± 0.19	16.98 ± 0.03	15.60 ± 0.13	15.80 ± 0.15
T60	-	-	16.92 ± 0.17	-	15.83 ± 0.06	-

CHAPTER 3

AMAZON RIVER PLUME TERRIGENOUS DISSOLVED ORGANIC CARBON FROM SATELLITE OBSERVATIONS. PART I: SEASONAL AND INTERANNUAL VARIABILITY[2]

[2]Martineac, R.P., Castelao, R.M., and Medeiros, P.M. To be submitted to Journal of Geophysical Research: Oceans.

Abstract

The Amazon River is a large source of freshwater and terrigenous dissolved organic carbon (tDOC) to the western tropical Atlantic Ocean. Understanding the distribution and fate of tDOC in the ocean is important because it influences a variety of biogeochemical processes. Here, we harness the near 2-decade-long time series of satellite observations of ocean color from Moderate Resolution Imaging Spectroradiometer (MODIS) to describe seasonal and interannual variability in tDOC content in the Amazon River plume. Our analyses revealed good agreement between surface salinity and tDOC content, suggesting that tDOC is a robust tracer of riverine water in the region. The tDOC distribution of the Amazon River plume has a distinct seasonal pattern, reaching northwest along the Atlantic coast of South America towards the Caribbean during maximum discharge periods, and moving eastward entrained in the North Brazil Current retroflection during minimum discharge periods. Maximum variability is found at the plume core, where seasonality accounts for 40% of the total variance. Elevated tDOC content extended beyond the shelfbreak in some capacity in all months of the year, suggesting that cross-shelf carbon transport occurs year-round. The long-time series also allowed for interannual variability to be quantified. Accounting for 15% of the total variance in the core of plume, interannual variability in tDOC is often associated with hydrological changes. Overall, we found MODIS-tDOC to be an effective tracer for the Amazon River plume, with great potential to be used for identifying events of increased off-shelf tDOC transport.

Keywords: terrigenous dissolved organic carbon, Amazon River plume, ocean-color, remote sensing, MODIS, SMOS.

1. Introduction

The dissolved organic matter (DOM) pool in the ocean holds an amount of carbon comparable to the atmospheric carbon pool, making DOM an important component of the global carbon cycle (Hansell, 2013). There are many sources of DOM in the ocean, each contribution highly variable and complex chemical compositions (Hopkinson, 1985). An important source is the export of organic carbon from rivers to the ocean. Rivers contribute enough carbon to maintain the steady-state concentration of oceanic dissolved organic carbon (DOC), upwards of 250-260 Tg C y^{-1} (1 Tg=10^{12} g) (Hedges *et al.*, 1997; Raymond and Spencer, 2015). Much remains to be learned about the fate of this terrigenous material in the ocean. Despite the large inputs, terrigenous DOC (tDOC) is thought to be altered over relatively short time scales (Benner and Opsahl, 2001; Hernes and Benner, 2003), with the coastal ocean serving as a major sink (Hedges *et al.*, 1997; Fichot and Benner, 2014). Main mechanisms responsible for removing tDOC in the coastal ocean include microbial degradation, photochemical processes, and flocculation (Sholkovitz, 1978; Hernes and Benner, 2003). The metabolic state of ocean margins, including the role of CO_2 exchange with the atmosphere, is directly affected by the mineralization of tDOC (Smith and Hollibaugh, 1993; Hedges *et al.*, 1997; Opsahl and Benner, 1997; Bianchi, 2011; Cai, 2011; Letscher *et al.*, 2011; Fichot and Benner, 2014).

Many studies have indicated that ocean margins can act as major filters of tDOC between the land and ocean (Hedges *et al.*, 1997; Opsahl and Benner, 1997). In the northern Gulf of Mexico (GoM), for example, recent studies have shown that over half of the tDOC from the Mississippi-Atchafalaya River system is mineralized along the margin each year (Fichot and Benner, 2014). Since it is likely that the terrigenous material will continue to be degraded as it is transported offshore, the fraction of terrigenous material exported from that continental margin is likely to be

even smaller. Despite intense mineralization occurring in many coastal regions, other studies have demonstrated that a large fraction of the tDOC from rivers can escape the continental margin (Medeiros *et al.*, 2015; Seidel *et al.*, 2015) and be transported to the open ocean (Medeiros *et al.*, 2016). Terrigenous DOC has indeed been observed in the deep Atlantic and Pacific Oceans (Opsahl and Benner, 1997; Medeiros *et al.*, 2016). In the Amazon River to ocean continuum, up to 75% of the tDOC delivered to the ocean by the river can be transported off the continental margin, particularly during high discharge conditions (Medeiros *et al.*, 2015). Since the Amazon River discharge is predicted to increase in future climate scenarios (Manabe *et al.*, 2004; Nohara *et al.*, 2006), the delivery of tDOC to the ocean and the export from the coastal margin may increase even further (Medeiros *et al.*, 2015).

Tracing the transport of tDOC in the ocean relying on *in situ* observations is challenging. Not only are such observations dependent on logistically difficult and expensive field campaigns that only provide snapshots in time, the transport often occurs in relatively narrow filaments that are easily missed by low-resolution *in situ* data. Long-term observations of that transport over large areas in the ocean can only be achieved via the use of well-calibrated satellite algorithms. Recent studies have shown that the spectral slope coefficient of chromophoric dissolved organic matter (CDOM) between 275 and 295 nm ($S_{275\text{-}295}$) can be used as a tracer of the percent tDOC in river-influenced ocean margins (Fichot and Benner, 2012; Fichot *et al.*, 2014; Medeiros *et al.*, 2017). Algorithms based on remote sensing reflectance (Rrs) data from the Moderate Resolution Imaging Spectroradiometer (MODIS) have been developed to estimate the spectral slope coefficient of CDOM absorbance from satellite ocean color data (Fichot *et al.*, 2013; 2014). Fichot *et al.* (2014) showed that $S_{275\text{-}295}$ from satellites agree with *in situ* $S_{275\text{-}295}$ measurements with an average uncertainty of 10%. By using a nonlinear regression to model the relationship

between *in situ* $S_{275\text{-}295}$ and tDOC concentration, estimates of tDOC content from ocean color can be obtained (Fichot *et al.*, 2014).

Although much has been learned about the distribution of Amazon River plume waters (e.g., Salisbury *et al.*, 2011; Fournier *et al.*, 2015) and the mechanisms driving offshore advection of freshwater into the tropical Atlantic Ocean (e.g., Fournier *et al.*, 2017) using satellite observations, many of these previous studies relied on relatively short time series lasting only a few years. This precluded the characterization of plume variability at seasonal and/or lower frequencies. With almost 20 years of satellite observations of ocean color now available, we adapted and refined the algorithm developed by Fichot *et al.* (2013, 2014) to provide a detailed characterization of seasonal and interannual variability in the distribution of terrigenous DOC from the Amazon River in the Atlantic Ocean. Identifying areas of enhanced offshore transport of tDOC as well as the mechanisms controlling the offshore transport are the focuses of Chapter 4.

2. Methods

2.1 In situ observations

In situ surface observations were collected in the Amazon River plume during two research cruises to the western tropical Atlantic Ocean, one in September/October 2011 and one in July 2012 (**Figure 3.1)**. Samples collected during September/October 2011 coincided with a low discharge period (~110,000 $m^3\ s^{-1}$), while sampling in July 2012 followed a record peak in river discharge (maximum of ~370,000 $m^3\ s^{-1}$). Data collection and chemical analyses are described in detail in Medeiros *et al.* (2015), Seidel *et al.* (2015) and Cao *et al.* (2016), and included DOC concentrations, bulk $\delta^{13}C$ ratios of DOC and $S_{275\text{-}295}$. The *in situ* concentration of

tDOC was determined as

$$[tDOC] = [DOC] \times f_{tDOC} \quad (1)$$

where [DOC] and [tDOC] are the *in situ* DOC and tDOC concentrations, respectively, and f_{tDOC}

$$f_{\mathrm{tDOC}} = \frac{^{13}C_{Sample} - ^{13}C_{marine}}{^{13}C_{terrigenous} - ^{13}C_{marine}} \quad (2)$$

is the fraction of terrigenous DOC in the sample estimated using $\delta^{13}C$ measured as reported in Medeiros *et al.* (2015) for marine and terrigenous end members, as well as the sample value. A nonlinear regression of the form (Fichot *et al.*, 2014)

$$\ln([\mathrm{tDOC}]) = \exp(\alpha - \beta \times S_{275\text{-}295}) + \exp(\gamma - \delta \times S_{275\text{-}295}) \quad (3)$$

was used to parameterize the relationship between the *in situ* spectral slope measurements and the *in situ* tDOC concentrations estimated using Eq. (1), where

$$\alpha=4.083,\ \beta=280.382,\ \gamma=1.886 \text{ and } \delta=36.418.$$

This allowed for tDOC to be estimated from $S_{275\text{-}295}$ measurements (**Figure 3.2a**). We noted a seemingly better agreement with 2011 data vs 2012. This could be due to data from 2012 extending closer to the river mouth, where high levels of suspended sediments are observed (Devol and Hedges, 2001). Errors in ocean-color remote sensing are generally increased under high-sediment conditions (e.g, Salisbury *et al.*, 2011).

2.2 Terrigenous DOC from satellite observations

To link *in situ* data and satellite observations, we followed Fichot *et al.* (2014) to obtain satellite-derived estimates of spectral slope via log-linearized Rrs(λ) at λ=443, 488, 555, 667 and 678 nm from MODIS:

$$\ln(S_{275\text{-}295}) = \varepsilon + \zeta \times \ln(\mathrm{Rrs}(443)) + \eta \times \ln(\mathrm{Rrs}(448)) + \theta \times \ln(\mathrm{Rrs}(555)) + \varphi \times \ln(\mathrm{Rrs}(667)) + \chi \times \ln(\mathrm{Rrs}(678)) \quad (4)$$

where

$$\varepsilon=-3.1221,\ \zeta=0.0673,\ \eta=0.3266,\ \theta=-0.07457,\ \varphi=-0.4599,\ \text{and}\ \chi=0.2917$$

are the derived regression coefficients from Fichot *et al.* (2014). The data collection during the research cruises to the Amazon River plume in 2011 and 2012 did not include *in situ* data of Rrs. As such, we use the regression coefficients listed in Eq. (4), which were derived by Fichot *et al.* (2014) using observations from the continental margin in the northern Gulf of Mexico, under the influence of the Mississippi River plume. We note that a nonlinear regression with form similar to Eq. (4) with slightly different coefficients was successfully used in the Arctic Ocean (Fichot *et al.*, 2013). Furthermore, Fichot *et al.* (2014) note that although region-specific parameterizations are always ideal, they applied the algorithm developed for the Gulf of Mexico (Eq. 4) to their Arctic Ocean data set (Fichot *et al.*, 2013) for testing purposes, which yielded accurate estimates of $S_{275\text{-}295}$ (within ±10% error). This led Fichot *et al.* (2014) to conclude that the algorithm should work well in other coastal environments under the influence of large tDOC inputs. To evaluate this, MODIS-derived spectral slopes derived from Eq. (4) were compared with *in situ* point-measurements of spectral slope. Comparisons between *in situ* and satellite-derived observations are always challenging, in part because *in situ* data represents a single location in space, while satellite observations represent averages over the satellite footprint size. In the case of MODIS-Aqua, a spatial resolution of 250 m was used in this study, with a footprint size of ~10 km. Additionally, substantial gaps in data coverage are observed in the region in daily satellite observations due to cloud cover. To address this, we built 7-day averages of the satellite observations centered around the time of *in situ* data collection before comparison with *in situ* measurements. Despite these uncertainties, *in situ* and remote-sensed spectral slope coefficients were found to be significantly correlated (r=0.83, $p<0.01$).

Once maps of $S_{275\text{-}295}$ were obtained based on MODIS data using Eq. (4), satellite-derived estimates of tDOC could be obtained using Eq. (3). The 7-day averages of satellite-derived tDOC were compared with the *in situ* point-measurements of tDOC from Eq. (1) (**Figure 3.2b**), which again resulted in a statistically significant correlation (r=0.78, p<0.01). The daily tDOC estimates from MODIS were then used to build monthly averages. This method has been shown to provide accurate estimates of tDOC concentrations in the Gulf of Mexico (Fichot *et al.*, 2014) and in the Arctic Ocean (Fichot *et al.*, 2013), suggesting that it can be applied successfully to other regions where optical data can be used to identify tDOC, as in the Amazon River plume (Cao *et al.*, 2016).

To quantify intraseasonal, seasonal and interannual variability in tDOC content in the western tropical Atlantic Ocean, we first low-pass filtered the monthly data using a 12-month filter (cosine-Lanczos filter; Mooers and Smith, 1968). That captured mostly interannual variability (Legaard and Thomas, 2006). The residue between the original time series and the low-pass filtered data includes variability at seasonal and higher frequencies. We then low-pass filtered the residue time series with a 6-month window to extract the seasonal signal. The new residue contains mostly intraseasonal variability. At each location, we follow Legaard and Thomas (2007) and approximate the total variance of the time series as the addition of the variance of the time series at the different frequency bands (i.e., intraseasonal, seasonal and interannual). The error associated with this assumption (i.e., the difference between the variance of the original data and the sum of the variances of the multiple time series for the different frequencies considered) is generally less than 15%.

2.3 Sea surface salinity from satellite observations

To track the temporal and spatial evolution of the Amazon River plume, satellite

observations of sea surface salinity (SSS) were obtained from the Soil Moisture Ocean Salinity (SMOS; Boutin *et al.*, 2022) mission. Observations are available since 2009, with 1000 km resolution and a footprint of ~40 km. We used the Level 3 debiased version 7 product distributed by LOCEAN. The overall accuracy of 10-day composites of SMOS salinity data in tropical regions is of the order of 0.3 practical salinity units (Reul *et al.*, 2013; Fournier *et al.*, 2014). SMOS has been successfully used previously to investigate salinity variability in the Amazon River plume (i.e., Grodsky *et al.*, 2014; Gouveia *et al.*, 2019a), as well as to identify variations in the offshore advection of plume waters (Fournier *et al.*, 2017). We focused on SMOS observations instead of data from the Soil Moisture Active Passive (SMAP) mission because the latter is only available since 2015, although good agreement of salinity observations was observed between the two products.

3. Results

Peak discharge from the main stem of the Amazon River occurs during May to June reaching an average maximum of ~240,000 m^3 s^1, and discharge minima is historically experienced between November – December (~80,000m^3 s^1; Richey *et al.*, 1990; Lentz, 1995). In the plume region, *in situ* observations of $\delta^{13}C$ and surface salinity were found to be highly correlated (r=0.88, p<0.001), with $\delta^{13}C$ signatures being depleted in riverine samples (~ -29.3 to -30‰) and enriched in the most oceanic samples (~ -21.8 to -22.4‰) (Medeiros *et al.*, 2015; Seidel *et al.*, 2015). Calculated fractions of the terrigenous portion of surface DOC based on *in situ* samples and obtained through equation (1) ranged from 0-3% near the distal portion of the plume to 40-60% on-shelf, reaching 100% in the river mouth. This is consistent with Medeiros *et al.* (2015) analyses, who used a two end-member mass balance based on high-resolution mass

spectrometry data to show that on-shelf plume waters were characterized by DOC with 40-60% of terrigenous content.

A 19-year long-term average of tDOC concentration (**Figure 3.3a**) reveals a picture that is largely consistent with the distribution of SSS from SMOS (e.g., Fournier *et al.*, 2015; **Figure 3.1**), with the bulk of the tDOC coinciding with the center of the Amazon River plume as identified by salinity observations. Averaged enhanced tDOC concentrations are generally constrained to within the 100 m isobath ranging from ~40-100 μmol L^{-1}, with substantially lower concentrations offshore extending to the northwest and to the east in the North Brazil Current (NBC) retroflection region (Fratantoni *et al.*, 1995; Garzoli *et al.*, 2004; Coles *et al.*, 2013) around 8ºN (**Figure 3.3a**). To better characterize the average reach of enhanced tDOC in the plume and surrounding ocean, we divide the number of times a pixel had tDOC concentrations larger than a given threshold (set to 10 μmol L^{-1} here) by the total number of months with available data for that pixel during the study period, yielding a frequency of plume occurrence (da Silva and Castelao, 2018). The analysis reveals that waters with high tDOC concentrations (i.e., > 10 μmol L^{-1}) are observed 100% of the time over the shelf, inshore of the 100 m isobath (**Figure 3.3b**). Even though tDOC concentrations off the shelf are low on average (**Figure 3.3a**), the signature of the plume is detected quite frequently, over 50% of the time in the northwest sector of our study area extending toward the Caribbean (Molleri *et al.*, 2010), and around 30-40% of the time in the retroflection region (**Figure 3.3b**).

Even though the influence of tDOC from the Amazon River is felt over the shelf in all months during the study period, tDOC concentrations are quite variable experiencing a large maximum range in excess of 200 μmol L^{-1} inshore of the 100 m isobath (**Figure 3.4**). That may be related to variations in the amount of tDOC exported from the Amazon River, but also due to

shifts in the position of the plume associated with winds or other forcing (Fournier *et al.*, 2017). Previous studies have observed shifts in the salinity plume core throughout the year, most recently observing a tight, nearshore plume from December-May, then moving offshore ~75 km during June-August (Ruault *et al.*, 2020). Enhanced variability is also observed in the NBC retroflection region as well, although substantially smaller than over the shelf.

The previous analyses indicated that substantial variability is observed in tDOC concentration and spatial distribution of the area under the influence of tDOC-enriched waters. That is expected, given that the Amazon River plume experiences substantial seasonal variability (e.g., Lentz, 1995; Lentz and Limeburner, 1995; Fournier *et al.*, 2015). Indeed, monthly averages of tDOC concentrations (**Figure 3.5**) and the frequency of plume occurrence based on tDOC data (**Figure 3.6**) reveal marked variability between months. From December to February, tDOC concentrations over the shelf are comparatively small (**Figure 3.5**), and high frequencies of plume occurrence are mostly restricted to the shelf, inshore of the 100 m isobath (**Figure 3.6**). tDOC concentrations over the shelf increase from March to May or June as the Amazon River discharge also increases (Richey *et al.*, 1990), with the plume extending beyond the continental margin toward the Caribbean 60-90% of the time. The frequency of plume occurrence remains quite small to the east, however. Concentrations begin to slowly decrease from June to August over the shelf, and the plume extends progressively eastward during that period under the influence of the NBC retroflection (Johns *et al.*, 1990). This is consistent with Lentz (1995), who used historical *in situ* salinity observations to show that the freshest water in the retroflection region is observed in July and August. Even though tDOC concentrations are low in that area compared to the shelf, the frequency of plume occurrence is high, exceeding 80%. The frequency of plume occurrence to the northwest toward the Caribbean decreases to around 50% during that

time. From August to November, the signature of the retroflection on tDOC concentrations and plume distribution is still clearly visible but it decreases progressively, and by December enhanced tDOC concentrations are once again mostly restricted to shelf waters.

The dominant modes of variability in the system were investigated through an empirical orthogonal function (EOF) decomposition of monthly tDOC concentrations (after removing the mean). Statistically significant modes were identified following Overland and Preisendorfer (1982). EOF 1 explains 21.9% of the total variance (i.e., the percentage of the variance explained over the entire domain), capturing the seasonal increase in tDOC concentrations primarily over the shelf (but also extending off the shelf toward the Caribbean) from April to June and a reduction in October-December (**Figure 3.7a,c**). Although the mode is dominated by seasonal variability, interannual variability is also clearly present (**Figure 3.7d**). Several years to note with amplitudes larger than the mean seasonal peaks (which indicate greater enhancement of tDOC than the seasonal pattern) include 2006, 2009, 2014, 2017, 2018, and 2021. The years 2009, 2012, 2014 and 2021 were flood years (Jiménez-Muñoz et al, 2013; Marengo *et al.*, 2015; Espinoza *et al.*, 2013, 2022). Though 2006 was not a flood year, it followed the severe drought during 2005 (Chen et al, 2010; Jiménez-Muñoz et al, 2016). Recent studies suggest that post-drought conditions in the Amazon River watershed contribute to the increased export of DOC (Kurek *et al.*, 2021). The peaks in the amplitude time series of EOF 1 during certain years are unusually wide, such as 2021, suggesting that the tDOC concentrations in the plume were enhanced over longer periods of time. This year was indeed associated with a historical extreme flood event, potentially increasing the amount of DOC exported from the watershed. The corresponding local variance explained (i.e., the percentage of the variance explained at each location) is ~40-60% over the shelf in the plume core, while at the portion of the plume off the

continental shelf (8-10ºN, 55ºW), EOF 1 explained ~30% of the local variance.

The second EOF mode explains 16.0% of the total variability (**Figure 3.8**), and it is characterized by a zero crossing over the shelf around 2°N (purple contour on **Figure 3.8a**). The second EOF shares characteristics with EOF1 in that the plume core appears to be captured, but instead it highlights an out-of-phase response between the region near the river mouth and the region farther north including the NBC retroflection region (**Figure 3.8a**). In those regions, the mode explains 20%-40% of the local variance (**Figure 3.8b**). The mode captures an increase in tDOC concentrations close to the river mouth near 0º latitude early in the year, from January to May (**Figure 3.8c**). This is consistent with Fournier *et al.* (2015), who also observed peak influence of plume waters near the mouth in April. Farther north near the shelfbreak and in the retroflection region, the mode captures increased concentrations from June to September. This general pattern was observed every year but with significant interannual variability in amplitude strength and peak month (**Figure 3.8d**). In particular, large anomalies were observed in 2006, 2009 and 2014. The intensification in amplitude was negative in 2006 and 2009, indicating lower tDOC concentrations in the retroflection region in those years. In 2014, on the other hand, the mode captured increased influence of the plume in the retroflection region.

Lastly, we computed the relative contribution of variability at the interannual, seasonal and intraseasonal frequency bands to the total variance at each pixel (**Figure 3.9**). Although there are several gaps in the observations, it is possible to see that the contribution of seasonal variability is increased over the shelf and in the retroflection region, which is consistent with the EOF decompositions. The largest variances are observed in the intraseasonal band, however. This indicates that variability at short time scales, such as due to shifts in the position of the plume associated with wind forcing (e.g., Fournier *et al.*, 2017) or due to meanders and eddies

(e.g., Fratantoni and Glickson, 2002), dominates tDOC variance in the region. Interannual variability, on the other hand, accounts for 10-15% of the total variance over the shelf and in the retroflection region.

4. Discussion

We used satellite-derived measurements of SSS from SMOS and estimates of tDOC from MODIS to describe variability in the Amazon River plume, and to quantify seasonal and interannual variability in tDOC distribution in the western tropical Atlantic Ocean. Our study builds on several previous studies that have characterized the Amazon River plume and its variability using *in situ* observations (e.g., Lentz, 1995) and satellite measurements of salinity (e.g., Fournier *et al.*, 2015, 2017) and ocean color (Müller-Karger *et al.*, 1988, 1995; Longhust, 1995; Fratantoni and Glickson, 2002; Del Vecchio and Subramaniam, 2004; Molleri *et al.*, 2009; Salisbury *et al.*, 2011; Gouveia *et al.*, 2019a). Several of these previous studies have used satellite imagery of chlorophyll, diffuse attenuation coefficient at 490 nm, or the absorption coefficient of colored detrital matter at the reference wavelength 443 nm (a_{cdm}) to track the position of the plume. Here, we use an algorithm (Fichot *et al.*, 2013, 2014) specifically designed to track the terrigenous component of the DOC pool, providing a link between limited and expensive *in situ* measurements and increasingly available satellite data. Satellite observations from MODIS are now available for almost 2 decades, and the use of a longer time series allows for the seasonal and interannual variability in tDOC concentrations to be quantified.

As expected, the average spatial distributions of the plume based on salinity and tDOC are quite similar to each other. Ocean color observations of the absorption coefficient of colored detrital material (a_{cdm}) have been shown to be highly correlated to salinity in the region, to the

point that local quasi-linear relationships between SSS and a_{cdm} have been used to extend SSS observations back in time (Fournier *et al.*, 2015). Analyses along a transect extending from the river mouth along the core of the river plume have shown significant deviations from conservative mixing, however (Salisbury *et al.*, 2011). A detailed analysis comparing SSS and tDOC along the core of the Amazon River plume is presented in Chapter 4.

We used the long-term observations to characterize the seasonal evolution of tDOC concentration in the western Atlantic Ocean. We also identified the evolution of the frequency of plume occurrence (da Silva and Castelao, 2018) through two decades based on tDOC observations. That is an important metric, because it reveals how often a specific location is under the influence of plume waters (which are typically concurrently enriched in nutrients and other substances) in each month. The presence of plume waters can influence a variety of biogeochemical processes, such as primary productivity stimulated by nutrients (Smith and Demaster, 1996; Gouveia *et al.*, 2019a) and the related CO_2 drawdown (e.g. Kortzinger, 2003; Chen *et al.*, 2012; Ibánhez *et al.*, 2015) associated with phytoplankton blooms (Smith and Demaster, 1996). Our observations are consistent with previous characterizations of the plume core movement that revealed three main dispersal patterns: *(1)* a narrow band of flow along the northeastern South American coast from December to March; *(2)* flow to the Caribbean region between April and July; and *(3)* flow to the Central Equatorial Atlantic Ocean with plume waters entrained in the NBC retroflection from August to November (e.g. Curtin, 1986; Lentz and Limeburner, 1995; Del Vecchio and Subramaniam, 2004; Molleri *et al.*, 2010; Salisbury *et al.*, 2011; Varona *et al.*, 2019). Elevated tDOC content extends beyond the shelfbreak in some capacity in all months of the year, suggesting that cross-shelf carbon transport occurs year-round. Even though tDOC concentrations are comparatively low in the retroflection region, our novel

estimates of the frequency of plume occurrence are quite high, exceeding 80% from July to September. That seasonal evolution of the plume accounts for as much as 40% of the total variance in tDOC concentrations over the shelf and in the retroflection.

Our long-term time series also allowed us to quantify interannual variability, something that has been difficult to achieve due to the use of comparatively short time series lasting only a few years (e.g., Salisbury *et al.*, 2011; Fournier *et al.*, 2015). Even though interannual variability only accounts for ~15% of the total variance in most locations, EOF decompositions have revealed large increases in tDOC concentrations in specific years. Much of the interannual variability we observed could be related to flood and drought conditions in the Amazon River watershed. Indeed, the largest increases in tDOC were often observed during flood years. Interannual variability in runoff has been shown to modulate the sea surface salinity of the Amazon plume (Gévaudan *et al.*, 2022), so it is reasonable to expect that it will also modulate variability in tDOC concentrations in the plume. That is important, because extreme floods have become more frequent over the last 3 decades (Gévaudan *et al.*, 2022). Studies have suggested that the hydrological cycle has intensified in the region; while previously the river experienced extreme events about once every ten years, it experienced three extreme events in the span of five years from 2005 to 2010 (Marengo *et al.*, 2011). The Amazon River plume may already be gradually getting fresher, by up to 3.5% per year (Gouveia et al, 2019b) due to increased precipitation extremes within the Amazon River watershed (de Almeida *et al.*, 2016; Lan *et al.*, 2016). It is likely that increased precipitation and/or discharge extremes will result in increased concentrations of tDOC over the shelf, and possibly in increased transport off the shelf into the interior of the basin.

Other factors that may impact the Amazon River watershed carbon supply, including forest fires which introduce black carbon (Coppola *et al.*, 2019) and deforestation which has been linked to increased tDOC output (Davidson *et al.*, 2012). It would be interesting to explore these relationships in future investigations as these anthropogenic phenomena become more prevalent. Another important source of interannual variability in the Amazon River plume is the occurrence of El Niño and/or La Niña events. La Niña years are generally characterized by increased precipitation and wetter conditions in the Amazon Basin, often resulting in flooding in the region, while the opposite is true during El Niño years resulting in droughts (Foley *et al.*, 2002; Ronchail, 2005; Espinoza *et al.*, 2013; Marengo *et al.*, 2013). The export of tDOC from the river into the ocean can increase substantially during La Niña years (e.g., Kurek *et al.*, 2021). This is likely to become even more important in the future, given that the effects of El Niño/La Niña cycles on the Amazon Basin have been amplified in relation to changes in the climate, and those events are predicted to increase in frequency and severity in the future (Cai *et al.*, 2015; Widlansky *et al.*, 2015).

As additional data are gathered and algorithms are refined and improved, remote sensing tools will become increasingly more valuable to investigate the distribution and variability of tDOC content in vast regions where *in situ* sampling is costly and difficult to obtain. They will also play a critical role on investigations of the importance of climate variability on carbon dynamics, be it on scales of a few years such those associated with El Niño/La Niña cycles or on longer time scales associated with anthropogenic-driven climate change. MODIS-tDOC also has a great potential to be used for identifying events of increased off-shelf tDOC transport, which are difficult to observe with *in situ* data. Our investigation of tDOC variability in the Amazon River plume supports the application of these methods in other coastal regions strongly

influenced by riverine inputs where tDOC export is high, and will hopefully stimulate comparisons with other coastal settings where river plumes interact with offshore boundary currents.

References

Benner, R., and Opsahl, S. (2001). Molecular indicators of the sources and transformations of dissolved organic matter in the Mississippi River plume. Org. Geochem., 32, 4, 597–611. doi: 10.1016/s0146-6380(00)00197-2

Bianchi, T. S. (2011). The role of terrestrially derived organic carbon in the coastal ocean: A changing paradigm and the priming effect. Proc. Natl. Acad. Sci. U.S.A., 108(49), 19473-19481. doi:10.1073/pnas.1017982108

Boutin J., Vergely J.-L., and Khvorostyanov D. (2022). SMOS SSS L3 maps generated by CATDS CEC LOCEAN. debias V7.0. SEANOE. doi: 10.17882/52804#91742

Cai, W. (2011). Estuarine and Coastal Ocean Carbon Paradox: CO2 Sinks or Sites of Terrestrial Carbon Incineration?. Annu. Rev. Mar. Sci., 3(1), 123-145. doi: 10.1146/annurev-marine-120709-142723

Cao, F., Medeiros, P. M. and Miller, W. L. (2016). Optical characterization of dissolved organic matter in the Amazon River plume and the Adjacent Ocean: Examining the relative role of mixing, photochemistry, and microbial alterations. Mar. Chem., 186, 178-188. doi: 10.1016/j.marchem.2016.09.007

Chen, J. L., Wilson, C. R. and Tapley, B. D. (2010). The 2009 exceptional Amazon flood and interannual terrestrial water storage change observed by GRACE. Water Resour. Res., 46(12). doi: 10.1029/2010WR009383

Chen, C.-T. A., Huang, T.-H., Fu, Y.-H., Bai, Y., & He, X. (2012). Strong sources of CO2 in upper estuaries become sinks of CO2 in large river plumes. Curr. Opin. Environ. Sustain., 4, 2, 179–185. doi: 10.1016/j.cosust.2012.02.003

Coles, V. J., Brooks, M. T. , Hopkins, J., Stukel, M. R., Yager, P. L. and Hood, R. R. (2013). The pathways and properties of the Amazon River Plume in the tropical North Atlantic Ocean. J. Geophys. Res. Oceans, 118(12), 6894-6913. doi: 10.1002/2013JC008981

Coppola, A.I., Seidel, M., Ward, N.D. *et al.* (2019). Marked isotopic variability within and between the Amazon River and marine dissolved black carbon pools. Nat. Commun., 10, 4018. doi: 10.1038/s41467-019-11543-9

Curtin, T. B. (1986). Physical observations in the plume region of the Amazon River during peak discharge—II. Water masses. Cont. Shelf Res., 6, 1–2, 53–7. doi: 10.1016/0278-4343(86)90053-1

da Silva, C. E., and Castelao, R. M. (2018). Mississippi River plume variability in the Gulf of Mexico from SMAP and MODIS-Aqua observations. J. Geophys. Res.: Oceans, 123, 6620– 6638. doi: 10.1029/2018JC014159

Davidson, E., de Araújo, A., Artaxo, P. *et al.* (2012). The Amazon basin in transition. Nature, 481, 321–328. doi: 10.1038/nature10717

de Almeida, C. T., Oliveira-Júnior, J. F., Delgado, R. C., Cubo, P., and Ramos, M. C. (2016). Spatiotemporal rainfall and temperature trends throughout the Brazilian Legal Amazon, 1973-2013. Int. J. Climatol., 37, 4, 2013–2026. doi: 10.1002/joc.4831

Del Vecchio, R. and Subramaniam, A. (2004). Influence of the Amazon River on the surface optical properties of the western tropical North Atlantic Ocean. J. Geophys. Res., 109, C11. doi: 10.1029/2004jc002503

Devol, A. H., and Hedges, J. I. (2001). Organic matter and nutrients in the main stem Amazon River. In The Biogeochemistry of the Amazon Basin, pp. 275–306.

Espinoza, J. C., Ronchail, J., Frappart, F., Lavado, W., Santini, W., & Guyot, J. L. (2013). The Major Floods in the Amazonas River and Tributaries (Western Amazon Basin) during the 1970–2012 Period: A Focus on the 2012 Flood. J. Hydrometeorol., 14(3), 1000-1008.

Espinoza, J., Marengo, J. A., Schongart, J. and Jimenez, J. C. (2022). The new historical flood of 2021 in the Amazon River compared to major floods of the 21st century: Atmospheric features in the context of the intensification of floods. Weather. Clim. Extremes, 35, 100406. doi: 10.1016/j.wace.2021.100406

Fichot, C. G. and Benner, R. (2012). The spectral slope coefficient of chromophoric dissolved organic matter (S275–295) as a tracer of terrigenous dissolved organic carbon in river-influenced ocean margins. Limnol. Oceanogr., 57(5), 1453-1466. doi: 10.4319/lo.2012.57.5.1453

Fichot, C. G., Kaiser, K., Hooker, S., Amon, R., Babin, M., Belanger, S., Walker, S., and Benner, R. (2013). Pan-Arctic distributions of continental runoff in the Arctic Ocean, Sci. Rep., 3, 1053. doi:10.1038/srep01053

Fichot, C. G. and Benner, R. (2014). The fate of terrigenous dissolved organic carbon in a river-influenced ocean margin. Global Biogeochem. Cycles, 28(3), 300-318. doi: 10.1002/2013GB004670

Fichot, C. G., Lohrenz, S. E., and Benner, R. (2014). Pulsed, cross-shelf export of terrigenous dissolved organic carbon to the Gulf of Mexico. J. Geophys. Res.: Oceans, 119, 2, 1176–1194. doi: 10.1002/2013jc009424

Foley, J. A., Botta, A., Coe, M. T. and Costa, M. H. (2002). El Niño–Southern oscillation and the climate, ecosystems and rivers of Amazonia. Global Biogeochem. Cycles, 16(4), 79-20. doi: 10.1029/2002GB001872

Fournier, S., Chapron, B., Salisbury, J., Vandemark, D. and Reul, N. (2015). Comparison of spaceborne measurements of sea surface salinity and colored detrital matter in the Amazon plume. J. Geophys. Res. Oceans, 120(5), 3177-3192. doi: 10.1002/2014JC010109

Fournier, S., Vandemark, D., Gaultier, L., Lee, T., Jonsson, B. and Gierach, M. M. (2017). Interannual Variation in Offshore Advection of Amazon-Orinoco Plume Waters: Observations, Forcing Mechanisms, and Impacts. J. Geophys. Res. Oceans, 122(11), 8966-

8982. doi: 10.1002/2017JC013103

Fratantoni, D. M., Johns, W. E., and Townsend, T. L. (1995). Rings of the North Brazil Current: Their structure and behavior inferred from observations and a numerical simulation. J. Geophys. Res.: Oceans, 100, C6, 10633. doi: 10.1029/95jc00925

Fratantoni, D. M. and Glickson, D. A. (2002). North Brazil Current Ring Generation and Evolution Observed with SeaWiFS. J. Phys. Oceanogr., 32(3), 1058-1074. doi: 10.1175/1520-0485(2002)032

Garzoli, S. L., Ffield, A., Johns, W. E. and Yao, Q. (2004). North Brazil Current retroflection and transports. J. Geophys. Res., 109. doi: 10.1029/2003JC001775

Gévaudan, M., Durand, F., and Jouanno, J. (2022). Influence of the Amazon-Orinoco discharge interannual variability on the western tropical Atlantic salinity and temperature. J. Geophys. Res. Oceans. 127, e2022JC018495. doi: 10.1029/2022JC018495

Gouveia, N. A., Gherardi, D. F. M., Wagner, F. H., Paes, E. T., Coles, V. J., and Aragão, L. E. O. C. (2019a). The Salinity Structure of the Amazon River Plume Drives Spatiotemporal Variation of Oceanic Primary Productivity. J. Geophys. Res. Biogeosci.,124, 1, 147–165. doi: 10.1029/2018jg004665

Gouveia, N. A., Gherardi, D. F. M., and Aragão, L. E. O. C. (2019b). The Role of the Amazon River Plume on the Intensification of the Hydrological Cycle. Geophys. Res. Lett., 46(21), 12221-12229. doi: 10.1029/2019GL084302

Grodsky, S. A., Reverdin, G., Carton, J. A., and Coles, V. J. (2014). Year-to-year salinity changes in the Amazon plume: Contrasting 2011 and 2012 Aquarius/SACD and SMOS satellite data. Remote Sens. Environ., 140, 14–22. doi: 10.1016/j.rse.2013.08.033

Hansell, D. A. (2013). Recalcitrant Dissolved Organic Carbon Fractions, Annu. Rev. Mar. Sci., 5(1), 421-445. doi: 10.1146/annurev-marine-120710-100757

Hedges, J. I., Keil, R. G. and Benner, R. (1997). What happens to terrestrial organic matter in the ocean?. Org. Geochem., 27(5), 195-212. doi: 10.1016/S0146-6380(97)00066-1

Hernes, P. J. and R. Benner (2003). Photochemical and microbial degradation of dissolved lignin phenols: Implications for the fate of terrigenous dissolved organic matter in marine environments, J. Geophys. Res., 108. doi: 10.1029/2002JC001421

Hopkinson Jr, C. S. (1985). Shallow-water benthic and pelagic metabolism: evidence of heterotrophy in the nearshore Georgia Bight, Mar. Biol., 87(1), 19-32.

Ibánhez, J. S. P., Diverrès, D., Araujo, M., & Lefèvre, N. (2015). Seasonal and interannual variability of sea-air CO2fluxes in the tropical Atlantic affected by the Amazon River plume. Glob. Biogeochem. Cycles, 29, 10, 1640–165. doi: 10.1002/2015gb005110

Jiménez-Muñoz, J. C., Sobrino, J. A., Mattar, C. and Malhi, Y. (2013). Spatial and temporal

patterns of the recent warming of the Amazon forest. J. Geophys. Res. Atmos., 118(11), 5204-5215. doi: 10.1002/jgrd.50456

Jiménez-Muñoz, J. C., Mattar, C., Barichivich, J., Santamaría-Artigas, A., Takahashi, K., Malhi, Y., Sobrino, J. A. and Schrier, G. v. d. (2016). Record-breaking warming and extreme drought in the Amazon rainforest during the course of El Niño 2015–2016. Sci. Rep., 6(1), 33130. doi: 10.1038/srep33130

Johns, W. E., Lee, T. N., Schott, F. A., Zantopp, R. J., and Evans, R. H. (1990). The North Brazil Current retroflection: Seasonal structure and eddy variability. J. Geophys. Res., 95(C12), 22103– 22120. doi: 10.1029/JC095iC12p22103.

Körtzinger, A. (2003). A significant CO2 sink in the tropical Atlantic Ocean associated with the Amazon River plume. Geophys. Res. Lett., 30, 24. doi: 10.1029/2003gl018841

Kurek, M. R., Stubbins, A., Drake, T. W., Moura, J. M. S., Holmes, R. M., Osterholz, H., Dittmar, T., Peucker-Ehrenbrink, B., Mitsuya, M., and Spencer, R. G. M. (2021). Drivers of Organic Molecular Signatures in the Amazon River. Glob. Biogeochem. Cycles, 35, 6. doi: 10.1029/2021gb006938

Lan, C., Lo, M., Chou, C., and Kumar, S. (2016). Terrestrial water flux responses to global warming in tropical rainforest areas. Earth's Future, 4, 5, 210–224. doi: 10.1002/2015ef000350

Legaard, K. R., and Thomas, A. C. (2006). Spatial patterns in seasonal and interannual variability of chlorophyll and sea surface temperature in the California Current. J. Geophys. Res., 111, C06032. doi: 10.1029/2005JC003282

Lentz, S. J. (1995a). Seasonal variations in the horizontal structure of the Amazon Plume inferred from historical hydrographic data. J. Geophys. Res., 100, 2391-2400, doi: 10.1029/94JC01847.

Lentz, S. J. and Limeburner, R. (1995). The Amazon River Plume during AMASSEDS: Spatial characteristics and salinity variability. J. Geophys. Res., 100, 2355-2375. doi: 10.1029/94JC01411

Letscher, R., D. A. Hansell, and D. Kadko. (2011). Rapid removal of terrigenous dissolved organic carbon over the Eurasian shelves of the Arctic Ocean. Mar. Chem., 123:78–87. doi: 10.1016/j.marchem.2010.10.002

Manabe, S., Wetherald, R. T., Milly, P., Delworth, T. L., and Stouffer, R. J. (2004). Century-scale change in water availability: CO 2-quadrupling experiment, Clim. Change, 64, 59-76.

Marengo, J. A., Tomasella, J., Alves, L. M., Soares, W. R., and Rodriguez, D. A. (2011). The drought of 2010 in the context of historical droughts in the Amazon region. Geophys. Res. Lett., 38, 12. doi: 10.1029/2011gl047436

Marengo, J. A., and Espinoza, J. C. (2015). Extreme seasonal droughts and floods in Amazonia:

causes, trends and impacts. Int. J. Climatol., 36, 3, 1033–1050. doi: 10.1002/joc.4420

Medeiros, P. M., Seidel, M., Ward, N. D., Carpenter, E. J., Gomes, H. R., Niggemann, J., Krusche, A. V., Richey, J. E., Yager, P. L. and Dittmar, T. (2015b). Fate of the Amazon River dissolved organic matter in the tropical Atlantic Ocean. Global Biogeochem. Cycles, 29(5), 677-690. doi: 10.1002/2015GB005115

Medeiros, P. M., Seidel, M., Niggemann, J., Spencer, R. G. M., Hernes, P. J., Yager, P. L., Miller, W. L., Dittmar, T. and Hansell, D. A. (2016). A novel molecular approach for tracing terrigenous dissolved organic matter into the deep ocean. Global Biogeochem. Cycles, 30(5), 689-699. doi: 10.1002/2015GB005320

Medeiros, P.M., Babcock-Adams, L., Seidel, M., Castelao, R.M., Di Iorio, D., Hollibaugh, J. T., *et al.* (2017a). Export of terrigenous dissolved organic matter in a broad continental shelf. Limnol. Oceanogr. 62, 1718-1731. doi: 10.1002/lno.10528

Molleri, G. S. F., Novo, E. M. L. de M. and Kampel, M. (2010). Space-time variability of the Amazon River plume based on satellite ocean color. Cont. Shelf Res., 30(3), 342-352. doi: 10.1016/j.csr.2009.11.015

Mooers, C. N. K., and Smith, R. L. (1968). Continental shelf waves off Oregon, J. Geophys. Res., 73(2), 549– 557. doi: 10.1029/JB073i002p00549

Müller-Karger, F., McClain, C. R. and Richardson, P. L. (1988). The dispersal of the Amazon's water. Nature, 333(6168), 56-59. doi: 10.1038/333056a0

Müller-Karger, F. E., Richardson, P. L., & Mcgillicuddy, D. (1995). On the offshore dispersal of the Amazon's Plume in the North Atlantic: Comments on the paper by A. Longhurst, "Seasonal cooling and blooming in tropical oceans." Deep Sea Res. Part I Oceanogr. Res. Pap., 42, 11–12: 2127–2137. doi: 10.1016/0967-0637(95)00085-2

Nohara, D., Kitoh, A., Hosaka, M., and Oki, T. (2006). Impact of climate change on river discharge projected by multimodel ensemble, J. Hydrometeorol., 7(5), 1076-1089.

Opsahl, S. and Benner, R. (1997). Distribution and cycling of terrigenous dissolved organic matter in the ocean, Nature, 386(6624), 480-482. doi: 10.1038/386480a0

Overland, J. E. and Preisendorfer, R. W. (1982). A Significance Test for Principal Components Applied to a Cyclone Climatology. Mon. Weather Rev., 110(1), 1-4. doi: 10.1175/1520-0493(1982)110

Raymond, P. A. and R. G. M. Spencer (2015). "Chapter 11 - Riverine DOM", in Biogeochemistry of Marine Dissolved Organic Matter (Second Edition), ed Hansell, D.A. and Carlson, C.A. (Boston MA: Academic Press) pp. 509-533.

Reul, N., *et al.* (2013). Sea surface salinity observations from space with the SMOS satellite: A new means to monitor the marine branch of the water cycle. Surv. Geophys., 35, 681–722.

Richey, J. E., Hedges, J. I., Devol, A. H., Quay, P. D., Victoria, R., Martinelli, L. and Forsberg, B. R. (1990). Biogeochemistry of carbon in the Amazon River. Limnol. Oceanogr., 35(2), 352-371. doi: 10.4319/lo.1990.35.2.0352

Ronchail, J., Labat, D., Cochonneau, G., Guyot, J.L., Filizola, N.m Oliveira, E. (2005). "Discharge variability within the Amazon basin." In Regional hydrological impacts of climatic change: hydroclimatic variability, (IAHS Press), 296, 21–32.

Ruault, V., Jouanno, J., Durand, F., Chanut, J., and Benshila, R. (2020). Role of the Tide on the Structure of the Amazon Plume: A Numerical Modeling Approach. J. Geophys. Res., 125, 2. doi: 10.1029/2019jc015495

Salisbury, J., Vandemark, D., Campbell, J., Hunt, C., Wisser, D., Reul, N., and Chapron, B. (2011). Spatial and temporal coherence between Amazon River discharge, salinity, and light absorption by colored organic carbon in western tropical Atlantic surface waters. J. Geophys. Res., 116, C7. doi: 10.1029/2011jc006989

Seidel, M., Yager, P. L., Ward, N. D., Carpenter, E. J., Gomes, H. R., Krusche, A. V., Richey, J. E., Dittmar, T., and Medeiros, P. M. (2015). Molecular-level changes of dissolved organic matter along the Amazon River-to-ocean continuum. Mar. Chem., 177, 218–231. doi: 10.1016/j.marchem.2015.06.019

Sholkovitz, E.R. (1976). Flocculation of dissolved organic and inorganic matter during the mixing of river water and seawater. Geochim. Cosmochim. Acta. 4, 831-845.

Smith, S. V. and J. T. Hollibaugh (1993). Coastal metabolism and the oceanic organic carbon balance. Rev. Geophys., 31(1), 75-89. doi: 10.1029/92RG02584

Smith, W. O., Jr, and Demaster, D. J. (1996). Phytoplankton biomass and productivity in the Amazon River plume: correlation with seasonal river discharge. Cont. Shelf Res., 16, 3, 291–319. doi: 10.1016/0278-4343(95)00007-n

Varona, H. L., Veleda, D., Silva, M., Cintra, M., and Araujo, M. (2019). Amazon River plume influence on Western Tropical Atlantic dynamic variability. Dyn. Atmospheres Oceans, 85, 1–15. doi: 10.1016/j.dynatmoce.2018.10.002

Widlansky, M. J., Timmermann, A., and Cai, W. (2015). Future extreme sea level seesaws in the tropical Pacific. Sci. Adv. 1-8. doi: 10.1126/sciadv.1500560

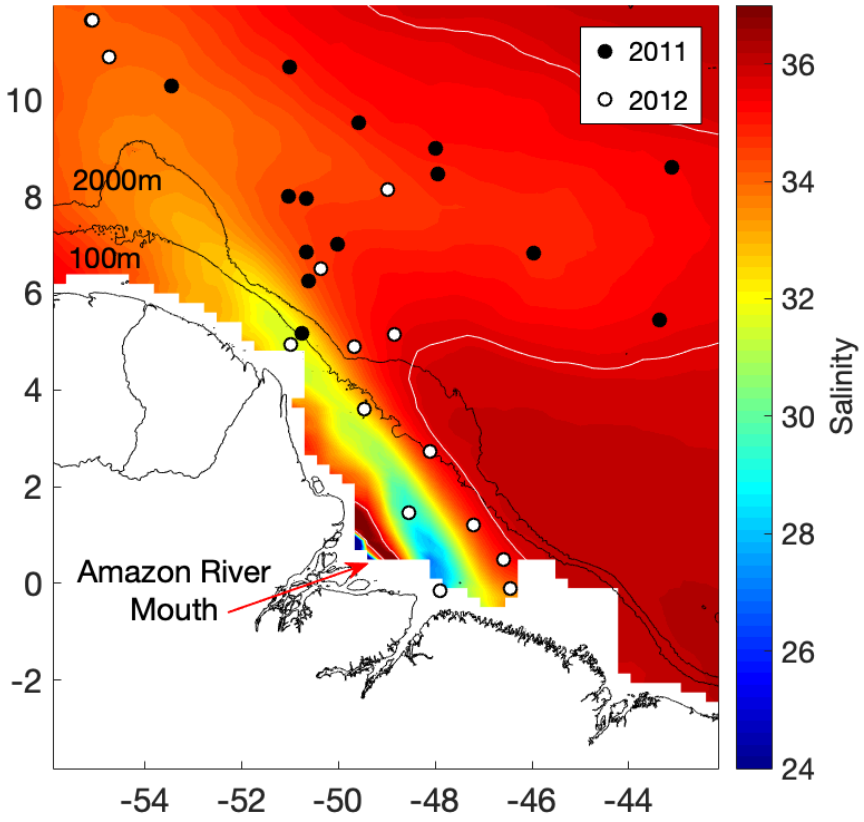

Figure 3.1: Long-term mean (January 2010 to December 2021) of sea surface salinity from SMOS. The 35.7 salinity contour is shown in white. Black contours are the 100 m and 2000 m isobaths. Sample stations where *in situ* data are available are plotted, color coded by year.

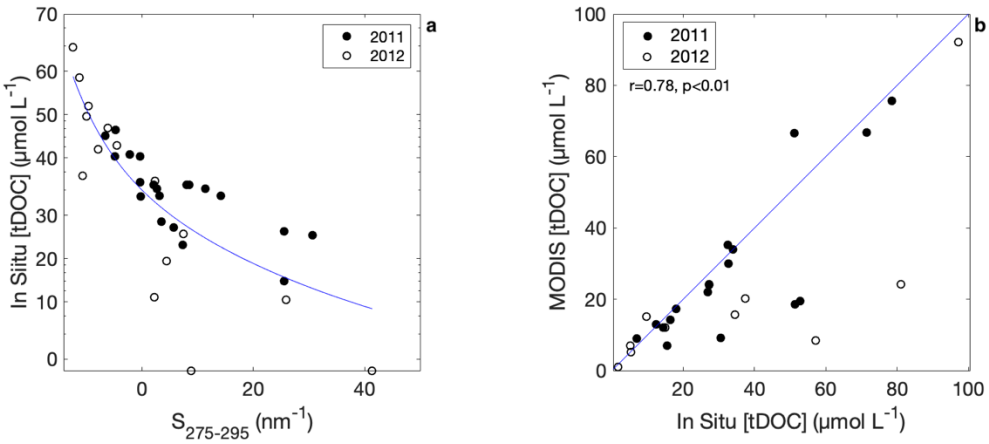

Figure 3.2: (**a**) Relationship between *in situ* measurements of CDOM spectral slope between 275-295 nm and *in situ* tDOC concentrations calculated using Eq. (1). The blue curve represents the nonlinear regression described in Eq. (3). (**b**) The *in situ* point measurements of tDOC concentrations from Eq. (1) were paired with 7-day averages of satellite-derived tDOC concentrations calculated using Eqs. (4) and (3). Correlation coefficients are also listed.

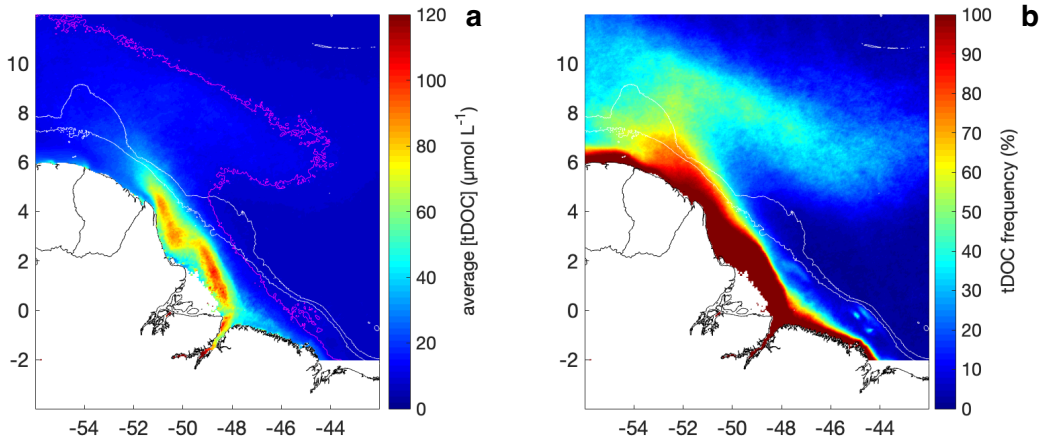

Figure 3.3: (**a**) Long-term mean of tDOC concentrations (µmol L^{-1}) over 19 years (2003-2021) in the Amazon River plume region. Magenta contour represents the boundary of the averaged plume, as defined by tDOC = 10 µmol L^{-1}. (**b**) The frequency of plume occurrence (%), defined as the ratio of the number of observations with tDOC > 10 µmol L^{-1} at a given pixel and the total number of valid observations at that pixel times 100. White contours are the 100 m and 2000 m isobaths.

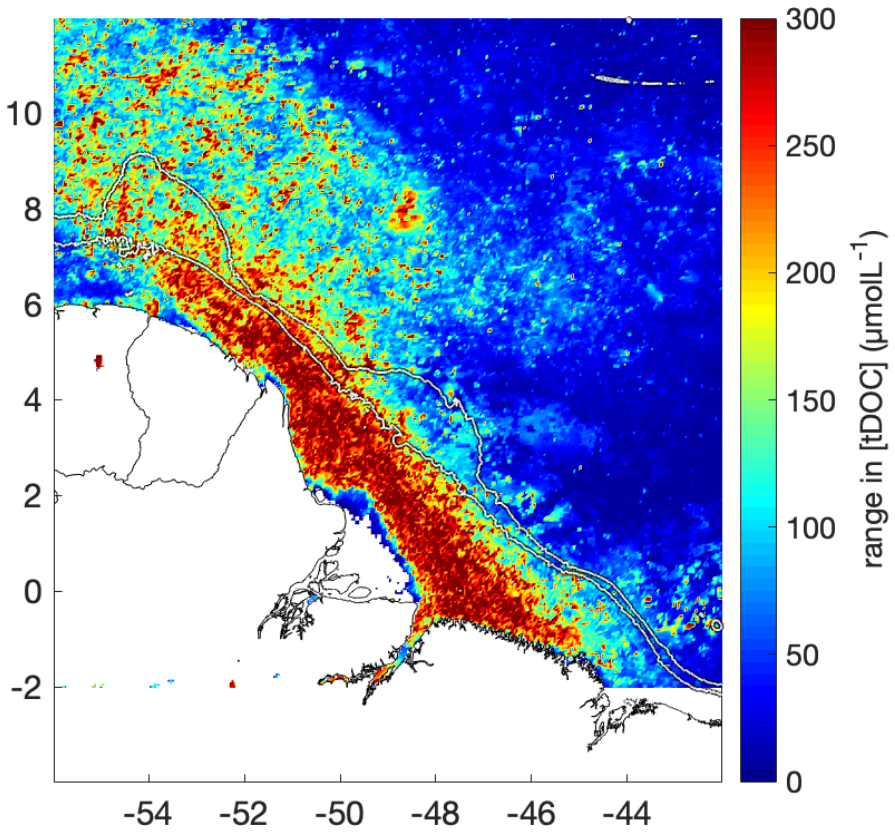

Figure 3.4: Range of tDOC concentration variability (µmol L^{-1}) at each pixel over the entire study period. White contours are the 100 m and 2000 m isobaths.

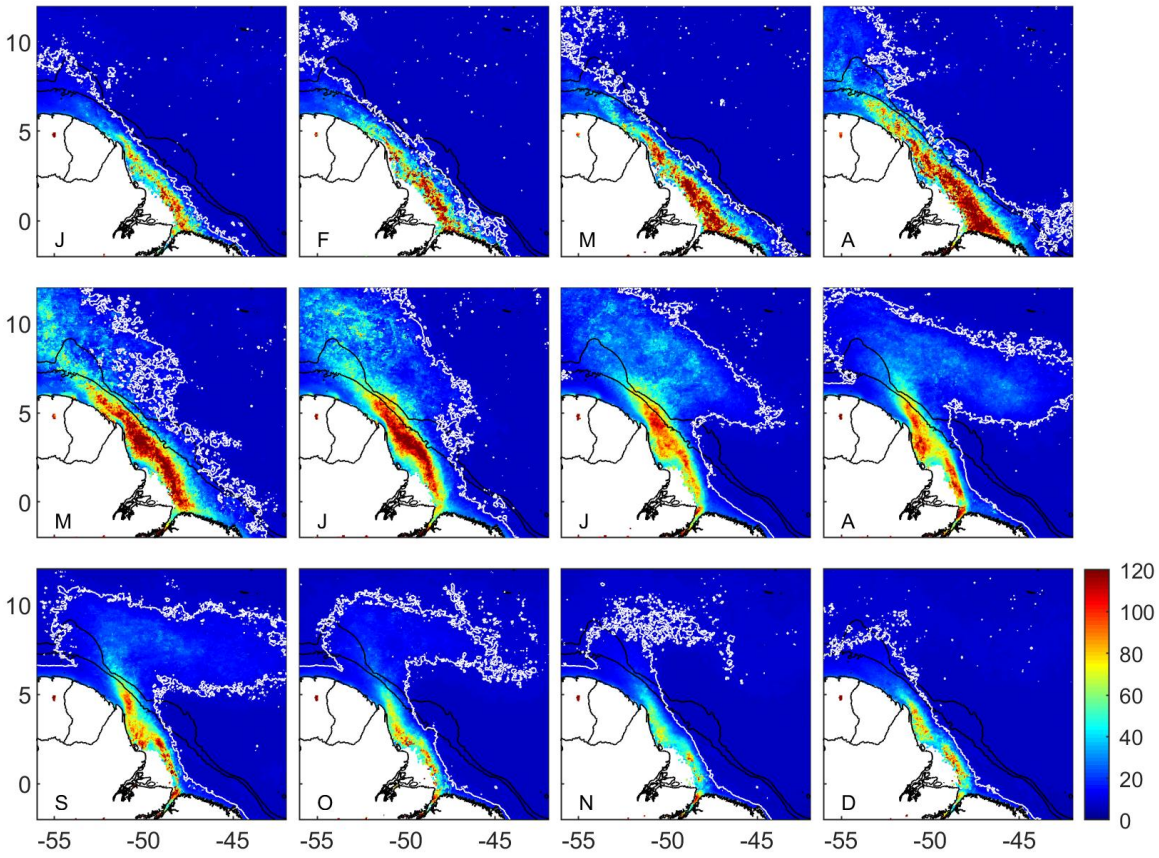

Figure 3.5: Monthly averages of tDOC concentration (µmol L^{-1}). The tDOC = 10 µmol L^{-1} contour is shown in white. Black contours are the 100 m and 2000 m isobaths.

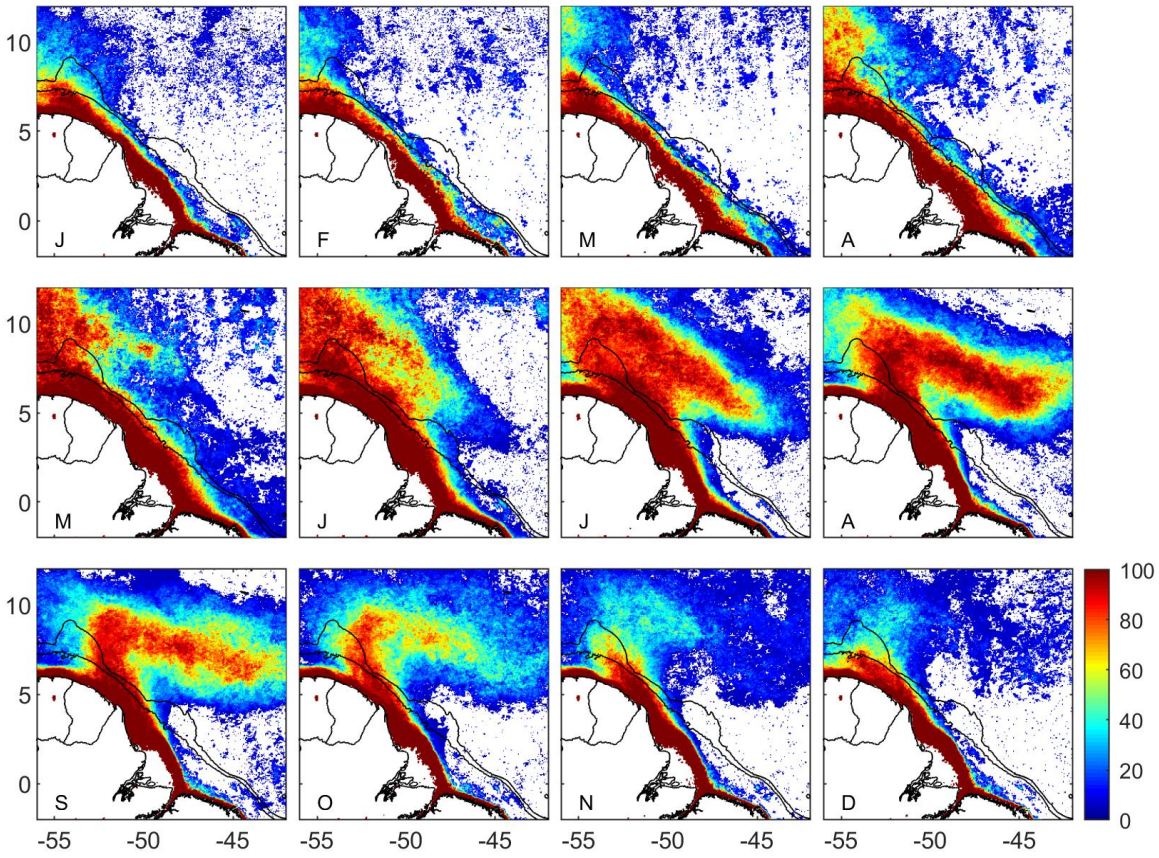

Figure 3.6: Frequency of plume occurrence (ratio of the number of observations with tDOC > 10 µmol L^{-1} at a given pixel and the number of valid observations at that pixel times 100 to yield a percentage) for each month. Zero frequency is shown in white. Black contours are the 100 m and 2000 m isobaths.

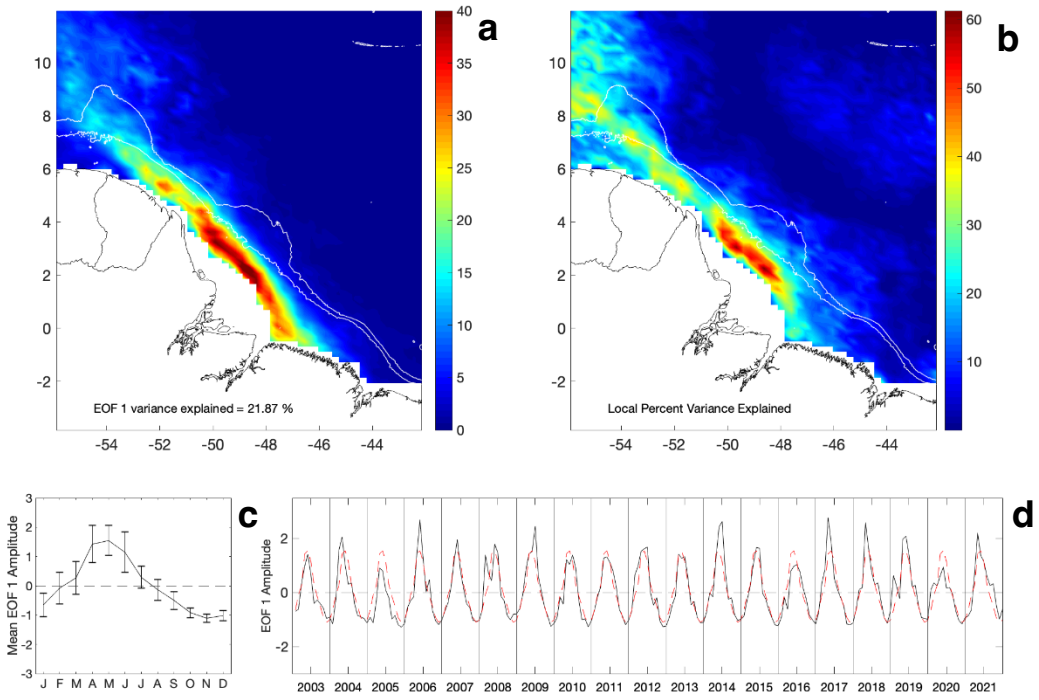

Figure 3.7: (**a**) EOF 1 of tDOC concentration (long-term average removed at each pixel). (**b**) Fraction of the local variance (%) explained by the first EOF mode. White contours are the 100 m and 2000 m isobaths. (**c**) Monthly average of the amplitude time series of EOF 1. (**d**) Amplitude time series of EOF 1. The red dashed lines are the overlay of the monthly-averaged amplitude time series (shown in c).

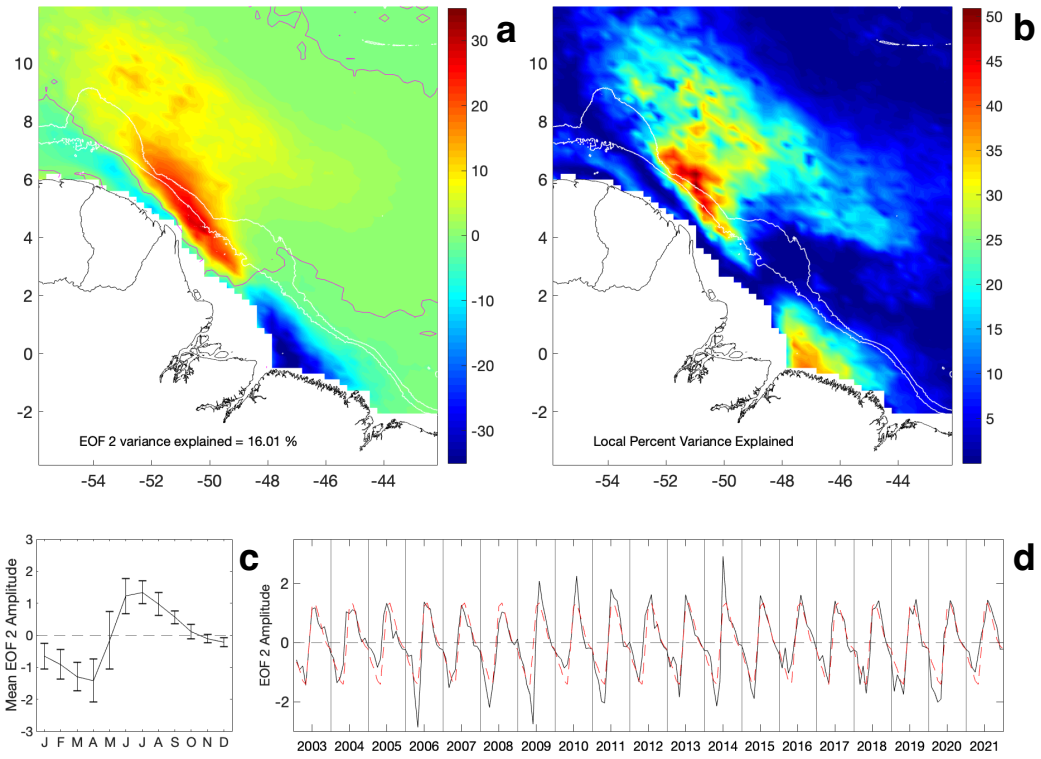

Figure 3.8: (**a**) EOF 2 of tDOC concentration (long-term average removed at each pixel). Purple contour outlines the 0-crossing of the EOF signal. (**b**) Fraction of the local variance (%) explained by the second EOF mode. White contours are the 100 m and 2000 m isobaths. (**c**) Monthly average of the amplitude time series of EOF 2. (**d**) Amplitude time series of EOF 2. The red dashed lines are the overlay of the monthly-averaged amplitude time series (shown in c).

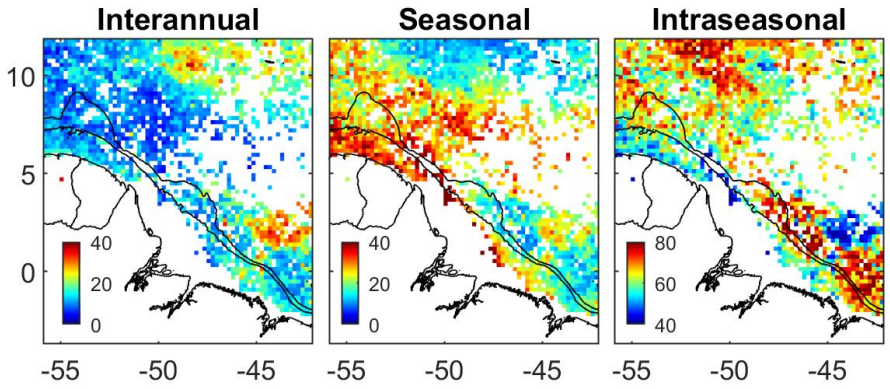

Figure 3.9: Fraction of total variance (%) explained by interannual (> 12 months), seasonal (between 6 and 12 months) and intraseasonal (< 6 months) variability. Colorbar on right panel is different because missing observations preclude the analyses in some pixels, and a different colorbar scale was used to better reveal spatial patterns. Black contours are the 100 m and 2000 m isobaths.

CHAPTER 4

AMAZON RIVER PLUME TERRIGENOUS DISSOLVED ORGANIC CARBON FROM SATELLITE OBSERVATIONS. PART II: DRIVERS OF OFF-SHELF VARIABILITY[3]

[3]Martineac, R.P., Castelao, R.M., and Medeiros, P.M. To be submitted to Journal of Geophysical Research: Oceans.

Abstract

Constraining the fate of terrigenous dissolved organic carbon (tDOC) delivered to the ocean by rivers is key to understanding the global carbon cycle. While mineralization of tDOC in the coastal ocean can directly influence air-sea CO_2 exchange and multiple biogeochemical processes, the fraction of the material that escapes the continental margin may be entrained in the large-scale circulation and potentially contribute to the long-term carbon storage of terrigenous organic matter in the deep ocean. Understanding mechanisms influencing the off-shelf transport of tDOC is challenging, however, because *in situ* observations are generally sparse. Here, we use satellite observations of tDOC and sea surface salinity to identify tDOC variability off the shelf in the Amazon River plume and to quantify tDOC degradation over the shelf. Our results reveal a clear seasonal cycle in tDOC degradation over the shelf, with increased consumption during high river discharge conditions. Furthermore, anomalies in tDOC degradation over the shelf with respect to the seasonal cycle are significantly correlated with anomalies in tDOC concentration offshore of the shelfbreak with a lag of around 40 days, so that years with anomalously high inshore tDOC degradation are associated with anomalously low tDOC content offshore. This suggests that seasonal variability in the offshore transport of tDOC in the Amazon River plume is modulated by interannual changes in tDOC degradation over the shelf. Our approach can be used to investigate the controls of tDOC variability offshore of other coastal margins characterized by large tDOC inputs.

Keywords: terrigenous dissolved organic carbon, Amazon River Plume, ocean-color, remote sensing, MODIS, SMOS

1. Introduction

Riverine transport is the largest delivery of organic matter from land to ocean (Hedges *et al.*, 1997; Raymond and Spencer, 2015), supplying a quantity sufficient to support the turnover of dissolved organic carbon (DOC) throughout the ocean (Williams and Druffel, 1987). Estimates of transport range from 0.17 Pg Cy r^{-1} (Dai et al, 2012) to 0.36 Pg C yr^{-1} (Aitkenhead and McDowell, 2000), with many other estimates over the past 5 decades falling in between (e.g., Meybeck, 1982; Smith and Hollibaugh, 1993; Ludwig *et al.*, 1996; Harrison *et al.*, 2005; Seitzinger *et al.*, 2005; Cai, 2011). The Amazon River alone is responsible for 12-20% of the global riverine DOC flux to the ocean (Meybeck, 1982; Richey *et al.*, 1986; Moreira-Turcq *et al.*, 2003; Raymond and Spencer, 2015), with a total DOC flux at the river mouth estimated to be 37.5 $tCyr^{-1}$ (Moreira-Turq *et al.*, 2003).

Research investigating dissolved organic matter (DOM) within the Amazon River shows many pathways contribute to degradation of this material. Microbial communities and photochemical degradation play a crucial role in breaking down this complex organic matter (Amon and Benner, 1996). Strong remineralization resulting in gas formation of CO_2 and CO have been reported, with losses of total organic carbon (TOC) from samples reaching 70% (Rodríguez-Zúñiga et al, 2008), suggesting that DOC is thoroughly degraded during transport to the river mouth. Consequently, the material that is exported to the coastal ocean has been shown to be quite stable, with a large fraction (50-76%) possibly escaping the continental margin in this region (Medeiros *et al.*, 2015b).

Understanding the conditions that control how much terrigenous DOC (tDOC) is laterally transported from the continental margin into offshore waters has important implications for climate. While tDOC mineralized in the coastal ocean can influence air-sea CO_2 exchange, the

material that escapes the continental margin may be entrained in the large-scale global circulation and potentially contribute to the long-term storage of organic matter of terrigenous origin in the deep ocean (Medeiros *et al.*, 2016). Previous studies have revealed that tDOC is rapidly and efficiently removed in coastal margins (e.g., Hedges *et al.*, 1997; Hernes and Benner, 2003), with more than half of the tDOC being consumed over the shelf in some systems (Fichot and Benner, 2014). Medeiros *et al.* (2015b) hypothesized that the apparent larger offshore transport of tDOC in the Amazon River plume may be related to the material being stable, possibly because it may have already been thoroughly degraded within the river prior to the export to the coastal ocean (Ward *et al.*, 2013). Medeiros *et al.* (2015b) also hypothesized that the large fraction of the terrigenous material being transported off the coastal margin may be a result of the short residence time of plume waters over the shelf, as plume waters are rapidly transported offshore due to interactions with the North Brazil Current (e.g., Coles *et al.*, 2013), offshore eddies and wind effects (e.g., Fournier *et al.*, 2017).

Identifying the relative contribution of different factors that may drive tDOC variability in the Amazon River plume offshore of the shelfbreak is difficult because *in situ* observations are scarce in the region. Although several studies have investigated tDOC degradation in the region (e.g., Amon and Benner, 1996; Ward *et al.*, 2013; Medeiros *et al.*, 2015b; Seidel *et al.*, 2015; 2016; Cao *et al.*, 2016), they only represent snapshots in time at a few locations. *In situ* observations of shelf circulation from shipboard surveys, mooring deployments and drifter trajectories are also scarce (e.g., Lentz, 1995a, b; Lentz and Limeburner, 1995; Coles *et al.*, 2013). Remote sensing can help fill that gap, providing observations over the large span of the Amazon River plume for longer periods of time. Indeed, much has been learned about the Amazon River plume using satellite measurements of salinity (e.g., Fournier *et al.*, 2015, 2017)

and ocean color (Müller-Karger *et al.*, 1988, 1995; Longhurst, 1993; Fratantoni and Glickson, 2002; Del Vecchio and Subramaniam, 2004; Molleri *et al.*, 2009; Salisbury *et al.*, 2011; Gouveia *et al.*, 2019a). In Chapter 3 (Martineac *et al.*, in prep.), we adapted and refined the algorithm developed by Fichot *et al.* (2013; 2014) to obtain estimates of tDOC concentrations from moderate resolution imaging spectroradiometer (MODIS) observations for the Amazon River plume region, and used it to characterize seasonal and interannual variability. Here, we use those satellite measurements to investigate tDOC degradation over the Amazonian shelf, and to relate it to tDOC variability offshore.

2. Methods

2.1 Remote sensing data

Daily observations of remote sensing reflectance (Rrs) from MODIS were used to estimate the spectral slope coefficient of CDOM absorbance in the 275-295 nm range ($S_{275\text{-}295}$) in the western tropical Atlantic Ocean based on the algorithm developed by Fichot *et al.* (2014). Satellite derived measurements of $S_{275\text{-}295}$ were then used to estimate tDOC concentrations based on a relationship derived using *in situ* observations from the Amazon River plume. A detailed description of the algorithm is provided in Chapter 3 (Martineac *et al.*, in prep.). Sea surface salinity (SSS) observations were obtained from the Soil Moisture Ocean Salinity (SMOS; Boutin *et al.*, 2022) mission. We use observations from January 2010 to December 2021 here when both MODIS and SMOS observations are available.

Upper-ocean currents were obtained from the Ocean Surface Current Analysis Real-time (OSCAR) data product (Bonjean and Lagerloef, 2002). Surface velocity vectors are calculated using satellite altimeter sea level anomalies and surface wind measurements, using a simplified

physical model comprising of a geostrophic term, a wind-driven term, and a thermal wind adjustment (Dohan and Maximenko, 2010).

2.2 tDOC degradation over the shelf

In order to obtain a measure of tDOC degradation over the shelf, we used 30-day averages of SSS and tDOC from satellite observations to identify deviations from conservative mixing. Specifically, we made scatter plots of bin-averages of SSS vs tDOC over the shelf in the area identified in **Figure 4.1**. Examples for two months are shown in **Figure 4.2**. The black solid line indicates conservative mixing between two end members, assuming that tDOC = 0 μM for a salinity of 36, and tDOC = 350 μM at the river mouth (0 psu). This value was chosen based on the average tDOC concentration measured at the river mouth by Medeiros *et al.* (2015) and Seidel *et al.* (2016). For each 30-day period, we integrated the difference between the bin-averaged pairs of SSS and tDOC and the conservative mixing line for salinity values larger than 25 psu, yielding an integrated deviation from conservative mixing (μM psu; we pursue the integration such that tDOC consumption is positive). That integrated deviation is related to the amount of tDOC degradation over the shelf. Large deviations, as in **Figure 4.2a**, indicate more degradation, while small values are consistent with less degradation.

3. Results

3.1 Variability in tDOC content offshore

We first present a short description of the seasonal cycle of tDOC concentrations in the Amazon River plume before focusing on deviations from that seasonal cycle. The amplitude and phase of the tDOC seasonal cycle was estimated over a 12-year period, from January 2010 to

December 2021. Amplitude of the seasonal cycle was greatest in the plume core (~ 80 μmol L^{-1}), with enhanced values stretching from the Amazon River mouth to the coast of French Guiana (**Figure 4.3a**). Slightly enhanced amplitudes were also observed extending northwestward past 7ºN and in the NBC retroflection region (Fratantoni *et al.*, 1995; Garzoli *et al.*, 2004). The phase of the seasonal cycle indicated greatest enhancement of tDOC concentrations along the coastline in March-June (**Figure 4.3b**), coinciding with the typical maximum riverine discharge season (e.g., Lentz, 1995; Smith and Demaster, 1996; Ward *et al.*, 2013). Near the shelf break and in the retroflection region, tDOC was most enhanced during July-September. Farther offshore to the northeast (~ 44°W, 10°N and surrounding area), the seasonal cycle peaked in November-January. Note, however, that the amplitude of the seasonal cycle was very small in those offshore areas. A detailed description of seasonal variability in tDOC concentrations in the region is presented in Chapter 3 (Martineac *et al.*, in prep.).

Our main goal here is to understand what drives interannual variability in tDOC in regions off the shelf. Given that the Amazon River plume is strongly modulated by seasonality (e.g., Müller-Karger *et al.*, 1988; Lentz, 1995; Fratantoni and Glickson, 2002; Coles *et al.*, 2013; Foltz *et al.*, 2015), we first removed the seasonal cycle by removing the monthly averages of the tDOC concentrations from the time series. This allowed for better identification of interannual anomalies in the dataset. Furthermore, we only considered observations from pixels offshore of the 2000 m isobath, so that we could identify offshore areas characterized by large anomalies. The first EOF mode of the tDOC anomalies offshore explains 12.2% of the total variance (**Figure 4.4a**), and it is characterized by a large signature offshore to the north of French Guiana, extending from the 2000 m isobath to around 12°N. The amplitude time series reveals that the mode is dominated by an event in June 2014 (**Figure 4.4c**), indicating increased tDOC content

offshore during that time. This followed exceptionally intense wet conditions in 2014 austral summer, when rainfall measured ~100% higher than average (Espinoza *et al.*, 2014). Fournier *et al.* (2017) used observations from SMOS to show that low-salinity waters in the core of the plume extended far beyond the shelfbreak in June 2014 (see their Figure 9), approximately coinciding with the area captured by the EOF mode (**Figure 4.4a**).

The second EOF mode explains 7.1% of the total variance (**Figure 4.4b**), and it is also characterized by enhanced values just offshore of the shelfbreak, but with an out-of-phase response to the east and to the west of ~51°W. In the region with enhanced signature to the east of 51°W, where EOF 2 is positive, the mode explains as much as 30% of the local variance (not shown). In that region, tDOC anomalies were enhanced (in comparison with the seasonal cycle) when the amplitude time series (**Figure 4.4d**) is positive, such as in mid-2012 and for several months in 2021, and depleted when the amplitude time series is negative, such as in mid-2013 and mid-2015. The opposite is true for the region to the west of 51°W, where EOF 2 is negative. EOF 2 explains less than 15% of the local variance at that location (note that this region spatially overlaps with the region with an enhanced signature in EOF 1).

3.2 tDOC variability offshore: The importance of tDOC degradation over the shelf

Interannual variability in tDOC content offshore of the shelfbreak in the Amazon River plume likely depends on a variety of processes, including variability in the DOC flux at the river mouth, as well as transport and transformations processes. In the previous section, we identified regions offshore of the shelfbreak characterized by large increases or decreases in tDOC content compared to the seasonal cycle. Here, we attempt to quantify tDOC degradation over the shelf, as well as its implications for tDOC variability in those offshore regions.

The comparisons of SSS and tDOC observations over the shelf and conservative mixing between the two end members yielded an integrated measure of degradation. Instances when tDOC behaves conservatively (e.g., **Figure 4.2b**) are consistent with the material being resistant to degradation, while large differences from conservative mixing (e.g., **Figure 4.2a**) would suggest tDOC removal (e.g., microbial-, photo-degradation) or the presence of additional water masses. There is considerable scatter in the relation between SSS and tDOC on a pixel-by-pixel level in the two examples shown in **Figure 4.2,** possibly related to uncertainties in the satellite observations (see discussion section for details). Despite this, there is a clear tendency for tDOC concentrations to be lower than the conservative mixing line in May 2010, while in June 2018 tDOC concentrations more closely matched conservative mixing. Monthly averages of the time series of deviations from conservative mixing (with the long-term average removed) present a clear seasonal cycle, suggesting enhanced consumption early in the year peaking in May during high river discharge conditions, and reduced consumption later in the year during low discharge, especially in August and September (**Figure 4.5**). We hypothesized that changes in tDOC degradation over the shelf may modulate tDOC content offshore. In other words, we hypothesized that enhanced tDOC degradation over the shelf may result in negative tDOC anomalies offshore, while periods where tDOC over the shelf behaves conservatively would be followed by positive tDOC anomalies offshore. To test this, we compared time series of tDOC content offshore with time series of tDOC degradation over the shelf (i.e., the time series of integrated deviations from conservative mixing; see **Figures 2** and **5**). The time series of tDOC anomaly offshore were computed by spatially averaging observations for the three regions identified in **Figure 4.4**, namely the area with large positive EOF 1 values in **Figure 4.4a** and the areas with large positive and negative EOF 2 values in **Figure 4.4b**. Before computing

correlations, we first removed the monthly averages from both time series, since they are both characterized by a strong seasonal cycle. Additionally, it is reasonable to expect that there should be a time lag between any possible impact of tDOC degradation anomaly over the shelf and tDOC anomalies offshore. Therefore, we computed multiple time series of tDOC degradation anomaly (i.e., time series of integrated deviations from conservative mixing with seasonal cycle removed) over the shelf, for lags of up to 70 days. For areas 1 and 2 (shown in **Figure 4.4**), no statistically significant correlations were observed. For area 3, where EOF 2 explains as much as 30% of the local variance, the time series were also found to be uncorrelated for small lags of up to 10 days and for lags larger than about 50 days (**Figure 4.6a**). Correlation coefficients are negative and increase in magnitude for intermediate lags, however. For lags between 22 and 44 days, correlation coefficients are statistically significant (at the 95% level), hovering around -0.2 to -0.3. A scatter plot of tDOC consumption anomaly over the shelf and tDOC anomaly offshore (both with the seasonal cycle removed) for a lag of 40 days is shown on **Figure 4.6b**. This supports the hypothesis that negative tDOC anomalies offshore can be associated with prior increases in degradation over the shelf (i.e., positive integrated deviations from conservative mixing).

3.3 The importance of shelf circulation

In this study, we had hoped to address how variability in ocean currents and residence time over the shelf could affect the lateral transport of tDOC toward the open ocean. We hypothesized that periods of strong mean northwestward flow over the shelf (e.g., in the area highlighted in **Figure 4.1)** would be followed by positive tDOC anomalies offshore, while periods of weak mean flow would be followed by negative tDOC anomalies offshore.

Unfortunately, however, the area of the shelf is characterized by low surface current data availability (**Figure 4.7a**). Even when data are available over the shelf, a very complex pattern of coastal currents is often captured (**Figure 4.7b**), possibly influenced by the strong tides observed in the region (e.g., Tchillibou *et al.*, 2022). These made comparisons between tDOC anomalies offshore and mean currents over the shelf unreliable.

4. Discussion

The fate of terrigenous material in the ocean is of fundamental importance. Many previous studies have indicated that coastal zones act as sinks of tDOC, with the organic material being efficiently and rapidly removed in ocean margins (e.g., Hedges *et al.*, 1997; Hernes and Benner, 2003; Fichot and Benner, 2014). Analyses at the molecular level have suggested that much of the Amazon River DOC is surprisingly stable in the coastal ocean, however, with 50-76% of the tDOC delivered to the ocean by the river being transported beyond the continental margin (Medeiros *et al.*, 2015b). Medeiros *et al.* (2015b) observed larger transport during high discharge conditions and relatively smaller transport during low flow conditions, suggesting that continued intensification of the hydrological cycle could result in increased offshore transport of tDOC in future climate scenarios. Their analysis was based on *in situ* observations during two research cruises to the Amazon River plume, and as such they were not able to investigate temporal variability in the transport other than during the two expeditions.

The recent advance of algorithms developed to estimate tDOC concentrations in the ocean using MODIS (Fichot *et al.*, 2013; 2014; Martineac, in prep.) have opened the possibility of investigating tDOC variability in the Amazon River plume over broad areas off the shelf over long periods. SSS and optical properties in the plume from satellite observations have been

shown to be strongly correlated to each other (Fournier *et al.*, 2015), but considerable deviation from conservative mixing has been reported. Salisbury *et al.* (2011) noted that negative anomalies indicating degradation of colored detrital matter (which includes absorption by both particulate detritus and CDOM) were often observed in the distal areas of the plume and suggested them to be related to photochemical oxidation. This motivated our current attempt to identify tDOC degradation over the shelf from satellite observations, and to relate it to tDOC variability off the shelf.

Despite noise in the data, our comparisons of SSS from SMOS and tDOC from MODIS have indicated a clear seasonal cycle in tDOC degradation over the shelf, with increased degradation occurring during the high discharge season. This is consistent with observations in other systems. Off coastal Georgia, U.S., for example, Letourneau and Medeiros (2019) showed that DOC utilization at the mouth of the Altamaha River is correlated with river discharge, increasing during peak river flow. Increased DOC losses have also been observed in Artic rivers during the spring freshet, both due to biological and photochemical pathways (Mann *et al.*, 2012). Although a large fraction of the dissolved macromolecules of terrigenous origin are respired in the Amazon River by microbes before export to the coastal ocean (Ward *et al.*, 2013), incubations of water collected near the Amazon River mouth have indicated that bio- and photo-transformations can alter up to 30% of the DOM molecular formulae (Seidel *et al.*, 2016). This is consistent with the statistically significant alterations in tDOC content observed here over the shelf after export from the river.

The monthly anomalies (i.e., seasonal cycle removed) in tDOC degradation over the shelf were found to be significantly correlated with anomalies in tDOC concentration in an area off the shelf, offshore of the 2000 m isobath, peaking for lags of about 40 days. Although correlation

coefficients are small, ranging in magnitude from 0.2 to 0.3, the change in correlation coefficients as a function of lag suggests that the analysis is robust: (1) Correlations coefficients are small for short lags as expected, since tDOC degradation over the shelf would not immediately lead to tDOC variability offshore due to the time it takes for the water to be transported offshore; (2) Coefficients are also small for large lags far exceeding the residence time over the shelf; (3) Coefficients are largest in magnitude for lags of about 40 days, which approximately coincide with the time it takes for drifters released near the river mouth to leave the shelf (i.e., < 30–60 days) (Limeburner *et al.*, 1995; Coles *et al.*, 2013), as they are entrained in the energetic and swift North Brazil Current (Coles *et al.*, 2013). We note that the main driver to tDOC variability offshore is likely to be variability in the tDOC flux at the river mouth. As captured by Medeiros *et al.* (2015b) mass balance approach, the largest offshore transport of tDOC occurs during peak discharge conditions. Our results suggest, however, that this seasonal variability in offshore tDOC transport seems to be modulated by interannual changes in tDOC degradation over the shelf.

Another related candidate for influencing tDOC variability off the shelf are variations in ocean circulation. Variations in the spatial extent of the plume offshore have been linked to river discharge, ocean rainfall, advection, wind forcing and turbulent mixing (e.g., Hu *et al.*, 2004; Molleri *et al.*, 2010; Coles *et al.*, 2013; Grodsky *et al.*, 2014). The containment of plume waters closer to the coast versus increased off-shelf advection has been shown to be more closely related to eddy-driven transport and cross-shore winds than to interannual variability in river discharge (Fournier *et al.*, 2017). The strength of surface currents over the shelf is likely to be particularly important for the offshore transport of tDOC. In particular, intensifications in coastal currents in comparison to the seasonal pattern would presumably lead to short residence times

over the shelf and to increased offshore transport. As such, it would be interesting to compare some metric of the intensity of coastal currents over the shelf that extends for several years with tDOC variability offshore. Our attempt to use surface currents from OSCAR revealed that data over the shelf are often missing, not allowing for robust comparisons. It may be possible to use surface drifter trajectories acquired from the Global Drifter Program Drifter Data Assembly Center (Hansen and Poulain, 1996) to obtain measures of variability in the transit time between the river mouth and the shelf break. Coles *et al.* (2013) analyzed drifter trajectories from 1979 to 2011 near the Amazon River mouth and noted that the temporal and spatial distribution of surface drifters are not uniform, however. Furthermore, they noted that a substantial fraction of the available drifters ran aground near the river mouth, leaving only 72 trajectories for their analysis. If the addition of drifters released since 2011 to the data set does not yield enough trajectories for a robust analysis, outputs from a well calibrated ocean model could be used to help identify the role of variability in shelf circulation on tDOC anomalies offshore.

There are many sources of uncertainties in the analysis pursued here. Biases on the order of 0.3-0.5 psu between *in situ* and SMOS salinity observations have been reported in the region, with the standard deviation of the *in situ* and satellite SSS differences increasing to 1 psu in plume waters (Fournier *et al.*, 2015). Optical measurements are also expected to have increased errors over the shelf and especially closer to the river mouth due to high sediment concentrations (Salisbury *et al.*, 2011). Direct comparisons between SMOS and MODIS data, as done for estimating deviations from conservative mixing, are also made more uncertain by the intrinsic characteristics of the datasets. Not only do SMOS and MODIS have different footprint sizes, but MODIS imagery cannot be obtained in cloudy conditions. The consequence is that data from different periods may have been used when computing monthly averages of SSS and tDOC (i.e.,

SSS data are available for all sampling periods at a given oceanic location at a given month, but tDOC will only be available during the cloudy-free portion of the month). Lastly, SSS measurements are representative of the top few centimeters of the ocean (Boutin *et al.*, 2016), while MODIS observations are representative of the first few meters (first optical depth). There are also uncertainties associated with the tDOC algorithm itself. Phytoplankton growth has been observed in all but the most turbid areas of the river plume (e.g., Hullburt and Corwin, 1969; Demaster *et al.*, 1996; Subramaniam *et al.*, 2008). Biological activity has been shown to increase in the northwestern part of the plume during summer (Westberry *et al.*, 2008). Large phytoplankton blooms and associated changes in ocean color could result in errors in the estimate of tDOC. Phytoplankton has been shown to change the DOM composition in the Amazon River plume by adding new compounds to the DOM pool (Medeiros *et al.*, 2015). As these newly added compounds are remineralized, they may modify the CDOM pool (e.g., Roberts *et al.*, 1998; Boss *et al.*, 2001; Twardowski and Donaghay, 2001; Yamashita and Tanoue, 2004), potentially modifying our satellite-based estimates of spectral slope even if there are no changes in the terrigenous component of the DOC. Despite all these sources of uncertainty, it is encouraging that the comparison captured a seasonal cycle in tDOC degradation that is consistent with that observed in other systems (e.g., Mann *et al.*, 2012; Letourneau *et al.*, 2019) and that anomalies (i.e., deviations from seasonal cycle) in tDOC degradation over the shelf seem to explain some of the variability in tDOC anomalies offshore. These suggest that a similar approach can be used to investigate the controls of tDOC variability in other coastal margins characterized by large tDOC inputs.

References

Aitkenhead, J. A. and W. H. McDowell (2000). Soil C:N ratio as a predictor of annual riverine DOC flux at local and global scales. Global Biogeochem. Cycles, 14(1), 127-138. doi: 10.1029/1999GB900083

Amon, R. M. W. and R. Benner (1996). Bacterial utilization of different size classes of dissolved organic matter. Limnol. Oceanogr., 41(1), 41-51. doi: 10.4319/lo.1996.41.1.0041

Bonjean, F., & Lagerloef, G. S. (2002). Diagnostic model and analysis of the surface currents in the tropical Pacific Ocean. J. Phys. Oceanogr., 32(10), 2938-2954.

Boss, E., Pegau, W. S., Zaneveld, J. R. V., & Barnard, A. H. (2001). Spatial and temporal variability of absorption by dissolved material at a continental shelf. J. Geophys. Res. Oc., 106(C5), 9499-9507.

Boutin J., Vergely J.-L., and Khvorostyanov D. (2022). SMOS SSS L3 maps generated by CATDS CEC LOCEAN. debias V7.0. SEANOE. doi: 10.17882/52804#91742

Cai, W. (2011). Estuarine and Coastal Ocean Carbon Paradox: CO2 Sinks or Sites of Terrestrial Carbon Incineration?. Annu. Rev. Mar. Sci., 3(1), 123-145. doi: 10.1146/annurev-marine-120709-142723

Cao, F., Medeiros, P. M. and Miller, W. L. (2016). Optical characterization of dissolved organic matter in the Amazon River plume and the Adjacent Ocean: Examining the relative role of mixing, photochemistry, and microbial alterations. Mar. Chem., 186, 178-188. doi: 10.1016/j.marchem.2016.09.007

Coles, V. J., Brooks, M. T. , Hopkins, J., Stukel, M. R., Yager, P. L. and Hood, R. R. (2013). The pathways and properties of the Amazon River Plume in the tropical North Atlantic Ocean. J. Geophys. Res. Oceans, 118(12), 6894-6913. doi: 10.1002/2013JC008981

Dai, M., Yin, Z. , Meng, F. , Liu, Q. and Cai W. (2012). Spatial distribution of riverine DOC inputs to the ocean: an updated global synthesis. Curr. Opin. Environ. Sustain., 4(2), 170-178. doi: 10.1016/j.cosust.2012.03.003

Del Vecchio, R. and Subramaniam, A. (2004). Influence of the Amazon River on the surface optical properties of the western tropical North Atlantic Ocean. J. Geophys. Res., 109, C11. doi: 10.1029/2004jc002503

Demaster, D. J. and Pope, R. H. (1996). Nutrient dynamics in Amazon shelf waters: results from AMASSEDS. Cont. Shelf Res., 16(3), 263-289.

Dohan, K., and Maximenko, N. (2010). Monitoring ocean currents with satellite sensors. Oceanography 23(4):94–103. doi:10.5670/oceanog.2010.08

Espinoza, J. C., Marengo, J. A., Ronchail, J., Carpio, J. M., Flores, L. N. and Guyot, J. L. (2014). The extreme 2014 flood in south-western Amazon basin: the role of tropical-subtropical

South Atlantic SST gradient. Environ. Res. Lett., 9(12), 124007. doi: 10.1088/1748-9326/9/12/124007

Fichot, C. G. and Benner, R. (2012). The spectral slope coefficient of chromophoric dissolved organic matter (S275–295) as a tracer of terrigenous dissolved organic carbon in river-influenced ocean margins. Limnol. Oceanogr., 57(5), 1453-1466. doi: 10.4319/lo.2012.57.5.1453

Fichot, C. G., Kaiser, K., Hooker, S., Amon, R., Babin, M., Belanger, S., Walker, S., and Benner, R. (2013). Pan-Arctic distributions of continental runoff in the Arctic Ocean, Sci. Rep., 3, 1053. doi:10.1038/srep01053

Fichot, C. G. and Benner, R. (2014). The fate of terrigenous dissolved organic carbon in a river-influenced ocean margin. Global Biogeochem. Cycles, 28(3), 300-318. doi: 10.1002/2013GB004670

Fichot, C. G., Lohrenz, S. E., and Benner, R. (2014). Pulsed, cross-shelf export of terrigenous dissolved organic carbon to the Gulf of Mexico. J. Geophys. Res.: Oceans, 119, 2, 1176–1194. doi: 10.1002/2013jc009424

Foltz, G. R., Schmid, C. and Lumpkin, R. (2015). Transport of Surface Freshwater from the Equatorial to the Subtropical North Atlantic Ocean. J. Phys. Oceanogr., 45(4), 1086-1102. doi: 10.1175/JPO-D-14-0189.1

Fournier, S., Chapron, B., Salisbury, J., Vandemark, D. and Reul, N. (2015). Comparison of spaceborne measurements of sea surface salinity and colored detrital matter in the Amazon plume. J. Geophys. Res. Oceans, 120(5), 3177-3192. doi: 10.1002/2014JC010109

Fournier, S., Vandemark, D., Gaultier, L., Lee, T., Jonsson, B. and Gierach, M. M. (2017). Interannual Variation in Offshore Advection of Amazon-Orinoco Plume Waters: Observations, Forcing Mechanisms, and Impacts. J. Geophys. Res. Oceans, 122(11), 8966-8982. doi: 10.1002/2017JC013103

Fratantoni, D. M. and Glickson, D. A. (2002). North Brazil Current Ring Generation and Evolution Observed with SeaWiFS. J. Phys. Oceanogr., 32(3), 1058-1074. doi: 10.1175/1520-0485(2002)032

Garzoli, S. L., Ffield, A., Johns, W. E. and Yao, Q. (2004). North Brazil Current retroflection and transports. J. Geophys. Res., 109. doi: 10.1029/2003JC001775

Gouveia, N. A., Gherardi, D. F. M., Wagner, F. H., Paes, E. T., Coles, V. J., and Aragão, L. E. O. C. (2019a). The Salinity Structure of the Amazon River Plume Drives Spatiotemporal Variation of Oceanic Primary Productivity. J. Geophys. Res. Biogeosci.,124, 1, 147–165. doi: 10.1029/2018jg004665

Gouveia, N. A., Gherardi, D. F. M., and Aragão, L. E. O. C. (2019b). The Role of the Amazon River Plume on the Intensification of the Hydrological Cycle. Geophys. Res. Lett., 46(21), 12221-12229. doi: 10.1029/2019GL084302

Grodsky, S. A., Reverdin, G., Carton, J. A., and Coles, V. J. (2014). Year-to-year salinity changes in the Amazon plume: Contrasting 2011 and 2012 Aquarius/SACD and SMOS satellite data. Remote Sens. Environ., 140, 14–22. doi: 10.1016/j.rse.2013.08.033

Hansen, D. and Poulain, P.-M. (1996). Quality control and interpolations of WOCE-TOGA drifter data. J. Atmos. Oceanic Technol., 13, 900–909.

Harrison, J. A., Caraco, N. and Seitzinger, S. P. (2005). Global patterns and sources of dissolved organic matter export to the coastal zone: Results from a spatially explicit, global model. Global Biogeochem. Cycles, 19(4). doi: 10.1029/2005GB002480

Hedges, J. I., Keil, R. G. and Benner, R. (1997). What happens to terrestrial organic matter in the ocean?. Org. Geochem., 27(5), 195-212. doi: 10.1016/S0146-6380(97)00066-1

Hernes, P. J. and R. Benner (2003). Photochemical and microbial degradation of dissolved lignin phenols: Implications for the fate of terrigenous dissolved organic matter in marine environments, J. Geophys. Res., 108. doi: 10.1029/2002JC001421

Hu, C., Montgomery, E. T., Schmitt, R. W., & Müller-Karger, F. E. (2004). The dispersal of the Amazon and Orinoco River water in the tropical Atlantic and Caribbean Sea: Observation from space and S-PALACE oats. Deep Sea Res. Part II Top. Stud. Oceanogr., 51, 1151–1171.

Hullburt, E.M. and Corwin, N. (1969). Influence of the Amazon River Outflow on the Ecology of the Western Tropical Atlantic. III. The Planktonic. Flora between the Amazon River and the Windward Islands. ICES J. Mar. Sci., 55–72.

Lentz, S. J. (1995a). Seasonal variations in the horizontal structure of the Amazon Plume inferred from historical hydrographic data. J. Geophys. Res., 100, 2391-2400, doi: 10.1029/94JC01847.

Lentz, S. J. (1995b). The Amazon River Plume during AMASSEDS: Subtidal current variability and the importance of wind forcing. J. Geophys. Res., 100(C2), 2377– 2390, doi:10.1029/94JC00343.

Lentz, S. J. and Limeburner, R. (1995). The Amazon River Plume during AMASSEDS: Spatial characteristics and salinity variability. J. Geophys. Res., 100, 2355-2375. doi: 10.1029/94JC01411

Letourneau, M. L. and Medeiros, P. M. (2019). Dissolved Organic Matter Composition in a Marsh-Dominated Estuary: Response to Seasonal Forcing and to the Passage of a Hurricane, J. Geophys. Res. Biogeosci., 124(6), 1545-1559. doi: 10.1029/2018JG004982

Limeburner, R., Beardsley, R. C., Soares, I. D., Lentz, S. J., & Candela, J. (1995). Lagrangian flow observations of the Amazon River discharge into the North Atlantic. J. Geophys. Res. Oc., 100(C2), 2401-2415.

Longhurst, A. (1993). Seasonal cooling and blooming in tropical oceans. Deep Sea Res. Part I

Oceanogr. Res. Pap., 40(11-12), 2145-2165.

Ludwig, W., Probst, J. and Kempe, S. (1996). Predicting the oceanic input of organic carbon by continental erosion. Global Biogeochem. Cycles, 10(1), 23-41. doi: 10.1029/95GB02925

Mann, P. J., Davydova, A., Zimov, N., Spencer, R. G. M., Davydov, S., Bulygina, E., Zimov, S., and Holmes, R. M. (2012). DOM composition and lability during the Arctic spring freshet on the River Kolyma, Northeast Siberia, J. Geophys. Res. Biogeo., 117, G01028. https://doi.org/10.1029/2011JG001798

Medeiros, P. M., Seidel, M., Ward, N. D., Carpenter, E. J., Gomes, H. R., Niggemann, J., Krusche, A. V., Richey, J. E., Yager, P. L. and Dittmar, T. (2015b). Fate of the Amazon River dissolved organic matter in the tropical Atlantic Ocean. Global Biogeochem. Cycles, 29(5), 677-690. doi: 10.1002/2015GB005115

Medeiros, P. M., Seidel, M., Niggemann, J., Spencer, R. G. M., Hernes, P. J., Yager, P. L., Miller, W. L., Dittmar, T. and Hansell, D. A. (2016). A novel molecular approach for tracing terrigenous dissolved organic matter into the deep ocean. Global Biogeochem. Cycles, 30(5), 689-699. doi: 10.1002/2015GB005320

Meybeck, M. (1982). Carbon, nitrogen, and phosphorus transport by world rivers, Am. J. Sci., 282(4), 401. doi: 10.2475/ajs.282.4.401

Molleri, G. S. F., Novo, E. M. L. de M. and Kampel, M. (2010). Space-time variability of the Amazon River plume based on satellite ocean color. Cont. Shelf Res., 30(3), 342-352. doi: 10.1016/j.csr.2009.11.015

Moreira-Turcq, P., Seyler, P., Guyot, J. L. and Etcheber, H. (2003). Exportation of organic carbon from the Amazon River and its main tributaries. Hydrol. Process., 17(7), 1329-1344. doi: 10.1002/hyp.1287

Müller-Karger, F., McClain, C. R. and Richardson, P. L. (1988). The dispersal of the Amazon's water. Nature, 333(6168), 56-59. doi: 10.1038/333056a0

Müller-Karger, F. E., Richardson, P. L., & Mcgillicuddy, D. (1995). On the offshore dispersal of the Amazon's Plume in the North Atlantic: Comments on the paper by A. Longhurst, "Seasonal cooling and blooming in tropical oceans." Deep Sea Res. Part I Oceanogr. Res. Pap., 42, 11–12: 2127–2137. doi: 10.1016/0967-0637(95)00085-2

Raymond, P. A. and R. G. M. Spencer (2015). "Chapter 11 - Riverine DOM", in Biogeochemistry of Marine Dissolved Organic Matter (Second Edition), ed Hansell, D.A. and Carlson, C.A. (Boston MA: Academic Press) pp. 509-533.

Richey, J. E., Meade, R. H., Salati, E., Devol, A. H., Nordin Jr, C. F., & Santos, U. D. (1986). Water discharge and suspended sediment concentrations in the Amazon River: 1982–1984. Water Resour. Res., 22(5), 756-764.

Roberts, D. A., Nelson, B. W., Adams, J. B., & Palmer, F. (1998). Spectral changes with leaf

aging in Amazon caatinga. Trees, 12, 315-325.

Rodríguez-Zúñiga, U. F., Milori, D. M. B. P., Da Silva, W. T. L., Martin-Neto, L., Oliveira, L. C., & Rocha, J. C. (2008). Changes in optical properties caused by UV-irradiation of aquatic humic substances from the Amazon River basin: seasonal variability evaluation. Environ. Sci. Technol., 42(6), 1948-1953.

Salisbury, J., Vandemark, D., Campbell, J., Hunt, C., Wisser, D., Reul, N., and Chapron, B. (2011). Spatial and temporal coherence between Amazon River discharge, salinity, and light absorption by colored organic carbon in western tropical Atlantic surface waters. J. Geophys. Res., 116, C7. doi: 10.1029/2011jc006989

Seidel, M., Dittmar, T., Ward, N. D., Krusche, A. V., Richey, J. E., Yager, P. L., & Medeiros, P. M. (2016). Seasonal and spatial variability of dissolved organic matter composition in the lower Amazon River. Biogeochem., 131, 281-302.

Seidel, M., Yager, P. L., Ward, N. D., Carpenter, E. J., Gomes, H. R., Krusche, A. V., Richey, J. E., Dittmar, T., and Medeiros, P. M. (2015). Molecular-level changes of dissolved organic matter along the Amazon River-to-ocean continuum. Mar. Chem., 177, 218–231. doi: 10.1016/j.marchem.2015.06.019

Seitzinger, S. P., Harrison, J. A., Dumont, E., Beusen, A. H. W., and Bouwman, A. F. (2005). Sources and delivery of carbon, nitrogen, and phosphorus to the coastal zone: An overview of Global Nutrient Export from Watersheds (NEWS) models and their application, Global Biogeochem. Cycles, 19(4). doi: 10.1029/2005GB002606

Smith, S. V. and J. T. Hollibaugh (1993). Coastal metabolism and the oceanic organic carbon balance. Rev. Geophys., 31(1), 75-89. doi: 10.1029/92RG02584

Smith, W. O., Jr, and Demaster, D. J. (1996). Phytoplankton biomass and productivity in the Amazon River plume: correlation with seasonal river discharge. Cont. Shelf Res., 16, 3, 291–319. doi: 10.1016/0278-4343(95)00007-n

Subramaniam, A., Yager, P. L., Carpenter, E. J., Mahaffey, C., Björkman, K., Cooley, S., ... & Capone, D. G. (2008). Amazon River enhances diazotrophy and carbon sequestration in the tropical North Atlantic Ocean. Proc. Natl. Acad. Sci. U.S.A., 105(30), 10460-10465.

Tchilibou, M., Koch-Larrouy, A., Barbot, S., Lyard, F., Morel, Y., Jouanno, J. and Morrow, R. (2022). Internal tides off the Amazon shelf during two contrasted seasons: interactions with background circulation and SSH imprints. Ocean Sci., 18(6), 1591-1618.

Twardowski, M. S., & Donaghay, P. L. (2001). Separating *in situ* and terrigenous sources of absorption by dissolved materials in coastal waters. J. Geophys. Res. Oc., 106(C2), 2545-2560.

Ward, N. D., R. G. Keil, P. M. Medeiros, D. C. Brito, A. C. Cunha, T. Dittmar, P. L. Yager, A. V. Krusche, and J. E. Richey (2013). Degradation of terrestrially derived macromolecules in the Amazon River, Nat. Geosci., 6, 530–533.

Westberry, T., Behrenfeld, M. J. , Siegel, D. A. and Boss, E. (2008). Carbon-based primary productivity modeling with vertically resolved photoacclimation. Global Biogeochem. Cycles, 22, GB2024. doi:10.1029/2007GB003078

Williams, P. M. and E. R. M. Druffel (1987). Radiocarbon in dissolved organic matter in the central North Pacific Ocean, Nature, 330(6145), 246-248. doi: 10.1038/330246a0

Yamashita, Y., and Tanoue, E. (2004). *In situ* production of chromophoric dissolved organic matter in coastal environments. Geophys. Res. Lett., 31(14).

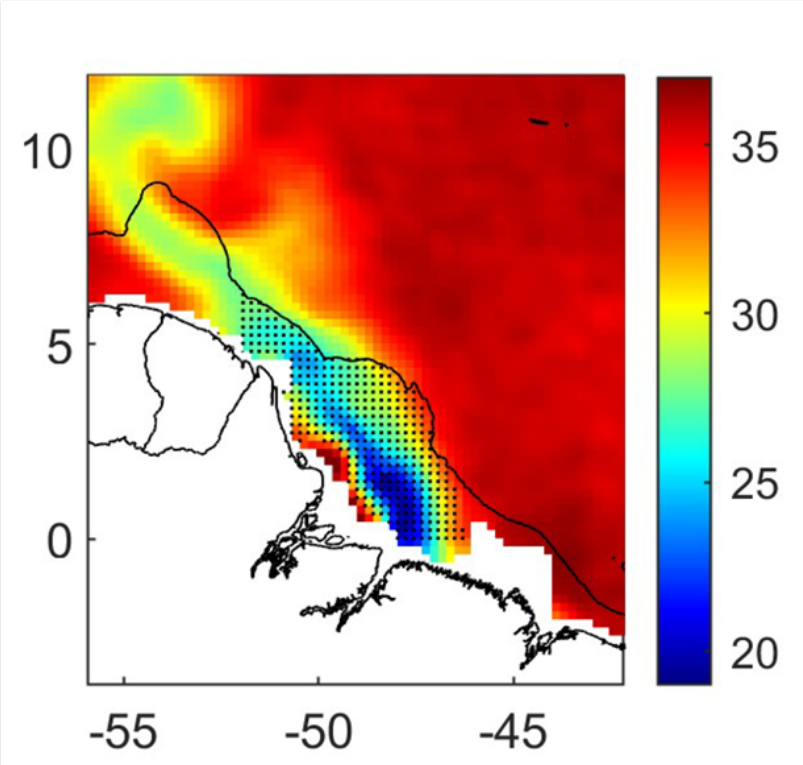

Figure 4.1: Sea surface salinity from SMOS on May 23, 2011. Small black dots indicate area where salinity and tDOC data were compared to estimate tDOC degradation over the shelf (see text for details).

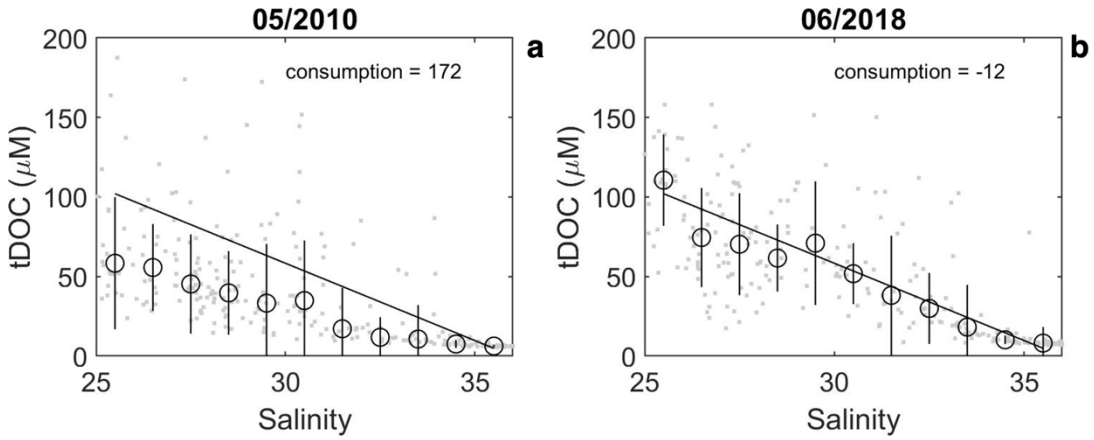

Figure 4.2: Scatter plots of SSS from SMOS and tDOC from MODIS over the shelf (in area identified in Figure 4.1) for (**a**) May 2010 and (**b**) June 2018. Gray dots represent comparison on a pixel-by-pixel basis, where large open circles are bin averages, with error bars representing the standard deviation within each bin. Black solid line represents conservative mixing. Integrated deviations from conservative mixing are also listed (μM psu), with larger positive values indicating larger tDOC degradation over the shelf.

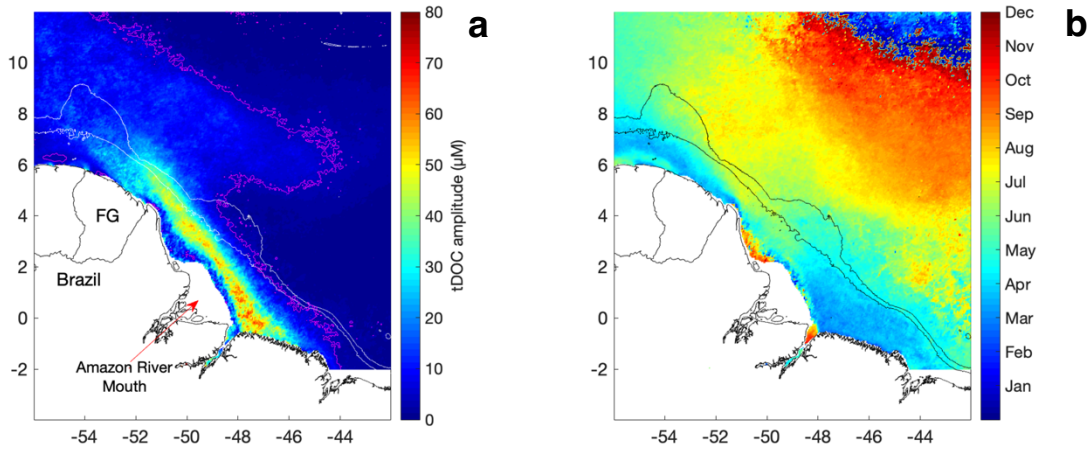

Figure 4.3: (**a**) Amplitude (mM) and (**b**) phase of the seasonal cycle of tDOC from MODIS. Magenta contour in (**a**) shows amplitude of 4 μM. Colors in (**b**) indicate the timing of the peak in the seasonal cycle. The 100 and 2000 m isobaths are shown. FG: French Guiana.

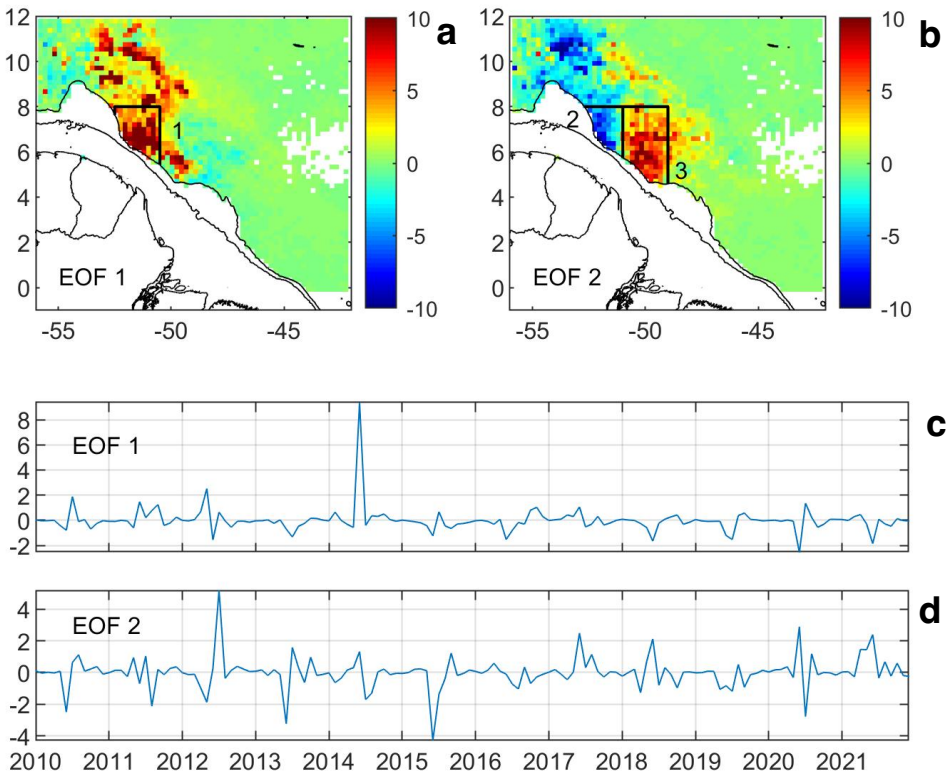

Figure 4.4: (**a**) EOF 1 and (**b**) EOF 2 of tDOC variability offshore of 2000 m isobath with seasonal cycle removed. The 100 and 2000 m isobaths are shown. Areas 1, 2, and 3 as referenced in text are denoted. Amplitude time series for EOF 1 and EOF 2 are shown in panels (**c**) and (**d**), respectively.

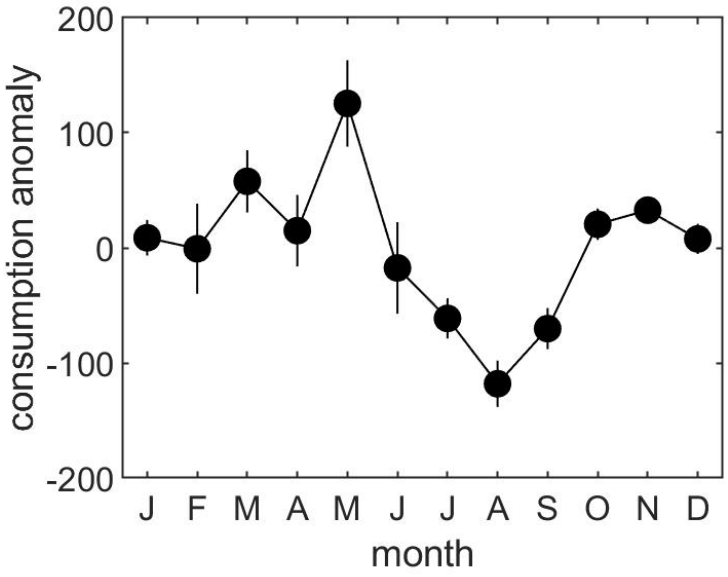

Figure 4.5: Monthly averages of tDOC consumption anomaly (μM psu) in the area identified in Figure 4.1, after removing the long-term average. Examples for two months are shown in Figure 4.2. Positive values indicate larger consumption than the long-term average.

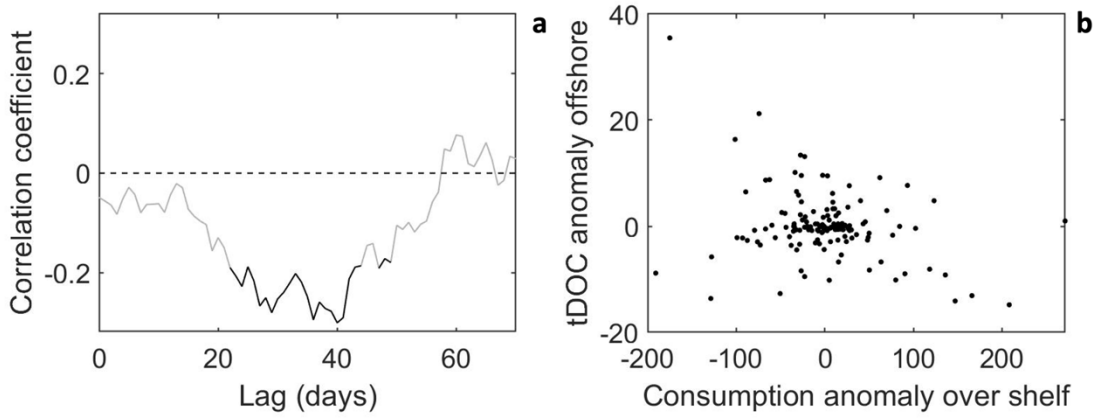

Figure 4.6: (**a**) Correlation coefficient between time series of spatially-averaged tDOC anomalies offshore (in the area with positive EOF 2 values in Figure 4.4b) and time series of tDOC degradation anomalies over the shelf in area identified in Figure 4.1. The seasonal cycle was removed from both time series. Negative correlations indicate that increased degradation over the shelf is associated with reduced tDOC anomaly offshore. Statistically significant correlations (at the 95% level) are shown in black. The correlation was computed based on 30-day averages for different lags. For example, a lag of 0 days indicates that the spatially averaged tDOC anomaly (seasonal cycle removed) offshore from June 1, 2010, to June 30, 2010 was compared with tDOC degradation anomaly (seasonal cycle removed) over the shelf during the same period. For a lag of 1 day, the same spatially averaged tDOC anomaly offshore was compared with tDOC degradation anomaly over the shelf from May 31, 2010 to June 29, 2010, and so forth. (**b**) Scatter plot of tDOC degradation anomaly (μM psu) over the shelf and spatially averaged tDOC anomaly (μM) offshore for a lag of 40 days, with seasonal cycle removed. A positive consumption anomaly indicates that tDOC degradation for that given month was larger than the average for that month.

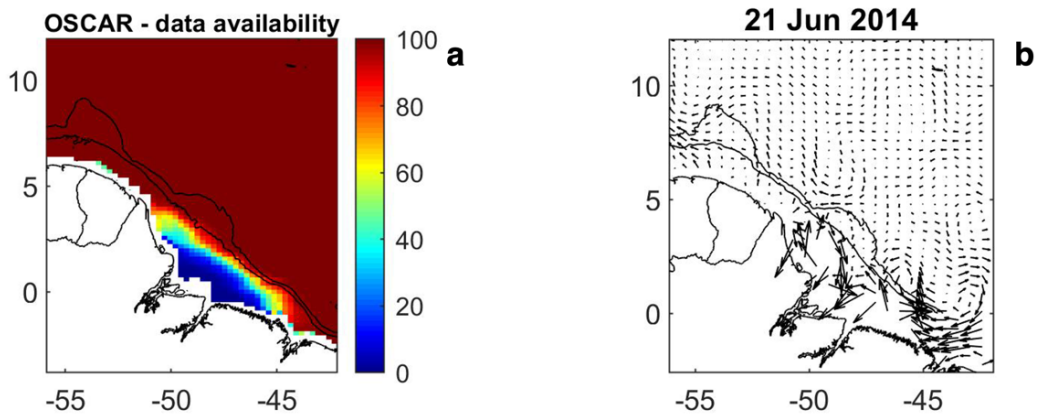

Figure 4.7: (**a**) Percentage of valid data in the OSCAR database in the Amazon River plume region. Note that data availability near the river mouth is substantially reduced. (**b**) Example of surface currents from OSCAR for 21 June 2014. Black contours are the 100 and 2000 m isobaths.

CHAPTER 5

CONCLUSIONS

This dissertation focused on better understanding transformation and transport of dissolved organic matter (DOM) in coastal systems using molecular and ocean color approaches. In one approach, I uncovered changes in DOM between freshwater and marine waters in coastal Georgia by exploring differences in DOM molecular composition. In the latter chapters of this dissertation, I adapted an algorithm to apply satellite observations to organic carbon estimates in the Amazon River plume. The research presented here aimed to answer four main questions: 1) What are the dominant patterns of variability modifying the DOM composition in an estuary off the Southeastern U.S.? 2) Is MODIS-tDOC an effective tracer for the Amazon River plume? 3) What are the patterns of seasonal and interannual variability in tDOC content in the Amazon River plume? 4) What controls the export of tDOC from the Amazon River to the continental margin?

Assessing the contribution of different drivers to DOM composition in estuaries is critically important to understand future changes in coastal regions. The analysis in CHAPTER 2 provides an assessment of the relative importance of seasonality, tides and microbial processing on variations in DOM composition in the estuary around Sapelo Island, off the Southeastern U.S. My analysis revealed that the primary mode of variability in DOM composition in Doboy Sound occurs at the seasonal scale and is associated with the terrigenous content of the DOM. Although

seasonal variability, likely due to riverine inputs, was dominant, the analyses also revealed significant increases in DOC during low tide conditions, which had not yet been investigated in this region. DOM composition between high and low tides did differ, however, with DOM from both tidal heights relatively enriched with aromatic compounds, yet, during low tide also relatively enriched with aliphatic compounds. I was also able to identify the relative contribution of microbial degradation to DOM compositional changes, which showed that on short time scales transformations due to microbial activity were small when compared to variations associated with seasonal or tidal variability. A comparison between molecular and metatranscriptomic data showed mirrored results, with tidal scale being of secondary importance relative to seasonal scale. As was the case for DOM composition, short-term incubations were found to have a smaller effect on variability in the microbial and molecular data. However, the molecular analyses indicate that over longer time scales, microbial activity has a significant impact on DOM chemistry. Therefore, if residence time is larger in comparison to the timescale of biodegradation, impacts of microbial activity on DOM composition become more important.

Future work is needed to fully resolve the relative significance of various drivers on DOM composition. Given that samples from CHAPTER 2 were collected during three instances in the year, I was unable to fully resolve seasonal variability in Doboy Sound. As such, variability at different scales (e.g., interannual) may have been aliased into the seasonal component of variability extracted by our analyses. Additionally, I focused on only a few factors that could be affecting DOM composition in estuaries, representing a first step toward assessing their relative importance. Therefore, future studies attempting to isolate and quantify the relative importance of other drivers, such as photochemistry, flocculation, and inputs associated with phytoplankton and zooplankton activity will advance community understanding of DOM

dynamics in complex coastal environments.

In CHAPTER 3, I used satellite-derived measurements of SSS from SMOS and estimates of tDOC from MODIS to describe variability in the Amazon River plume, and to quantify seasonal and interannual variability in terrigenous dissolved organic carbon (tDOC) distribution in the western tropical Atlantic Ocean. Remote sensing tools are becoming increasingly more valuable to investigate the distribution and variability of tDOC content in vast regions where *in situ* sampling is costly and difficult to obtain. Overall, MODIS-tDOC proved to be a successful tracer of the Amazon River Plume. My observations were consistent with previous characterizations of the plume core movement that revealed three main dispersal patterns: *(1)* a narrow band of flow along the northeastern South American coast from December to March; *(2)* flow to the Caribbean region between April and July; and *(3)* flow to the Central Equatorial Atlantic Ocean with plume waters entrained in the North Brazil Current retroflection from August to November. Identifying the seasonal evolution of tDOC in the plume and the frequency of occurrence provides insight on how often specific locations are influenced by plume waters, which can influence a variety of biogeochemical processes. Interestingly, these analyses also suggested cross-shelf transport of tDOC occurs year-round. Additionally, the long-term time series also allowed me to quantify interannual variability, something that has been difficult to achieve before due to the use of comparatively short time series lasting only a few years. Much of the interannual variability observed could be related to flood and drought conditions in the Amazon River watershed, with the largest increases in tDOC often observed during flood years. This is important to consider, as extreme weather events are increasing over the Amazon River watershed, potentially due to intensification of the hydrological cycle.

Although in CHAPTER 3 I connected interannual variability of the Amazon River Plume

tDOC to extreme events such as flood and drought, there are also other factors that may impact the Amazon River watershed carbon supply, such as forest fires which introduce black carbon and deforestation which have been linked to increased tDOC output. It would be interesting to explore these relationships in future investigations as these anthropogenic phenomena become more prevalent. In general, as additional data are gathered and algorithms are refined and improved, better estimates of tDOC variability will be attainable using remote sensing.

Research in CHAPTER 4 observed clear seasonal degradation of Amazon River plume tDOC over the shelf region. Additionally, the monthly anomalies in tDOC degradation over the shelf were significantly correlated with anomalies of offshore (beyond 2000 m isobath) tDOC concentration. The correlation was with a specific offshore region identified by empirical orthogonal function (EOF) decomposition. Additionally, these correlations were associated with a lag of about 40 days, which coincides with the time it takes drifters released near the river mouth to leave the shelf.

The analyses in CHAPTER 4 also attempted to correlate offshore tDOC anomalies with the magnitude of velocity of surface currents over the shelf and plume core region. However, the analyses revealed that data over the shelf are often missing, not allowing for robust comparisons. It may be possible to use surface drifter trajectories acquired from the Global Drifter Program Drifter Data Assembly Center. However, prior studies found that the distribution of surface drifters is not uniform in this region, and that a substantial fraction of the available drifters ran aground near the river mouth. If the recent addition of drifters to the data set does not yield enough trajectories for a robust analysis, outputs from a well calibrated ocean model could be used to help identify the role of variability in shelf circulation on tDOC anomalies offshore.

This dissertation provided an insight to patterns of seasonal and interannual variability of

DOM in coastal regions. Investigating the transport and fate of DOM using molecular techniques uncovered nuances between the importance of various factors impacting DOM composition. Ocean-color techniques allowed estimates of tDOC over the continental shelf near the Amazon River mouth to reveal patterns of interannual, seasonal, and intraseasonal variability, as well as provide an estimate of when and how tDOC is exported from the continental shelf from the Amazon River. This dissertation advanced the knowledge of DOM in coastal regions by improving our understanding of the drivers of variability impacting DOM composition, transport, and fate in two relevant coastal environments of our planet: a typical estuarine area in the southeastern U.S. and a major riverine plume in the Atlantic Ocean. Two different techniques, and yet complementary, were successfully employed in the studies reported here; while FT-ICR MS and metatranscriptomics unraveled the relative importance of seasonality, tides and microbial degradation changing the composition of DOM, MODIS-tDOC was an effective tracer not only to identify seasonal and interannual variability of the Amazon River plume terrigenous organic carbon, but also to quantify tDOC degradation over the shelf. The rapid advance of techniques, from molecular level to satellites, to the detection and analysis of organic matter is becoming a powerful ally to the research community studying changes in composition of organic matter in aquatic environments on both short and large time scales.

BIBLIOGRAPHY

Aitkenhead, J. A. and W. H. McDowell (2000). Soil C:N ratio as a predictor of annual riverine DOC flux at local and global scales. Global Biogeochem. Cycles, 14(1), 127-138. doi: 10.1029/1999GB900083

Aitkenhead-Peterson, J.A., McDowell, W.H., and Neff, J.C. (2003). "Sources, Production, and Regulation of Allochthonous Dissolved Organic Matter Inputs to Surface Waters." In Aquatic Ecosystems (Cambridge, MA: Elsevier), p. 25-70.

Amon, R. M. W. and R. Benner (1996). Bacterial utilization of different size classes of dissolved organic matter. Limnol. Oceanogr., 41(1), 41-51. doi: 10.4319/lo.1996.41.1.0041

Aufdenkampe, A. K., Mayorga, E., Raymond, P. A., Melack, J. M., Doney, S. C., Alin, S. R., Aalto, R. E. and Yoo, K. (2011). Riverine coupling of biogeochemical cycles between land, oceans, and atmosphere. Front. Ecol. Environ., 9(1), 53-60. doi: 10.1890/100014

Battin, T. J., Luyssaert, S., Kaplan, L. A., Aufdenkampe, A. K., Richter, A. and Tranvik, L. J. (2009). The boundless carbon cycle. Nat. Geosci, 2(9), 598-600. doi: 10.1038/ngeo618

Bauer J., Cai, W.J., Raymond, P., Bianchi, T.S., Hopkinson, C.S., and Regnier, P.A.G. (2013). The changing carbon cycle of the coastal ocean. Nature. 504, 61-70. doi: 10.1038/nature12857

Benner, R., and Opsahl, S. (2001). Molecular indicators of the sources and transformations of dissolved organic matter in the Mississippi River plume. Org. Geochem., 32, 4, 597–611. doi: 10.1016/s0146-6380(00)00197-2

Benner, R., Benitez-Nelson, B., Kaiser, K. and Amon, R. M. W. (2004). Export of young terrigenous dissolved organic carbon from rivers to the Arctic Ocean. Geophys. Res. Lett., 31(5). doi: 10.1029/2003GL019251

Bianchi, T.S. (2006). “Organic Matter Cycling,” in Biogeochemistry of Estuaries. (New York, NY: Oxford University Press), p. 177-221.

Bianchi, T. S. (2011). The role of terrestrially derived organic carbon in the coastal ocean: A changing paradigm and the priming effect. Proc. Natl. Acad. Sci. U.S.A., 108(49), 19473-19481. doi:10.1073/pnas.1017982108

Bonjean, F., & Lagerloef, G. S. (2002). Diagnostic model and analysis of the surface currents in the tropical Pacific Ocean. J. Phys. Oceanogr., 32(10), 2938-2954.

Borges, A. V., Delille, B., and Frankignoulle, M. (2005). Budgeting sinks and sources of CO2 in the coastal ocean: Diversity of ecosystems counts, Geophys. Res. Lett., 32(14).

Boss, E., Pegau, W. S., Zaneveld, J. R. V., & Barnard, A. H. (2001). Spatial and temporal

variability of absorption by dissolved material at a continental shelf. J. Geophys. Res. Oc., 106(C5), 9499-9507.

Boutin, J., Chao, Y., Asher, W.E., Delcroix, T., Drucker, R., Drushka, K., Kolodziejczyk, N.; Lee, T., Reul, N., Reverdin, G., *et al.* (2016). Satellite and *In situ* Salinity: Understanding Near-Surface Stratification and Subfootprint Variability. Bull. Am. Meteorol. Soc., 97, 1391–1407

Boutin J., Vergely J.-L., and Khvorostyanov D. (2022). SMOS SSS L3 maps generated by CATDS CEC LOCEAN. debias V7.0. SEANOE. doi: 10.17882/52804#91742

Bro, R., and Smilde, A. (2014). Principal component analysis. Anal. Methods. 6, 2812-2831.

Cai, W. (2011). Estuarine and Coastal Ocean Carbon Paradox: CO2 Sinks or Sites of Terrestrial Carbon Incineration?. Annu. Rev. Mar. Sci., 3(1), 123-145. doi: 10.1146/annurev-marine-120709-142723

Canuel, E.A., and Hardison, A.K. (2016). Sources, ages, and alteration of organic matter in estuaries. Ann. Rev. Mar. Sci. 8, 409-434. doi:10.1146/annurev-marine-122414-034058

Cao, F., Medeiros, P. M. and Miller, W. L. (2016). Optical characterization of dissolved organic matter in the Amazon River plume and the Adjacent Ocean: Examining the relative role of mixing, photochemistry, and microbial alterations. Mar. Chem., 186, 178-188. doi: 10.1016/j.marchem.2016.09.007

Cao, F., Tzortziou, M., Hu, C., Mannino, A., Fichot, C.G., Del Vecchio, R., Najjar, R.G., and Novak, M. (2018). Remote sensing retrievals of colored dissolved organic matter and dissolved organic carbon dynamics in North American estuaries and their margins. Remote Sens. Environ. 205, 151-165. doi: 10.1016/j.rse.2017.11.014

Cao, F., and Tzortziou, M. (2021). Capturing dissolved organic carbon dynamics with Landsat-8 and Sentinel-2 in tidally influenced wetland–estuarine systems. Sci. Total Environ. 777, 145910. doi: 10.1016/j.scitotenv.2021.145910

Chen, C. A. and Borges, A. V. (2009). Reconciling opposing views on carbon cycling in the coastal ocean: Continental shelves as sinks and near-shore ecosystems as sources of atmospheric CO2, Deep Sea Res. Part II Top. Stud. Oceanogr., 56(8-10), 578-590.

Chen, J. L., Wilson, C. R. and Tapley, B. D. (2010). The 2009 exceptional Amazon flood and interannual terrestrial water storage change observed by GRACE. Water Resour. Res., 46(12). doi: 10.1029/2010WR009383

Chen, C.-T. A., Huang, T.-H., Fu, Y.-H., Bai, Y., & He, X. (2012). Strong sources of CO2 in upper estuaries become sinks of CO2 in large river plumes. Curr. Opin. Environ. Sustain., 4, 2, 179–185. doi: 10.1016/j.cosust.2012.02.003

Coles, V. J., Brooks, M. T., Hopkins, J., Stukel, M. R., Yager, P. L. and Hood, R. R. (2013). The pathways and properties of the Amazon River Plume in the tropical North Atlantic Ocean.

J. Geophys. Res. Oceans, 118(12), 6894-6913. doi: 10.1002/2013JC008981

Coppola, A.I., Seidel, M., Ward, N.D. *et al.* (2019). Marked isotopic variability within and between the Amazon River and marine dissolved black carbon pools. Nat. Commun., 10, 4018. doi: 10.1038/s41467-019-11543-9

Corilo, Y.E. (2014). PetroOrg software. Florida State University. All rights reserved. (https://nationalmaglab.org/user-facilities/icr/icr-software).

Crump, B.C., Peterson, B.J., Raymond, P.A., Amon, R.M.W., Rinehart, A., McClelland, J.W., and Holmes, R.M. (2009). Circumpolar synchrony in big river bacterioplankton. Proc. Natl. Acad. Sci. U.S.A. 106, 21208-21212. doi: 10.1073/pnas.0906149106

Curtin, T. B. and Legeckis, R. V. (1986). Physical observations in the plume region of the Amazon River during peak discharge—I. Surface variability. Cont. Shelf Res., 6(1), 31-51. doi: 10.1016/0278-4343(86)90052-X

Curtin, T. B. (1986). Physical observations in the plume region of the Amazon River during peak discharge—II. Water masses. Cont. Shelf Res., 6, 1–2, 53–7. doi: 10.1016/0278-4343(86)90053-1

D'Sa, E.J., Steward, R.G., Vodacek, A., Blough, N. V., and Phinney, D. (1999). Determining optical absorption of colored dissolved organic matter in seawater with a liquid capillary waveguide. Limnol. Oceanogr. 44, 1142-1148. doi: 10.4319/ lo.1999.44.4.1142

da Silva, C. E., and Castelao, R. M. (2018). Mississippi River plume variability in the Gulf of Mexico from SMAP and MODIS-Aqua observations. J. Geophys. Res.: Oceans, 123, 6620– 6638. doi: 10.1029/2018JC014159

Dai, M., Yin, Z. , Meng, F. , Liu, Q. and Cai W. (2012). Spatial distribution of riverine DOC inputs to the ocean: an updated global synthesis. Curr. Opin. Environ. Sustain., 4(2), 170-178. doi: 10.1016/j.cosust.2012.03.003

Davidson, E., de Araújo, A., Artaxo, P. *et al.* (2012). The Amazon basin in transition. Nature, 481, 321–328. doi: 10.1038/nature10717

de Almeida, C. T., Oliveira-Júnior, J. F., Delgado, R. C., Cubo, P., and Ramos, M. C. (2016). Spatiotemporal rainfall and temperature trends throughout the Brazilian Legal Amazon, 1973-2013. Int. J. Climatol., 37, 4, 2013–2026. doi: 10.1002/joc.4831

Demaster, D. J. and Pope, R. H. (1996). Nutrient dynamics in Amazon shelf waters: results from AMASSEDS. Cont. Shelf Res., 16(3), 263-289.

Del Vecchio, R. and Subramaniam, A. (2004). Influence of the Amazon River on the surface optical properties of the western tropical North Atlantic Ocean. J. Geophys. Res., 109, C11. doi: 10.1029/2004jc002503

Devol, A. H., and Hedges, J. I. (2001). Organic matter and nutrients in the main stem Amazon

River. In The Biogeochemistry of the Amazon Basin, pp. 275–306.

Di Iorio, D., and Castelao, R.M. (2013). The dynamical response of salinity to freshwater discharge and wind forcing in adjacent estuaries on the Georgia coast. Oceanography. 26, 44-51. doi: 10.5670/oceanog.2013.44

Dittmar, T. and Paeng, J. (2009). A heat-induced molecular signature in marine dissolved organic matter. Nat. Geosci., 2(3), 175-179. doi: 10.1038/ngeo440

Dohan, K., and Maximenko, N. (2010). Monitoring ocean currents with satellite sensors. Oceanography 23(4):94–103. doi:10.5670/oceanog.2010.08

Espinoza, J. C., Ronchail, J., Frappart, F., Lavado, W., Santini, W., & Guyot, J. L. (2013). The Major Floods in the Amazonas River and Tributaries (Western Amazon Basin) during the 1970–2012 Period: A Focus on the 2012 Flood. J. Hydrometeorol., 14(3), 1000-1008.

Espinoza, J. C., Marengo, J. A., Ronchail, J., Carpio, J. M., Flores, L. N. and Guyot, J. L. (2014). The extreme 2014 flood in south-western Amazon basin: the role of tropical-subtropical South Atlantic SST gradient. Environ. Res. Lett., 9(12), 124007. doi: 10.1088/1748-9326/9/12/124007

Espinoza, J., Marengo, J. A., Schongart, J. and Jimenez, J. C. (2022). The new historical flood of 2021 in the Amazon River compared to major floods of the 21st century: Atmospheric features in the context of the intensification of floods. Weather. Clim. Extremes, 35, 100406. doi: 10.1016/j.wace.2021.100406

Fichot, C. G. and Benner, R. (2012). The spectral slope coefficient of chromophoric dissolved organic matter (S275–295) as a tracer of terrigenous dissolved organic carbon in river-influenced ocean margins. Limnol. Oceanogr., 57(5), 1453-1466. doi: 10.4319/lo.2012.57.5.1453

Fichot, C. G., Kaiser, K., Hooker, S., Amon, R., Babin, M., Belanger, S., Walker, S., and Benner, R. (2013). Pan-Arctic distributions of continental runoff in the Arctic Ocean, Sci. Rep., 3, 1053. doi:10.1038/srep01053

Fichot, C. G. and Benner, R. (2014). The fate of terrigenous dissolved organic carbon in a river-influenced ocean margin. Global Biogeochem. Cycles, 28(3), 300-318. doi: 10.1002/2013GB004670

Fichot, C. G., Lohrenz, S. E., and Benner, R. (2014). Pulsed, cross-shelf export of terrigenous dissolved organic carbon to the Gulf of Mexico. J. Geophys. Res.: Oceans, 119, 2, 1176–1194. doi: 10.1002/2013jc009424

Foley, J. A., Botta, A., Coe, M. T. and Costa, M. H. (2002). El Niño–Southern oscillation and the climate, ecosystems and rivers of Amazonia. Global Biogeochem. Cycles, 16(4), 79-20. doi: 10.1029/2002GB001872

Foltz, G. R., Schmid, C. and Lumpkin, R. (2015). Transport of Surface Freshwater from the

Equatorial to the Subtropical North Atlantic Ocean. J. Phys. Oceanogr., 45(4), 1086-1102. doi: 10.1175/JPO-D-14-0189.1

Fournier, S., Chapron, B., Salisbury, J., Vandemark, D. and Reul, N. (2015). Comparison of spaceborne measurements of sea surface salinity and colored detrital matter in the Amazon plume. J. Geophys. Res. Oceans, 120(5), 3177-3192. doi: 10.1002/2014JC010109

Fournier, S., Vandemark, D., Gaultier, L., Lee, T., Jonsson, B. and Gierach, M. M. (2017). Interannual Variation in Offshore Advection of Amazon-Orinoco Plume Waters: Observations, Forcing Mechanisms, and Impacts. J. Geophys. Res. Oceans, 122(11), 8966-8982. doi: 10.1002/2017JC013103

Fratantoni, D. M., Johns, W. E., and Townsend, T. L. (1995). Rings of the North Brazil Current: Their structure and behavior inferred from observations and a numerical simulation. J. Geophys. Res.: Oceans, 100, C6, 10633. doi: 10.1029/95jc00925

Fratantoni, D. M. and Glickson, D. A. (2002). North Brazil Current Ring Generation and Evolution Observed with SeaWiFS. J. Phys. Oceanogr., 32(3), 1058-1074. doi: 10.1175/1520-0485(2002)032

Garzoli, S. L., Ffield, A., Johns, W. E. and Yao, Q. (2004). North Brazil Current retroflection and transports. J. Geophys. Res., 109. doi: 10.1029/2003JC001775

Gévaudan, M., Durand, F., and Jouanno, J. (2022). Influence of the Amazon-Orinoco discharge interannual variability on the western tropical Atlantic salinity and temperature. J. Geophys. Res. Oceans. 127, e2022JC018495. doi: 10.1029/2022JC018495

Gifford, S.M., Sharma, S., Rinta-Kanto, J.M., and Moran, M.A. (2011). Quantitative analysis of a deeply sequenced marine microbial metatranscriptome. ISME J. 5, 461-472.

Gifford, S.M., Sharma, S., Booth, M., and Moran, M.A. (2013). Expression patterns reveal niche diversification in a marine microbial assemblage. ISME J. 7, 281-298.

Gouveia, N. A., Gherardi, D. F. M., Wagner, F. H., Paes, E. T., Coles, V. J., and Aragão, L. E. O. C. (2019a). The Salinity Structure of the Amazon River Plume Drives Spatiotemporal Variation of Oceanic Primary Productivity. J. Geophys. Res. Biogeosci.,124, 1, 147–165. doi: 10.1029/2018jg004665

Gouveia, N. A., Gherardi, D. F. M., and Aragão, L. E. O. C. (2019b). The Role of the Amazon River Plume on the Intensification of the Hydrological Cycle. Geophys. Res. Lett., 46(21), 12221-12229. doi: 10.1029/2019GL084302

Grodsky, S. A., Reverdin, G., Carton, J. A., and Coles, V. J. (2014). Year-to-year salinity changes in the Amazon plume: Contrasting 2011 and 2012 Aquarius/SACD and SMOS satellite data. Remote Sens. Environ., 140, 14–22. doi: 10.1016/j.rse.2013.08.033

Häggi, C., Hopmans, E. C., Schefuß, E., Sawakuchi, A. O., Schreuder, L. T., Bertassoli Jr, D. J. and Schouten, S. (2021). Negligible quantities of particulate low-temperature pyrogenic

carbon reach the Atlantic Ocean via the Amazon River. Global Biogeochem. Cycles, 35(9), e2021GB006990. doi: 10.1029/2021GB006990

Hansell, D.A. (2005). Dissolved organic carbon reference material program. Eos. 86:35, 318-318. doi: 10.1029/2005EO350003

Hansell, D.A., Carlson, C.A., Repeta, D.J., and Schlitzer, R. (2009). Dissolved organic matter in the ocean: A controversy stimulates new insights. Oceanography. 22, 202-211. doi: 10.5670/oceanog.2009.109

Hansell, D. A. (2013). Recalcitrant Dissolved Organic Carbon Fractions, Annu. Rev. Mar. Sci., 5(1), 421-445. doi: 10.1146/annurev-marine-120710-100757

Hansen, D. and Poulain, P.-M. (1996). Quality control and interpolations of WOCE-TOGA drifter data. J. Atmos. Oceanic Technol., 13, 900–909.

Harrison, J. A., Caraco, N. and Seitzinger, S. P. (2005). Global patterns and sources of dissolved organic matter export to the coastal zone: Results from a spatially explicit, global model. Global Biogeochem. Cycles, 19(4). doi: 10.1029/2005GB002480

Hedges, J. I. (1992). Global biogeochemical cycles: progress and problems. Mar. Chem., 39(1), 67-93. doi: 10.1016/0304-4203(92)90096-S

Hedges, J. I., Keil, R. G. and Benner, R. (1997). What happens to terrestrial organic matter in the ocean?. Org. Geochem., 27(5), 195-212. doi: 10.1016/S0146-6380(97)00066-1

Helms, J.R., Stubbins, A., Ritchie, J.D., Minor, E.C., Kieber, D.J., and Mopper, K. (2008). Absorption spectral slopes and slope ratios as indicators of molecular weight, source, and photobleaching of chromophoric dissolved organic matter. Limnol. Oceanogr. 53, 955-969.

Hernes, P. J. and R. Benner (2003). Photochemical and microbial degradation of dissolved lignin phenols: Implications for the fate of terrigenous dissolved organic matter in marine environments, J. Geophys. Res., 108. doi: 10.1029/2002JC001421

Hertkorn, N., Benner, R., Frommberger, M., Schmitt-Kopplin, P., Witt, M., Kaiser, K., Kettrup, A., and Hedges, J. I. (2006). Characterization of a major refractory component of marine dissolved organic matter, Geochim. Cosmochim. Acta, 70(12), 2990-3010.

Hollibaugh, J., Gifford, S., Sharma, S., Bano, N. and Moran, M.A. (2011). Metatranscriptomic analysis of ammonia-oxidizing organisms in an estuarine bacterioplankton assemblage. ISME J. 5, 866-878. doi: 10.1038/ismej.2010.172

Hollibaugh, J., Gifford, S., Moran, M.A., Ross, M.J., Sharma, S., and Tolar, B.B. (2013). Seasonal variation in the metratranscriptomes of a Thaumarchaeota population from SE USA coastal waters. ISME J. 8, 685-698. doi: 10.1038/ismej.2013.171

Hopkinson Jr, C. S. (1985). Shallow-water benthic and pelagic metabolism: evidence of heterotrophy in the nearshore Georgia Bight, Mar. Biol., 87(1), 19-32.

Hu, C., Montgomery, E. T., Schmitt, R. W., & Müller-Karger, F. E. (2004). The dispersal of the Amazon and Orinoco River water in the tropical Atlantic and Caribbean Sea: Observation from space and S-PALACE oats. Deep Sea Res. Part II Top. Stud. Oceanogr., 51, 1151–1171.

Hullburt, E.M. and Corwin, N. (1969). Influence of the Amazon River Outflow on the Ecology of the Western Tropical Atlantic. III. The Planktonic. Flora between the Amazon River and the Windward Islands. ICES J. Mar. Sci., 55–72.

Ibánhez, J. S. P., Diverrès, D., Araujo, M., & Lefèvre, N. (2015). Seasonal and interannual variability of sea-air CO2fluxes in the tropical Atlantic affected by the Amazon River plume. Glob. Biogeochem. Cycles, 29, 10, 1640–165. doi: 10.1002/2015gb005110

Jiménez-Muñoz, J. C., Sobrino, J. A., Mattar, C. and Malhi, Y. (2013). Spatial and temporal patterns of the recent warming of the Amazon forest. J. Geophys. Res. Atmos., 118(11), 5204-5215. doi: 10.1002/jgrd.50456

Jiménez-Muñoz, J. C., Mattar, C., Barichivich, J., Santamaría-Artigas, A., Takahashi, K., Malhi, Y., Sobrino, J. A. and Schrier, G. v. d. (2016). Record-breaking warming and extreme drought in the Amazon rainforest during the course of El Niño 2015–2016. Sci. Rep., 6(1), 33130. doi: 10.1038/srep33130

Johns, W. E., Lee, T. N., Schott, F. A., Zantopp, R. J., and Evans, R. H. (1990). The North Brazil Current retroflection: Seasonal structure and eddy variability. J. Geophys. Res., 95(C12), 22103– 22120. doi: 10.1029/JC095iC12p22103.

Kara, E., and Shade, A. (2009). Temporal dynamics of south end tidal creek (Sapelo Island, Georgia) bacterial communities. Appl. Environ. Microbiol. 75, 1058-1064.

Kieber, R. J., Zhou, X., and Mopper, K. (1990). Formation of carbonyl compounds from UV-induced photodegradation of humic substances in natural waters: Fate of riverine carbon in the sea, Limnol. Oceanogr., 35(7), 1503-1515.

Kim, S., Kramer, R. W., and Hatcher, P. G. (2003). Graphical Method for Analysis of Ultrahigh-Resolution Broadband Mass Spectra of Natural Organic Matter, the Van Krevelen Diagram, Anal. Chem., 75(20), 5336-5344. doi: 10.1021/ac034415p

Koch, B.P., and Dittmar, T. (2006). From mass to structure: an aromaticity index for high-resolution mass data of natural organic matter. Rapid Commun. Mass Spectrom., 20, 926-932. doi: 10.1002/rcm.2386

Koch, B.P., and Dittmar, T. (2016). From mass to structure: an aromaticity index for high-resolution mass data of natural organic matter. Rapid Commun. Mass Spectrom., 30, 250. doi: 10.1002/rcm.7433.

Körtzinger, A. (2003). A significant CO2 sink in the tropical Atlantic Ocean associated with the Amazon River plume. Geophys. Res. Lett., 30, 24. doi: 10.1029/2003gl018841

Kuhlbrodt, T., Griesel, A., Montoya, M., Levermann, A., Hofmann, M. and Rahmstorf, S. (2007). On the driving processes of the Atlantic meridional overturning circulation, Rev. Geophys., 45(2). doi: 10.1029/2004RG000166

Kujawinski, E.B. (2011). The impact of microbial metabolism on marine dissolved organic matter. Ann. Rev. Mar. Sci. 3, 567-599. doi: 10.1146/annurev-marine-120308-081003

Kurek, M. R., Stubbins, A., Drake, T. W., Moura, J. M. S., Holmes, R. M., Osterholz, H., Dittmar, T., Peucker-Ehrenbrink, B., Mitsuya, M., and Spencer, R. G. M. (2021). Drivers of Organic Molecular Signatures in the Amazon River. Glob. Biogeochem. Cycles, 35, 6. doi: 10.1029/2021gb006938

Lan, C., Lo, M., Chou, C., and Kumar, S. (2016). Terrestrial water flux responses to global warming in tropical rainforest areas. Earth's Future, 4, 5, 210–224. doi: 10.1002/2015ef000350

Lechtenfeld, O. J., Hertkorn, N., Shen, Y., Witt, M., and Benner, R. (2015). Marine sequestration of carbon in bacterial metabolites, Nat. Commun., 6(1), 6711.

Legaard, K. R., and Thomas, A. C. (2006). Spatial patterns in seasonal and interannual variability of chlorophyll and sea surface temperature in the California Current. J. Geophys. Res., 111, C06032. doi: 10.1029/2005JC003282

Lentz, S. J. (1995a). Seasonal variations in the horizontal structure of the Amazon Plume inferred from historical hydrographic data. J. Geophys. Res., 100, 2391-2400, doi: 10.1029/94JC01847.

Lentz, S. J. (1995b). The Amazon River Plume during AMASSEDS: Subtidal current variability and the importance of wind forcing. J. Geophys. Res., 100 (C2), 2377– 2390, doi:10.1029/94JC00343.

Lentz, S. J. and Limeburner, R. (1995). The Amazon River Plume during AMASSEDS: Spatial characteristics and salinity variability. J. Geophys. Res., 100, 2355-2375. doi: 10.1029/94JC01411

Letourneau, M. L. and Medeiros, P. M. (2019). Dissolved Organic Matter Composition in a Marsh-Dominated Estuary: Response to Seasonal Forcing and to the Passage of a Hurricane, J. Geophys. Res. Biogeosci., 124(6), 1545-1559. doi: 10.1029/2018JG004982

Letourneau, M. L., Schaefer, S. C., Chen, H., McKenna, A. M., Alber, M., and Medeiros, P. M. (2021). Spatio-temporal changes in dissolved organic matter composition along the salinity gradient of a marsh-influenced estuarine complex, Limnol. Oceanogr., 66(8), 3040-3054. doi: 10.1002/lno.11857

Letscher, R., D. A. Hansell, and D. Kadko. (2011). Rapid removal of terrigenous dissolved organic carbon over the Eurasian shelves of the Arctic Ocean. Mar. Chem., 123:78–87. doi: 10.1016/j.marchem.2010.10.002

Limeburner, R., Beardsley, R. C., Soares, I. D., Lentz, S. J., & Candela, J. (1995). Lagrangian flow observations of the Amazon River discharge into the North Atlantic. J. Geophys. Res. Oc., 100(C2), 2401-2415.

Logozzo, L., Tzortziou, M., Neale, P., and Clark, J.B. (2021). Photochemical and microbial degradation of chromophoric dissolved organic matter exported from tidal marshes, J. Geophys. Res.-Biogeosci., 126. doi:10.1029/2020JG005744

Longhurst, A. (1993). Seasonal cooling and blooming in tropical oceans. Deep Sea Res. Part I Oceanogr. Res. Pap., 40(11-12), 2145-2165.

Love, M.I., Huber, W. and Anders, S. (2014). Moderated estimation of fold change and dispersion for RNA-seq data with DESeq2. Genome Biol. 15, 550. doi: 10.1186/s13059-014-0550-8

Ludwig, W., Probst, J. and Kempe, S. (1996). Predicting the oceanic input of organic carbon by continental erosion. Global Biogeochem. Cycles, 10(1), 23-41. doi: 10.1029/95GB02925

Manabe, S., Wetherald, R. T., Milly, P., Delworth, T. L., and Stouffer, R. J. (2004). Century-scale change in water availability: CO 2-quadrupling experiment, Clim. Change, 64, 59-76.

Mann, P. J., Davydova, A., Zimov, N., Spencer, R. G. M., Davydov, S., Bulygina, E., Zimov, S., and Holmes, R. M. (2012). DOM composition and lability during the Arctic spring freshet on the River Kolyma, Northeast Siberia, J. Geophys. Res. Biogeo., 117, G01028. https://doi.org/10.1029/2011JG001798

Marengo, J. A., Tomasella, J., Alves, L. M., Soares, W. R., and Rodriguez, D. A. (2011). The drought of 2010 in the context of historical droughts in the Amazon region. Geophys. Res. Lett., 38, 12. doi: 10.1029/2011gl047436

Marengo, J. A., and Espinoza, J. C. (2015). Extreme seasonal droughts and floods in Amazonia: causes, trends and impacts. Int. J. Climatol., 36, 3, 1033–1050. doi: 10.1002/joc.4420

Medeiros, P.M., Seidel, M., Dittmar, T., Whitman, W.B., and Moran, M.A. (2015a). Drought-induced variability in dissolved organic matter composition in a marsh-dominated estuary. Geophys. Res. Lett. 42, 6446-6453. doi:10.1002/ 2015GL064653

Medeiros, P. M., Seidel, M., Ward, N. D., Carpenter, E. J., Gomes, H. R., Niggemann, J., Krusche, A. V., Richey, J. E., Yager, P. L. and Dittmar, T. (2015b). Fate of the Amazon River dissolved organic matter in the tropical Atlantic Ocean. Global Biogeochem. Cycles, 29(5), 677-690. doi: 10.1002/2015GB005115

Medeiros, P. M., Seidel, M., Powers, L. C., Dittmar, T., Hansell, D. A., and Miller, W. L. (2015c). Dissolved organic matter composition and photochemical transformations in the northern North Pacific Ocean, Geophys. Res. Lett., 42(3), 863-870.

Medeiros, P. M., Seidel, M., Niggemann, J., Spencer, R. G. M., Hernes, P. J., Yager, P. L., Miller, W. L., Dittmar, T. and Hansell, D. A. (2016). A novel molecular approach for

tracing terrigenous dissolved organic matter into the deep ocean. Global Biogeochem. Cycles, 30(5), 689-699. doi: 10.1002/2015GB005320

Medeiros, P.M., Babcock-Adams, L., Seidel, M., Castelao, R.M., Di Iorio, D., Hollibaugh, J. T., *et al.* (2017a). Export of terrigenous dissolved organic matter in a broad continental shelf. Limnol. Oceanogr. 62, 1718-1731. doi: 10.1002/lno.10528

Medeiros, P.M., Seidel, M., Gifford, S.M., Ballantyne, F., Dittmar, T., Whitman, W. B., *et al.* (2017b). Microbially-mediated transformations of estuarine dissolved organic matter. Front. Mar. Sci. 4. doi:10.3389/fmars.2017.00069

Meybeck, M. (1982). Carbon, nitrogen, and phosphorus transport by world rivers, Am. J. Sci., 282(4), 401. doi: 10.2475/ajs.282.4.401

Meyer, J. L., Edwards, R. T., and Risley, R. (1987). Bacterial growth on dissolved organic carbon from a blackwater river, Microb. Ecol., 13(1), 13-29. doi: 10.1007/BF02014960

Miller, W.L., and Moran, M.A. (1997). Interaction of photochemical and microbial processes in the degradation of refractory dissolved organic matter from a coastal marine environment. Limnol. Oceanogr. 42, 1317-1324. doi: 10.4319/lo.1997.42.6.1317

Molion, L. and Moraes, J. (1987). Oscilaçao sul e descarga de rios na América do Sul Tropical. Rev.Bras.Eng., Caderno de Hidrologia, 5(1), 53-63.

Molleri, G. S. F., Novo, E. M. L. de M. and Kampel, M. (2010). Space-time variability of the Amazon River plume based on satellite ocean color. Cont. Shelf Res., 30(3), 342-352. doi: 10.1016/j.csr.2009.11.015

Mooers, C. N. K., and Smith, R. L. (1968). Continental shelf waves off Oregon, J. Geophys. Res., 73(2), 549– 557. doi: 10.1029/JB073i002p00549

Moran, M. A. and Hodson, R. E. (1989). Formation and bacterial utilization of dissolved organic carbon derived from detrital lignocellulose, Limnol. Oceanogr., 34(6), 1034-1047.

Moran, M. A. and Hodson, R. E. (1994). Dissolved humic substances of vascular plant origin in a coastal marine environment, Limnol. Oceanogr., 39(4), 762-771.

Moran, M. A., Sheldon, W. M., and Sheldon, J. E. (1999). Biodegradation of riverine dissolved organic carbon in five estuaries of the southeastern United States, Estuaries, 22, 55-64.

Moran M.A, Kujawinski E.B., Stubbins A., Fatland R., Aluwihare L.I., Buchan A., *et al.* (2016). Deciphering ocean carbon in a changing world. Proc. Natl. Acad. Sci. U.S.A. 113, 3143-3151. doi: 10.1073/pnas.1514645113

Moreira-Turcq, P., Seyler, P., Guyot, J. L. and Etcheber, H. (2003). Exportation of organic carbon from the Amazon River and its main tributaries. Hydrol. Process., 17(7), 1329-1344. doi: 10.1002/hyp.1287

Müller-Karger, F., McClain, C. R. and Richardson, P. L. (1988). The dispersal of the Amazon's water. Nature, 333(6168), 56-59. doi: 10.1038/333056a0

Müller-Karger, F. E., Richardson, P. L., & Mcgillicuddy, D. (1995). On the offshore dispersal of the Amazon's Plume in the North Atlantic: Comments on the paper by A. Longhurst, "Seasonal cooling and blooming in tropical oceans." Deep Sea Res. Part I Oceanogr. Res. Pap., 42, 11–12: 2127–2137. doi: 10.1016/0967-0637(95)00085-2

Nohara, D., Kitoh, A., Hosaka, M., and Oki, T. (2006). Impact of climate change on river discharge projected by multimodel ensemble, J. Hydrometeorol., 7(5), 1076-1089.

Noriega, C., and Araujo, M. (2014). Carbon dioxide emissions from estuaries of northern and northeastern Brazil. Sci. Rep. 4, 6164. doi: 10.1038/srep06164

Obernosterer, I., and Benner, R. (2004). Competition between biological and photochemical processes in the mineralization of dissolved organic carbon. Limnol. Oceanogr. 49, 117-124.

Opsahl, S. and Benner, R. (1997). Distribution and cycling of terrigenous dissolved organic matter in the ocean, Nature, 386(6624), 480-482. doi: 10.1038/386480a0

Osburn, C.L., Atar, J.N., Boyd, T.J., and Montgomery, M.T. (2019). Antecedent precipitation influences the bacterial processing of terrestrial dissolved organic matter in a North Carolina estuary. Estuar. Coast. Shelf Sci. 221, 119-131. doi: 10.1016/j.ecss.2019.03.016

Osterholz, H., Singer, G., Wemheuer, B., Daniel, R., Simon, M., Niggemann, J., *et al.* (2016a). Deciphering associations between dissolved organic molecules and bacterial communities in a pelagic marine system. ISME J. 10, 1717-1730. doi: 10.1038/ismej.2015.231

Osterholz, H., Kirchman, D. L., Niggemann, J., and Dittmar, T. (2016b). Environmental drivers of dissolved organic matter molecular composition in the Delaware Estuary, Front. Earth Sci., 4, 95.

Osterholz, H., Kirchman, D. L., Niggemann, J., and Dittmar, T. (2018). Diversity of bacterial communities and dissolved organic matter in a temperate estuary. FEMS Microbiol. Ecol. 94:8. doi: 10.1093/femsec/fiy119

Overland, J. E. and Preisendorfer, R. W. (1982). A Significance Test for Principal Components Applied to a Cyclone Climatology. Mon. Weather Rev., 110(1), 1-4. doi: 10.1175/1520-0493(1982)110

Peuravuori, J., and Pihlaja, K. (1997). Molecular size distribution and spectroscopic properties of aquatic humic substances. Anal. Chim. Acta. 337, 133-149. doi: 10.1016/s0003-2670(96)00412-6

Pomeroy, L. R. (1974). The ocean's food web, a changing paradigm. Bioscience, 24(9), 499-504.

Pomeroy, L. R, Williams, P. J. leB., Azam, F., and Hobbie, J. E. (2007). The microbial loop,

Oceanography, 20(2), 28-33.

Poretsky, R.S., Bano, N., Buchan, A., LeCleir, G. Kleikemper, J., Pickering, M., *et al.* (2005). Analysis of microbial gene transcripts in environmental samples. Appl. Environ. Microbiol. 71, 7. doi: 10.1128/AEM.71.7.4121-4126.2005

Poretsky, R.S., Sun, S., Mou, X., and Moran, M.A. (2010). Transporter genes expressed by coastal bacterioplankton in response to dissolved organic carbon. Environ. Microbiol. 12, 616-627. doi: 10.1111/j.1462-2920.2009.02102.x

Raymond, P. A., and J. E. Bauer (2001). Riverine export of aged terrestrial organic matter to the North Atlantic Ocean. Nature, 409, 497–500.

Raymond, P. A. and R. G. M. Spencer (2015). "Chapter 11 - Riverine DOM", in Biogeochemistry of Marine Dissolved Organic Matter (Second Edition), ed Hansell, D.A. and Carlson, C.A. (Boston MA: Academic Press) pp. 509-533.

Reul, N., *et al.* (2013). Sea surface salinity observations from space with the SMOS satellite: A new means to monitor the marine branch of the water cycle. Surv. Geophys., 35, 681–722.

Rich, J., Ducklow, H., and Kirchman, D.L. (1996). Concentrations and uptake of neutral monosaccharides along 14°W in the equatorial Pacific: Contribution of glucose to heterotrophic bacterial activity and the DOM flux. Limnol. Oceanogr. 41, 595-604.

Richey, J. E., Meade, R. H., Salati, E., Devol, A. H., Nordin Jr, C. F., & Santos, U. D. (1986). Water discharge and suspended sediment concentrations in the Amazon River: 1982–1984. Water Resour. Res., 22(5), 756-764.

Richey, J. E., Nobre, C. and Deser, C. (1989). Amazon River Discharge and Climate Variability: 1903 to 1985. Science, 246(4926), 101-103. doi: 10.1126/science.246.4926.101

Richey, J. E., Hedges, J. I., Devol, A. H., Quay, P. D., Victoria, R., Martinelli, L. and Forsberg, B. R. (1990). Biogeochemistry of carbon in the Amazon River. Limnol. Oceanogr., 35(2), 352-371. doi: 10.4319/lo.1990.35.2.0352

Roberts, D. A., Nelson, B. W., Adams, J. B., & Palmer, F. (1998). Spectral changes with leaf aging in Amazon caatinga. Trees, 12, 315-325.

Rodríguez-Zúñiga, U. F., Milori, D. M. B. P., Da Silva, W. T. L., Martin-Neto, L., Oliveira, L. C., & Rocha, J. C. (2008). Changes in optical properties caused by UV-irradiation of aquatic humic substances from the Amazon River basin: seasonal variability evaluation. Environ. Sci. Technol., 42(6), 1948-1953.

Ronchail, J., Labat, D., Cochonneau, G., Guyot, J.L., Filizola, N.m Oliveira, E. (2005). "Discharge variability within the Amazon basin." In Regional hydrological impacts of climatic change: hydroclimatic variability, (IAHS Press), 296, 21–32.

Ruault, V., Jouanno, J., Durand, F., Chanut, J., and Benshila, R. (2020). Role of the Tide on the

Structure of the Amazon Plume: A Numerical Modeling Approach. J. Geophys. Res., 125, 2. doi: 10.1029/2019jc015495

Salisbury, J., Vandemark, D., Campbell, J., Hunt, C., Wisser, D., Reul, N., and Chapron, B. (2011). Spatial and temporal coherence between Amazon River discharge, salinity, and light absorption by colored organic carbon in western tropical Atlantic surface waters. J. Geophys. Res., 116, C7. doi: 10.1029/2011jc006989

Satyamurty, P., Da Costa, C. P. W., Manzi, A. O., & Candido, L. A. (2013). A quick look at the 2012 record flood in the Amazon Basin. Geophys. Res. Lett., 40(7), 1396-1401.

Savory, J.J., Kaiser, N.K., McKenna, A.M., Xian, F., Blakney, G.T., Rodgers, R.P., Hendrickson, C.L., and Marshall, A.G. (2011). Parts-per-billion Fourier transform ion cyclotron resonance mass measurement accuracy with a "walking" calibration equation. Anal. Chem. 83, 1732-1736, doi: 10.1021/ac102943z

Schaefer, S.C., and Alber, M. (2007). Temperature controls a latitudinal gradient in the proportion of watershed nitrogen exported to coastal ecosystems. Biogeochemistry. 85, 333-346.

Seager, R., Tzanova, A., and Nakamura, J. (2009). Drought in the southeastern United States: causes, variability over the last millennium, and the potential for future hydroclimate change. J. Clim. 22, 5021-5045. doi: 10.1175/2009jcli2683.1

Seidel, M., Beck, M., Riedel, T., Waska, H., Suryaputra, I. G. N. A., Schnetger, B., *et al.* (2014). Biogeochemistry of dissolved organic matter in an anoxic intertidal creek bank. Geochim. Cosmochim. Acta. 140, 418-434. doi: 10.1016/j.gca.2014.05.038

Seidel, M., Yager, P. L., Ward, N. D., Carpenter, E. J., Gomes, H. R., Krusche, A. V., Richey, J. E., Dittmar, T., and Medeiros, P. M. (2015). Molecular-level changes of dissolved organic matter along the Amazon River-to-ocean continuum. Mar. Chem., 177, 218–231. doi: 10.1016/j.marchem.2015.06.019

Seidel, M., Dittmar, T., Ward, N. D., Krusche, A. V., Richey, J. E., Yager, P. L., & Medeiros, P. M. (2016). Seasonal and spatial variability of dissolved organic matter composition in the lower Amazon River. Biogeochem., 131, 281-302.

Seitzinger, S. P., Harrison, J. A., Dumont, E., Beusen, A. H. W., and Bouwman, A. F. (2005). Sources and delivery of carbon, nitrogen, and phosphorus to the coastal zone: An overview of Global Nutrient Export from Watersheds (NEWS) models and their application, Global Biogeochem. Cycles, 19(4). doi: 10.1029/2005GB002606

Sheldon, J.E., and Alber, M. (2002). A comparison of residence time calculations using simple compartment models of the Altamaha River estuary, Georgia. Estuar. Coast. 25, 1304-1317. doi: 10.1007 /bf02692226

Sholkovitz, E.R. (1976). Flocculation of dissolved organic and inorganic matter during the mixing of river water and seawater. Geochim. Cosmochim. Acta. 4, 831-845.

Sleighter, R.L., and Hatcher, P.G. (2008). Molecular characterization of dissolved organic matter (DOM) along a river to ocean transect of the lower Chesapeake Bay by ultrahigh resolution electrospray ionization Fourier transform ion cyclotron resonance mass spectrometry. Mar. Chem. 110, 140-152. doi: 10.1016/j.marchem.2008.04.008

Smith, S. V. and J. T. Hollibaugh (1993). Coastal metabolism and the oceanic organic carbon balance. Rev. Geophys., 31(1), 75-89. doi: 10.1029/92RG02584

Smith, W. O., Jr, and Demaster, D. J. (1996). Phytoplankton biomass and productivity in the Amazon River plume: correlation with seasonal river discharge. Cont. Shelf Res., 16, 3, 291–319. doi: 10.1016/0278-4343(95)00007-n

Subramaniam, A., Yager, P. L., Carpenter, E. J., Mahaffey, C., Björkman, K., Cooley, S., ... & Capone, D. G. (2008). Amazon River enhances diazotrophy and carbon sequestration in the tropical North Atlantic Ocean. Proc. Natl. Acad. Sci. U.S.A., 105(30), 10460-10465.

Sunagawa, S., Coelho, L. P., Chaffron, S., Kultima, J. R., Labadie, K., Salazar, G., Djahanschiri, B, Zeller, G., Mende, D. R., and Alberti, A. (2015). Structure and function of the global ocean microbiome, Science, 348(6237), 1261359.

Tchilibou, M., Koch-Larrouy, A., Barbot, S., Lyard, F., Morel, Y., Jouanno, J. and Morrow, R. (2022). Internal tides off the Amazon shelf during two contrasted seasons: interactions with background circulation and SSH imprints. Ocean Sci., 18(6), 1591-1618.

Twardowski, M. S., & Donaghay, P. L. (2001). Separating *in situ* and terrigenous sources of absorption by dissolved materials in coastal waters. J. Geophys. Res. Oc., 106(C2), 2545-2560.

Tzortziou, M., Neale, P.J., Osburn, C.L., Megonigal, J. P., Maie, N., and Jaffe, R. (2008). Tidal marshes as a source of optically and chemically distinctive colored dissolved organic matter in the Chesapeake Bay. Limnol. Oceanogr. 53, 148-159.

Tzortziou, M., P. J. Neale, J. P. Megonigal, C. L. Pow, and M. Butterworth (2011). Spatial gradients in dissolved carbon due to tidal marsh outwelling into a Chesapeake Bay estuary, Mar. Ecol. Prog. Ser., 426, 41-56.

Varona, H. L., Veleda, D., Silva, M., Cintra, M., and Araujo, M. (2019). Amazon River plume influence on Western Tropical Atlantic dynamic variability. Dyn. Atmospheres Oceans, 85, 1–15. doi: 10.1016/j.dynatmoce.2018.10.002

Vorobev, A., S. Sharma, M. Yu, J. Lee, B. J. Washington, W. B. Whitman, F. Ballantyne IV, P. M. Medeiros, and M. A. Moran (2018). Identifying labile DOM components in a coastal ocean through depleted bacterial transcripts and chemical signals, Environ. Microbiol., 20(8), 3012-3030.

Walsh, J. J. (1991). Importance of continental margins in the marine biogeochemical cycling of carbon and nitrogen, Nature, 350(6313), 53-55.

Walther, J.V. (2013). “Understanding the Earth's natural resources: An introduction,” in Earth's Natural Resources, (Burlington, MA: Jones and Bartlett Learning), p 1-26.

Wang, Y., Castelao, R.M., and Di Iorio, D. (2017). Salinity variability and water exchange in interconnected estuaries. Estuar. Coast. 40, 917-929. doi: 10.1007/s12237-016-0195-9

Ward, N. D., R. G. Keil, P. M. Medeiros, D. C. Brito, A. C. Cunha, T. Dittmar, P. L. Yager, A. V. Krusche, and J. E. Richey (2013). Degradation of terrestrially derived macromolecules in the Amazon River, Nat. Geosci., 6, 530–533.

Watanabe, K., and Kuwae, T. (2015). How organic carbon derived from multiple sources contributes to carbon sequestration processes in a shallow coastal system? Glob. Change Biol. 21, 2612-2623. doi: 10.1111/gcb.12924

Westberry, T., Behrenfeld, M. J. , Siegel, D. A. and Boss, E. (2008). Carbon-based primary productivity modeling with vertically resolved photoacclimation. Global Biogeochem. Cycles, 22, GB2024. doi:10.1029/2007GB003078

Widlansky, M. J., Timmermann, A., and Cai, W. (2015). Future extreme sea level seesaws in the tropical Pacific. Sci. Adv. 1-8. doi: 10.1126/sciadv.1500560

Williams, P. M. and E. R. M. Druffel (1987). Radiocarbon in dissolved organic matter in the central North Pacific Ocean, Nature, 330(6145), 246-248. doi: 10.1038/330246a0

Wu, Z., Rodgers, R.P., and Marshall, A.G. (2004). Two- and three-dimensional van Krevelen diagrams: A graphical analysis complementary to the Kendrick mass plot for sorting elemental compositions of complex organic mixtures based on ultrahigh-resolution broadband Fourier transform ion cyclotron resonance mass measurements. Anal. Chem. 76, 2511-2516. doi: 10.1021/ ac0355449

Yamashita, Y., and Tanoue, E. (2004). *In situ* production of chromophoric dissolved organic matter in coastal environments. Geophys. Res. Lett., 31(14).